Control of Alternative Energy Hybrid System for Residential and Low Power Applications

By
Emil A. Jimenez-Brea

A thesis submitted in partial fulfillment for the degree of

MASTER OF SCIENCE
In
Electrical Engineering

UNIVERSITY OF PUERTO RICO
MAYAGUEZ CAMPUS
2009

Approved by:

_____	_____
Miguel Vélez Reyes, Ph.D. Member, Graduate Committee	Date
_____	_____
Andrés Díaz, Ph.D. Member, Graduate Committee	Date
_____	_____
Eduardo I. Ortiz Rivera, Ph.D. President, Graduate Committee	Date
_____	_____
Pedro Vázquez, D. Sc. Representative of Graduate Studies	Date
_____	_____
Jaime Seguel, Ph.D. Associate Dean for Academic Affairs College of Engineering	Date

ABSTRACT

This work presents the design and simulation of a control strategy for the interconnection of a hybrid alternative energy system capable of regulating the load's voltage and controlling the power generation of the energy sources. The control strategy consists of controlling the power generated by each energy source, in a hierarchical form using sliding mode control, while taking in consideration factors that affect each power source and transform the power generated to suitable conditions for low power and residential applications. The hybrid alternative energy system is composed of photovoltaic cells, fuel cells and batteries. A mathematical equation to estimate the optimal voltage of photovoltaic systems for any solar irradiance and temperature conditions is proposed. Simulations of one or more systems interconnected to the load with the proposed control scheme, under different environmental and load conditions, are presented to show the efficacy of the method.

RESUMEN

Este trabajo presenta el diseño y simulación de una estrategia de control, para la interconexión de sistemas de energías alternas, capaz de controlar la potencia generada por las fuentes de energías y conseguir una regulación de voltaje en la carga. La estrategia de control consiste en controlar la potencia generada por el sistema de energía alterna de forma jerárquica, usando control de modo deslizante, considerando factores que afectan los sistemas de energías y convirtiendo la potencia generada en condiciones adecuadas para poder ser utilizadas en aplicaciones residenciales y de baja potencia. El sistema hibrido de energía alterna está compuesto de celdas fotovoltaicas, celdas de combustible y baterías. Una ecuación matemática para estimar el punto de voltaje óptimo de las celdas fotovoltaicas para diferentes condiciones es propuesta. Simulaciones de uno o más sistemas interconectados con el esquema propuesto de control son presentados para demostrar la eficacia del método.

DEDICATION

This thesis is dedicated to God, who gave me the necessary strength to start and finish this journey. It's also dedicated to my parents Luis Jimenez Berroa and Mayra Brea Perez., my brothers Luis Jimenez Jr. and Michael Jimenez, and all the people who, directly and indirectly, gave me their support during this journey. This journey would not have been possible without their help, motivation and encouragement. Thanks for your support.

ACKNOWLEDGEMENTS

I would like to thank my advisor, Professor Eduardo Ortiz Rivera, for all the support, guidance, patience and motivation he has given me during this time. Thanks for letting me part of your team and help me achieve a lot of goals during my time under your supervision. I will be grateful of your support.

Thanks to my family and friends for believing in me and for giving me a lot of support. Thanks to the group Minds 2 Create for all the time we spent together; to the Electrical and Computer Engineering Department faculty and staff; and to all of the people who directly or indirectly have helped through this process. I would like to thank Dr. Miguel Velez and Dr. Andres Diaz for being part of my graduate committee.

Finally I would like to thank God. If it was not for him, none of my goals would have been achieved.

Table of Contents

Title **Page**

Table List

Tables **Page**

.

Figure List

Figures Page

1 INTRODUCTION

The use of alternative and renewable energies to satisfy the power demand has been increasing over the last years. The need of producing a cleaner energy to reduce the greenhouse gases that create environmental problems like global warming, a decrease in the cost of the materials used to develop this technologies and the increment in the cost of the fossil fuel among others, are some of the reasons that have been pushing this increment [1, 2, 3]. Of all alternative energy systems, photovoltaic cells (technology that generates an electric power from the sun using the photovoltaic effect), wind turbines (technology that generates electric power by using the kinetic energy of the wind) and fuel cells (technology that generates electric power by the chemical reaction of two reactants) are among the most popular.

The power generated by photovoltaic or solar cells, wind turbines and fuel cells, beside depending on factors as solar irradiation and temperature for solar cells, wind speed for wind turbine and fuel flow for fuel cells, depends greatly in the load values. These factors affect the system's output power, creating unregulated voltages and power deficiency [4]. Since we cannot control most of these factors, alternative energy systems are usually composed of two or more systems in order for one system to compensate the other.

The use of renewable energy system has some problems. One is that the interconnection of one or more of these systems to a load, without a proper control strategy, can lead to power quality and stability problems [5,6,7]. Because of that, a control strategy must be developed to control and supervise the power distribution of the hybrid system in order to provide the demanded power to the load while maintaining stability, regulation and quality of the power in the system.

The second problem is that of the three mentioned alternative energy technologies, the wind and photovoltaic are intermittent power sources. Their power generation depends on factors that are variable and cannot be controlled causing fluctuations in the maximum power they could provide. This creates situations where enough power cannot be generated to satisfy the demand. For this reason we are going to restrict our alternative energy hybrid system to be composed of one intermittent alternative energy technology, photovoltaic, a controllable non intermittent alternative energy technology, fuel cells, and an energy storage system, batteries.

This work presents the design, simulation and implementation of a control strategy, based on sliding mode control, for the interconnection of one or more alternative energy system, composed of photovoltaic cells, fuel cells and batteries for energy storage, for residential and low power applications taking into consideration different factors that affects each technology while achieving high power efficiencies and voltage regulation. Simulations of different configuration of systems composed of one or more energy systems

interconnected with the controller, under different conditions and for different arrangement, are presented to show the efficacy of the method.

1.1 Motivation

A control strategy for the interconnection of one or more technologies plays a vital part in the implementation of hybrid systems. Stand-alone applications require a control system capable of generating the demanded power at all times to satisfy the load demand. These control strategies need to operate well under dynamic operating conditions, have a good response to load changes and improve the power management.

Different control strategies has been designed and implemented and successful results have been obtained. Examples of control strategies that has been used in the past are: fuzzy logic[8,9], sliding mode control[10,11], neural network[12,13,14], pid control[15], hierarchical control[16], predictive control[16,17], genetic algorithms [18], etc. Even though these control strategies showed good efficiency, stability and were able to control the power generation, some of them contained advanced mathematics, their adaptability to changes in the operating points are debatable, had too many assumptions that may not be valid or don't take into consideration important factors that would affect the system.

In this document, we present a dynamic control strategy capable of controlling the power generation of one or more alternative energy system, capable of adapting to environmental variations and simple enough that can be adapted to almost any power system. A series of simulations of the control strategy are presented to show the adaptability that this control strategy exhibit.

1.2 Objectives of the Thesis

The main objective for this research is to design and implement a control strategy, using a sliding mode-based control law, for a hybrid alternative power system composed of photovoltaic cells, fuel cells and batteries. The controller must be capable of managing the energy generation, energy quality and distribution of the energy produced by the system and to convert it to a suitable condition so it can be used for residential and low power applications. The controller must be able to operate well under varying loads conditions and under different operating and environmental conditions. The system must be simulated and the results must show the expected behavior and improvement described in the theory.

1.3 Literature Review

1.3.1 Photovoltaic Cell

Through the years, different circuit models have been used to study and simulate the behavior of a photovoltaic cell. The simplest method used to simulate photovoltaic cells was to implement it as a DC voltage source [5]. The problem with this method is that a photovoltaic cell does not behave completely as a dc voltage source. Assumed assumptions, like constant environmental conditions, constant output voltage and that the cell is working at its maximum power make this method of modeling inefficient.

Anotherr approach to simulate a photovoltaic cell, with an acceptable precision, is using the one diode model [19]. Figure 1.1 shows the equivalent one-diode model. It's composed of a DC current source, I_L, in parallel with a diode, and two resistors, Rs and Rsh, to simulate internal losses.

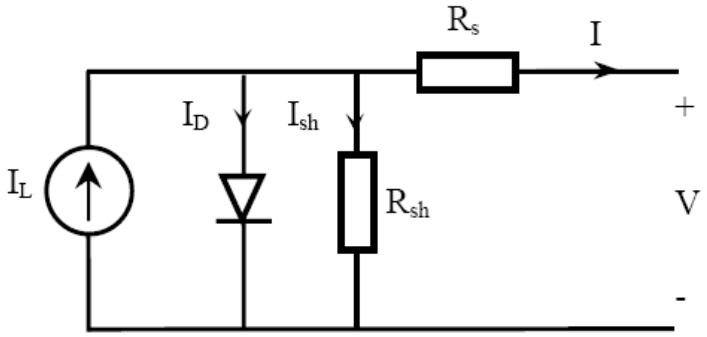

Fig 1.1: One Diode Solar Cell model

The problems with this model are that it requires information that is not easily found in a data sheet, some of the variables are very difficult to be determined and there is no explicit way to determine the effect of variations in the solar irradiance.

Other methods, like the two diode model [20] and Neural Networks [21] among others [22, 23], are also used to simulate the photovoltaic cells behavior. As with the one diode model, these methods require parameters that are not available in the manufacturer's datasheet, require curve fitting, have poor performance during variations in the solar irradiation, or need too much computational power.

For this work, we are going to use a model presented in [24]. In [24], a more practical PV cell model is presented. The advantage of this model over the others relies in that all the parameters can be obtained using the manufacturer sheet, has excellent performance under different irradiation levels and does not need too much computational power. More about this model, its equations, and its structure is presented in Chapter 2.

1.3.2 Fuel Cell Model

In [25], a dynamic electrochemical-based proton exchange membrane fuel cell model, suitable for an electrical engineering automation approach, for the representation, simulation and evaluation of the performance of the power generation of the system is presented. In the paper, the model is used to predict the output voltage, efficiency and power of the fuel cells

as a function of the load current and parameters of the cells. An electric equivalent circuit is presented. The results validate the accuracy of the model.

In [26], a dynamic electrochemical model for representation, simulation, and evaluation of the performance of low power generation systems proton exchange membrane fuel cell stacks is presented. The model is used to predict the output voltage, efficiency, and power of fuel cells as a function of the load's current and parameters of the cells. The dynamic response of the models discussed was tested by varying the loads. Comparisons of this model against other fuel cell models are shown in the results.

In [27], a dynamic electromechanical fuel cell model is presented. This model takes into considerations the pressures of oxygen and hydrogen. Also it takes into consideration the flow rate of air and hydrogen into the cell. The fuel cell model presented very good accuracy compared to different types of fuel cells like PEM fuel cells. Another advantage of this model, besides that it's able to reproduce the effects of pressure and flow of reactants, is that it only uses parameters that either can be obtained directly from the manufacturer's data sheet or can be estimated from it.

In [28], a simple fuel cell model is presented capable of reproducing the fuel cell's V-I curve for a fuel cell operating at given conditions. The advantages of this model are that all the information needed can be obtained directly from the manufacturer's voltage-current curve and power-voltage curve.

For this work, the model presented at [28] will be the one used for simulations of FC. The structure and equations of this model is going to be explained further at Chapter 3.

1.3.3 Control Strategies

Maximum power point trackers are devices capable of searching for the point of maximum power and, using DC-DC converters, extracting the maximum power available by the cell. Several methods have been designed and implemented to search for this operation point. A common method used is the Perturb and Observe (P&O) algorithm which are discussed in [29, 30]. Classical P&O algorithms tend to measure the converter’s output power in order to modify the input voltage by modifying the converter’s duty cycle. Another common method is the hill climbing method [31, 32].This method is based on a trial and error algorithm where the voltage is increased until you reach such a voltage level where the PV exhibits maximum power. Other MPPT algorithms sample the open circuit voltage and operate the PV module at a fixed percent of this voltage. Incremental conductance algorithms are another method to track the MPP and are discussed in [33, 34, 35]. Other methods that have been used to obtain the maximum power are variable structure maximum power point

trackers as shown in [36, 37, 38], neural networks as shown in [39] and linear reoriented method discussed in [40]. Some of the disadvantages with these methods are that some of them require doing a lot of iterations to calculate the optimal steady state duty ratio, uses approximate values that does not guarantee near maximum power output can be very complex methods, can be slow and the system can become instable if the MPP moves abruptly.

In [36, 37,38], maximum power point trackers, using sliding mode control and power electronics devices, are implemented to obtain the maximum power possible from the PV cells and to interconnect the PV cells to the grid. In these papers, sliding mode control shows its capability in tracking the maximum power point. Even though these papers show effectiveness, they do not take into consideration changes in environmental factors such as solar irradiance and the temperature at the surface of the cell.

In [39] a neural network controller maximum power point tracker is applied to extract the maximum power of a PV system while interconnecting the system to the grid. It uses a voltage source inverter with optimized sinusoidal PWM strategy to eliminate harmonics up to the 17^{th}.

In [41], a sliding mode-based inverter for grid connection is described. The controller is capable of operating the PV module at its maximum power while taking into consideration the quality of the output signal. In this paper, some chattering, due to switching, is visible in the output signal which can cause power quality problems in the grid.

In [42], a power conditioner control system for a fuel cell system is presented. There, the output waveform of the fuel cell is inverted and corrected to a sinusoidal waveform to connect the system to the grid.

In [43], an equivalent circuit model for a PEMFC, which is simple and at the same time includes all the important characteristics of a fuel cell stack, is presented. The model uses the nonlinearity of a junction diode and the current control feature of bipolar junction transistors. The model is justified through experiments performed on a commercial PEMFC stack for both static and dynamic responses.

In [44], the hybridization of solar energy, as a renewable energy source, natural gas fuel cells, as a fossil fuel, and the improvement of the power plant efficiency, by using power electronics technology and electric energy storages, are discusses**.** Other aspects of this hybrid power plant are the using of renewable energy sources as a reliable power supply with stand-alone and grid-connected systems which can increase network power quality**.**

1.4 Summary of Chapters

Background theory and an introduction of this work were presented in Chapter 1. Chapter 2 deals with the characteristics and modeling of the photovoltaic cells. Chapter 3 presents the characteristics and modeling of the fuel cells. Chapter 4 present background information and the theory behind sliding mode control. Information regarding the basic topologies of DC/DC converters is shown in chapter 5.Chapter 6 details the steps followed to achieve the control strategy and all the information regarding the control strategy. Chapter 7 contains the simulations results of the implementation of our proposed system. Chapter 8 contains the conclusions of this work and future works. References and appendix are at the end of this work.

2 Photovoltaic Power System

2.1 Introduction

Photovoltaic power systems are power systems that use solar cells to generate electrical power. Photovoltaic cells are devices that are capable of generating electric energy from a light source by the photovoltaic effect. An electric current is generated when photons in light hit the photovoltaic cell and get absorbed by the semiconducting material. After absorption, electrons are knocked loose from the atom and travels through the material, producing an electric current.

Photovoltaic cells, or solar cells, are typically arranged in two forms:

- Modules: Two or more interconnected cells encapsulated in a weatherproof material. The cells are connected in series to increase the voltage output or in parallel to increase its current output.
- Arrays: Two or more interconnected modules. The modules are connected in series to increase the voltage output or in parallel to increase its current output.

Since it can virtually produce power anywhere where there is direct sunlight, photovoltaic cells are very attractive technology to be used as an alternative energy system.

2.2 History

The history of the photovoltaic cells begin with the discovery of the photovoltaic effect by the French physicist Alexander-Edmond Becquerel in the year 1839 while experimenting with an electrode in a conductive solution exposed to light[45,46]. He noted that when certain cells, built using materials that later were known to be photoconductive, were exposed to light the generation of electricity increased. It was not until 1883 that Charles Fritts, by coating selenium with a thin layer of gold to form the junctions, built the first solar cell. His first device was not very efficient, around 1% [47].

After the first solar cell was built, a lot of researches were being conducted to increase the capacity of the cells. It was not until 1954 when Bell Laboratories, while experimenting with semiconductors, found out that silicon, doped with certain impurities, was very sensitive to sunlight. Daryl Chapin, with some colleagues from Bell Labs, built the first modern practical solar cell, the silicon solar cell with an efficiency of 6% [48

After the first solar cell was presented to the world, it rapidly found applications mainly in space programs due to its ability of producing electric power directly from sunlight. The first satellite to use solar cells, the Vanguard 1, was launched by US four years after the first solar cell was built, in March 1958[47]. This event woke up a great interest in the use of solar cells as power supply in communications satellites.

Even though solar cells were successful for space applications, it was not being successful for terrestrial applications mainly due to its high production cost and low power output. During the next years a lot of researches were conducted in increasing the efficiency of solar cells. Different materials were being used to build the solar cell. By August 2009, the most efficient photovoltaic cell was reported to have an efficiency of 41.6% [47].

Even though solar cells' efficiencies were increasing, its cost-per-watts was still too high when compared to fossil fuels cost-per-watts making it only viable to places that were not connected to the utility lines and for low power appliances as calculators and watches. Lately the production costs of solar cells are declining rapidly making it economically more viable to be used not only in stand-alone applications but as power systems [49]. Figure 2.1 shows the world production of PV power, in megawatts peak from 1980 to 2007[50].

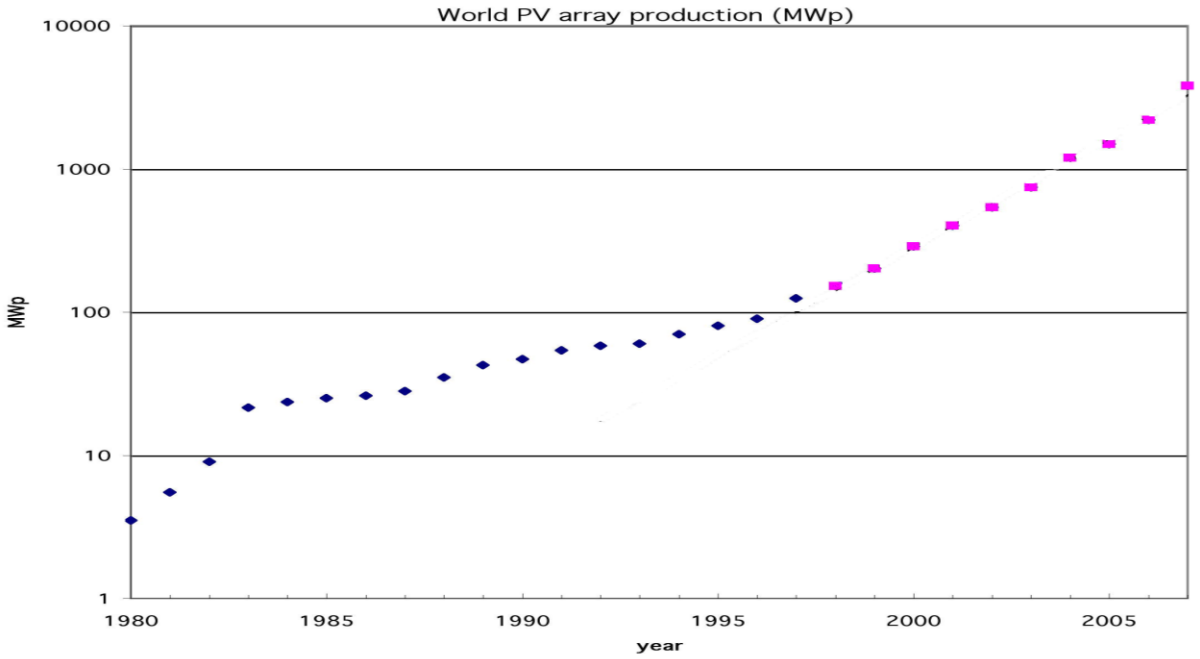

Fig 2.1: World production of photovoltaic arrays from 1980 to 2007 [50]

2.3 Photovoltaic as a power systems

2.3.1 Power Availability

Around 174 petawatts of solar radiation is received at the Earth's upper atmosphere. 70% of that energy, around 121.4PW, reaches Earth's surface and it is used as an energy source for a lot of natural processes, such as the water cycle and photosynthesis, or is simply absorbed and dissipated as heat. In 2004, the solar energy was so vast that it could have supplied 8000 times the energy consumption of that year. Table 2.1 shows how vast are the solar energy that it would be sufficient to supply all our energy needs.

Yearly Solar Fluxes& Human energy Consumption	
Solar	3,850,000 EJ[50]
Wind	2,250 EJ[51]
Biomass	3,000 EJ[52]
Primary energy use (2005)	487 EJ[53]
Electricity (2005)	56.7 EJ[54]

Table 2.1: Comparison of Renewable Energy Availability and World Energy Consumption

Solar energy is not evenly distributed across the Earth, having places in Earth's surface with more energy availability than other places. Most of the solar energy, in the form of solar irradiance, is concentrated between the tropic lines. Figure 2.2 shows the average solar irradiation, in W/m^2, received at Earth's surface sampled in a period of three years. The black points in the figure represent the amount of area that has to be covered with 8% efficient solar panels to replace the primary energy supply as the electricity source [55].

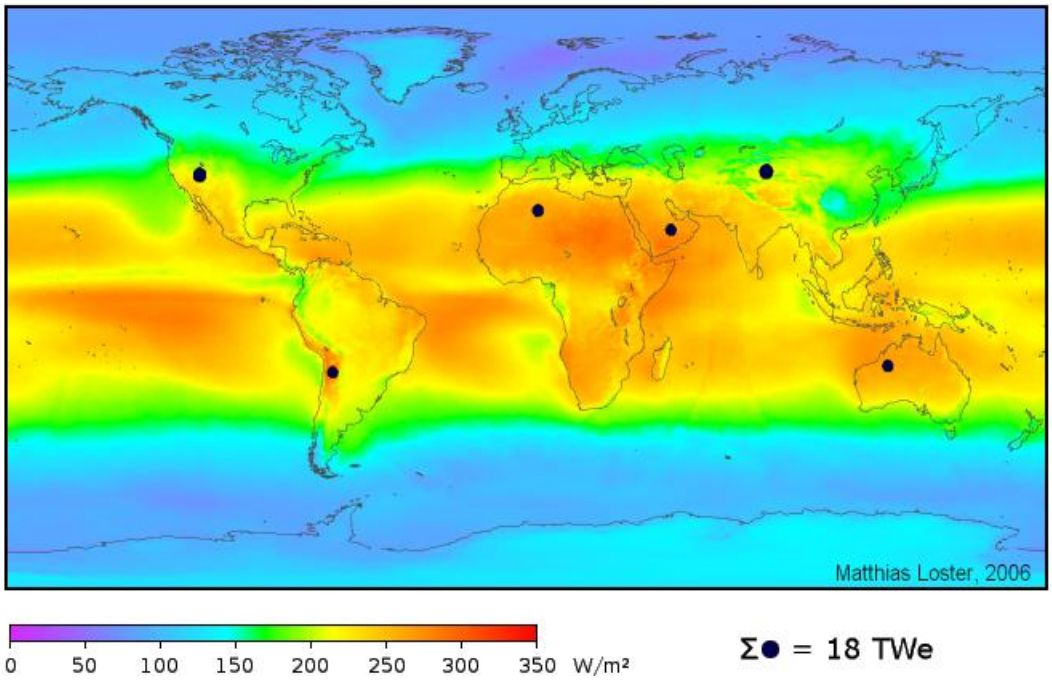

Fig 2.2: Average Solar irradiance from 1991 to 1993

2.3.2 Photovoltaic Cells Electric Characteristics

Photovoltaic cells produce an electric current, by absorbing solar irradiation and converting it to electricity as described by the photovoltaic effect. The relation between the solar cell's current and voltage is a nonlinear relation. Figure 2.3 shows the nonlinear relation between the current and voltage for a typical solar cell at standard test conditions (1000W/m^2 of solar irradiation and 25^{o}C of temperature). The area of the shaded rectangle represents the maximum power of the PV. It can be seen that the solar cell has a maximum output current, called short-circuit current (Isc), and a maximum output voltage, called open circuit voltage (Voc). Also is seen that the higher the voltage the lower the current and vice versa.

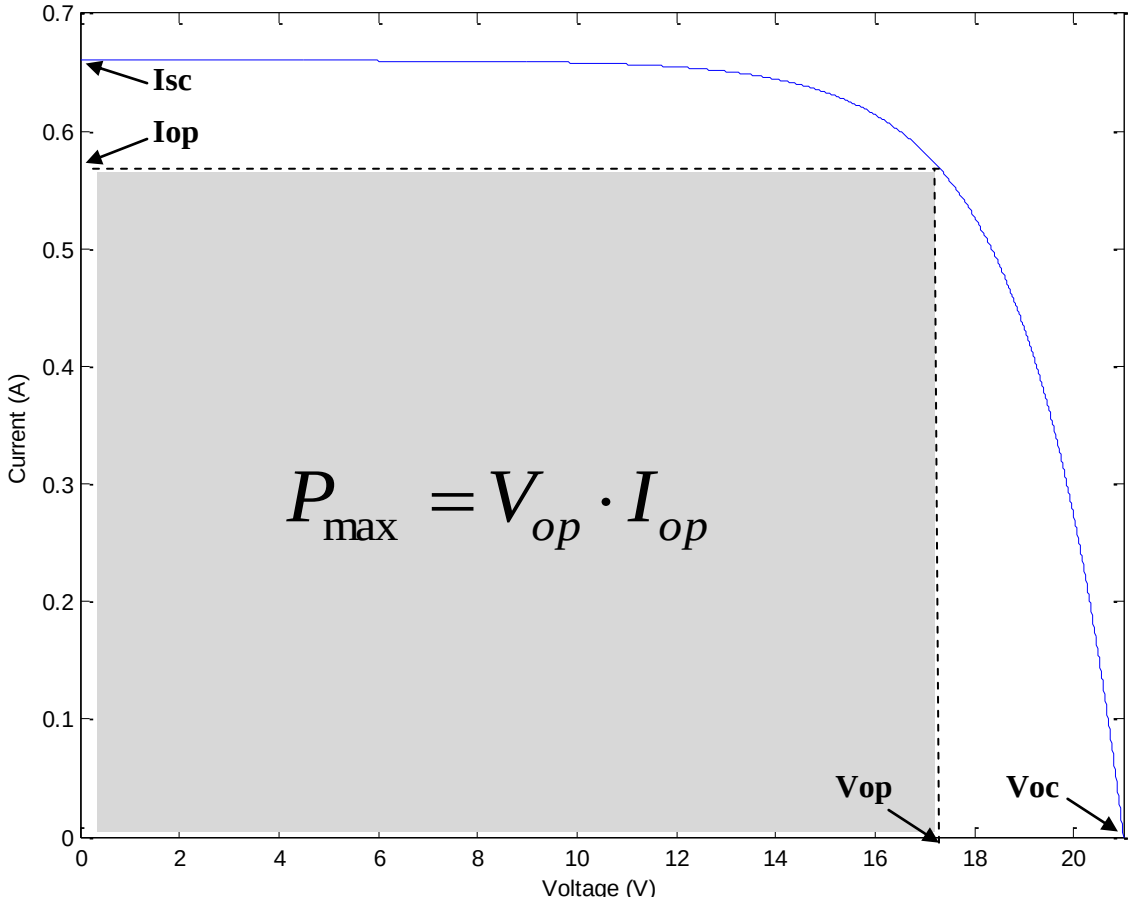

Fig 2.3: Photovoltaic Cell Current vs. Voltage Relation at STC

Due to the non linear relation between its voltage and current, photovoltaic cells has only one operation point where it exhibits a maximum power. Figure 2.4 shows the relation between the photovoltaic cell output power versus its output voltage. The maximum power operation point corresponds to a unique voltage value, Vop, a unique current value, Iop and, by Ohm's law, a unique resistive load, Rop. The optimal resistance value means that the photovoltaic module will only produce its maximum power when it is connected directly to a resistive load of value Rop. Any other resistive load value will result in a sub-optimal power operation point.

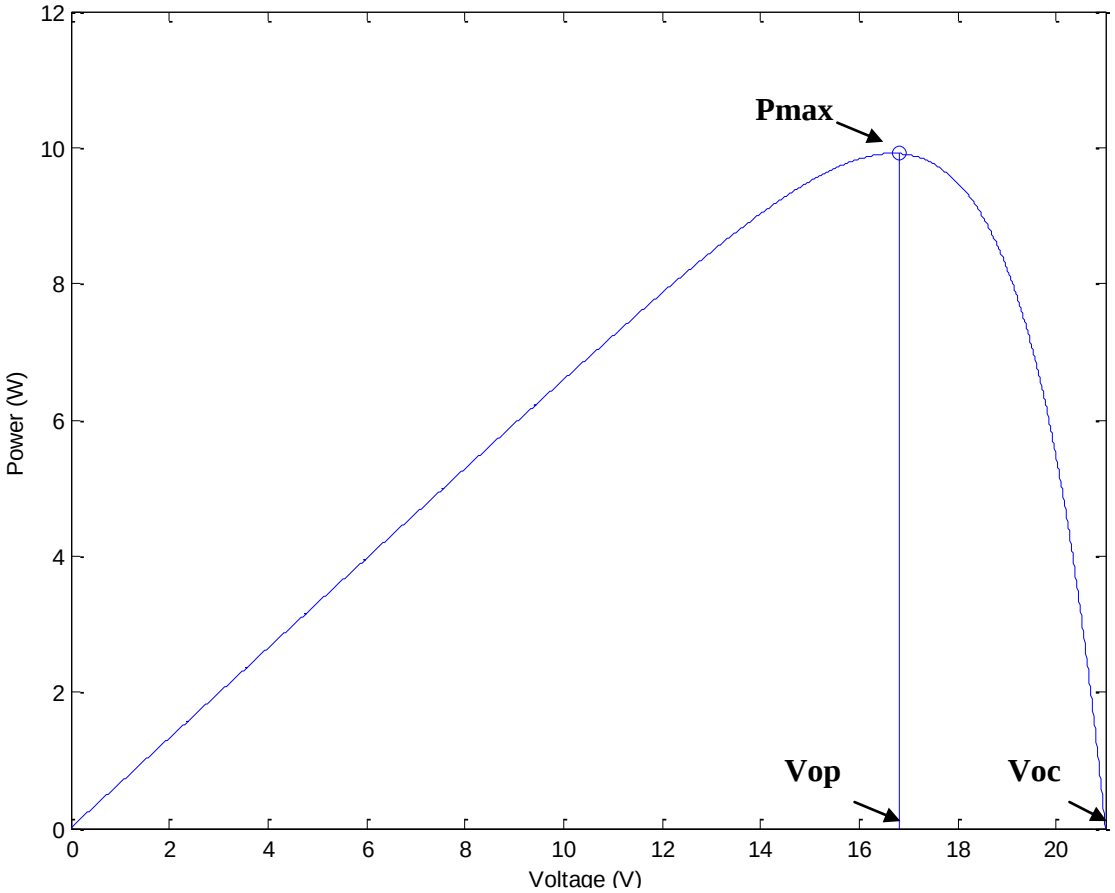

Fig 2.4: Photovoltaic Cell Power vs. Voltage relation at STC

Photovoltaic cells are considered intermittent energy sources. It does not provide a constant power. The power availability of photovoltaic cells depends greatly in the solar irradiation, which is a dynamic factor. Figure 2.5 shows the changes in the current-voltage curve under different irradiation levels at 25^{o}C. It is noted that changes in the irradiation affects significantly the short circuit currents.

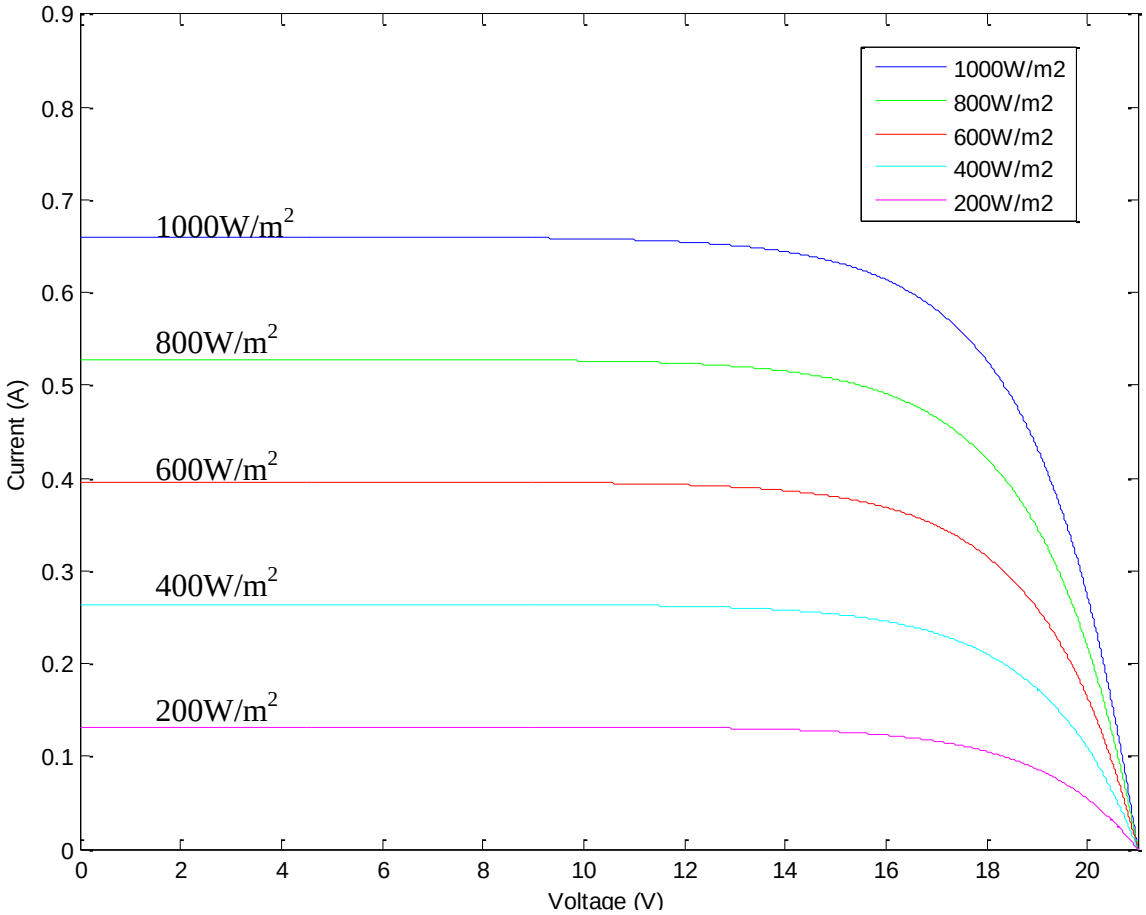

Fig 2.5: Current-Voltage curve behavior for different irradiance level at 25^{o}C

Figure 2.6 shows the changes in the power-voltage curve under different irradiation levels at 25^{o}C. It's noted that the power output is drastically reduced under lower irradiation levels. Also should be noted that the voltage where maximum power is produced, Vop, changes too.

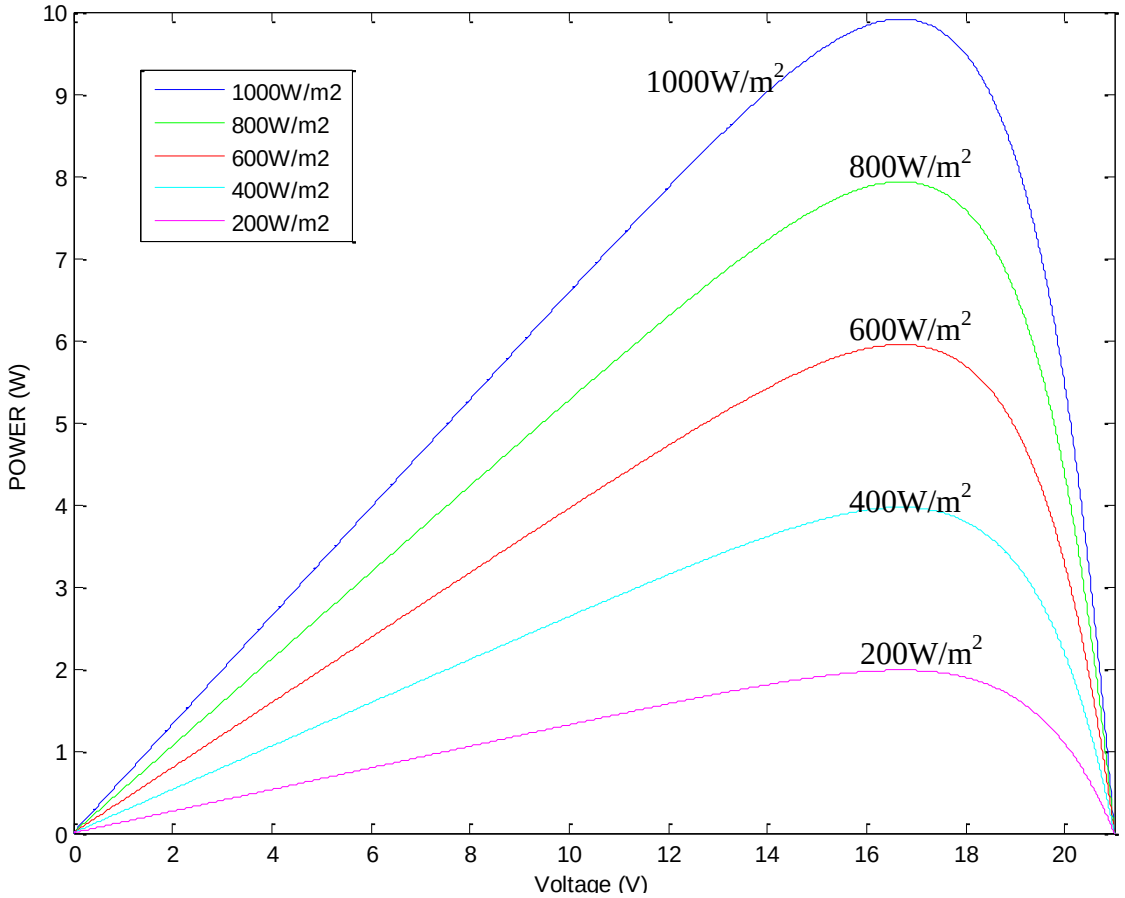

Fig 2.6: Power versus voltage curve for different irradiance level at 25^{o}C

The cell's surface temperature also affects electric characteristics of the cell such as its maximum power, its open circuit voltage, its short circuit current and its maximum power operation point voltage and current values.

Figure 2.7 shows the behavior of the current-voltage curve at different temperature values under a constant irradiance level of 1000w/m^2. It is noted that the open circuit voltage is significantly reduced as the temperature increase. Also can be noted that the short-circuit current it's not greatly affected by the changes in temperature.

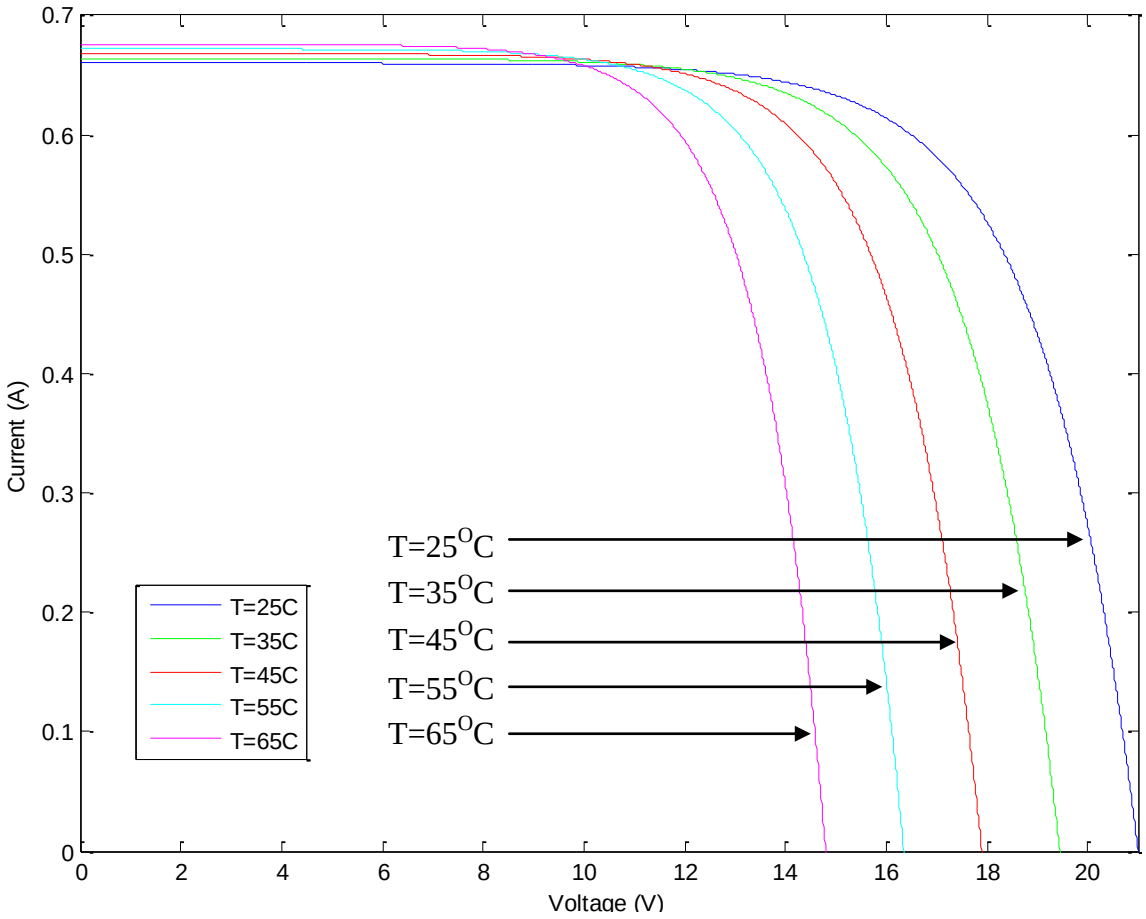

Fig 2.7: Current-Voltage curve behavior for different temperatures at 1000W/m^2

Figure 2.8 shows the behavior of the power-voltage curve for different temperatures under a constant irradiance level of 1000W/m^2. It can be seen that the power is significantly reduced by temperatures changes. Also, it's noted that the open circuit value, Voc, and optimal voltage value, Vop, changes too.

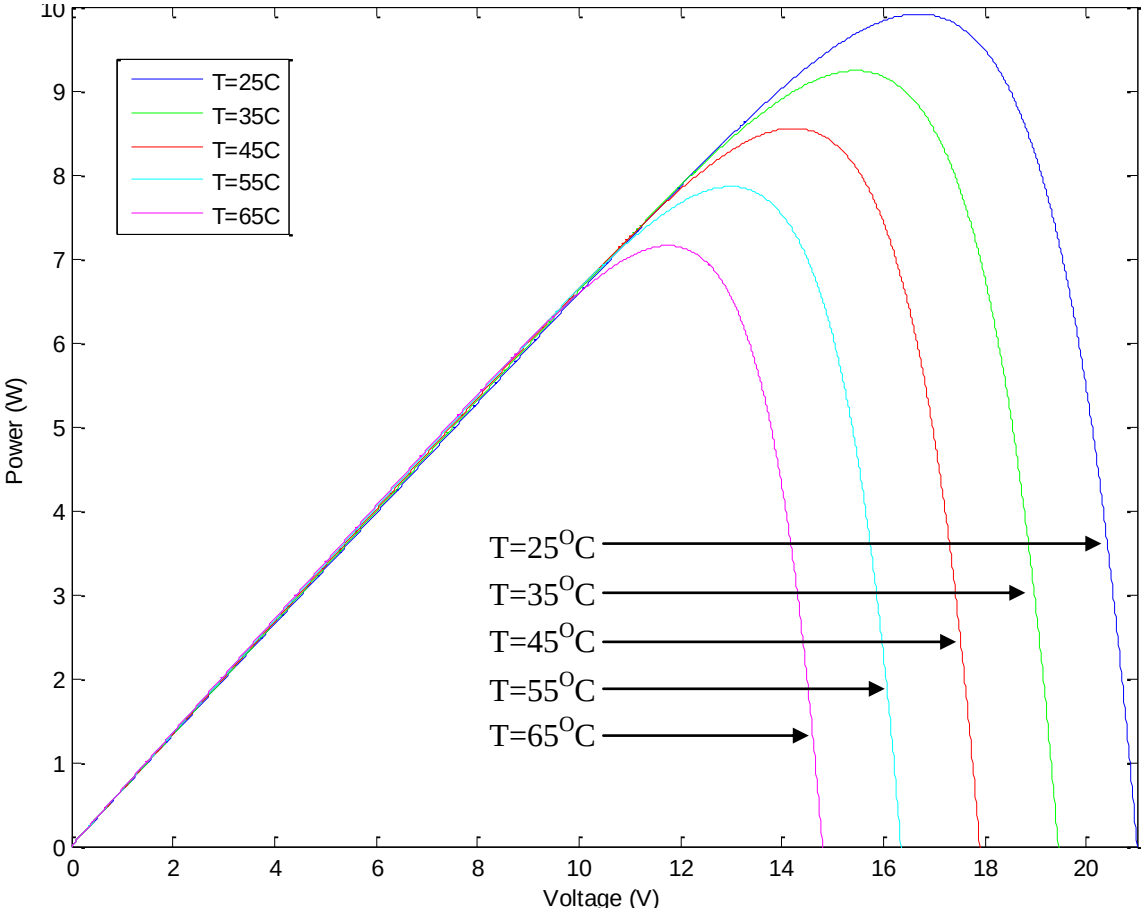

Fig 2.8: Power versus voltage curve for different temperatures

2.4 Photovoltaic Electrical Circuit Model

In this thesis, we are going to use the model presented at [24] where a photovoltaic cell model based on the electrical characteristics provided by the manufacturer is presented. The model predicts power production by the photovoltaic cell for different temperatures and irradiation levels. The following equations that describe the behavior of a photovoltaic cell are given:

$$I(V) = \frac{Ix}{1-\exp\left(\frac{-1}{b}\right)}\left[1-\exp\left(\frac{V}{b\cdot Vx}-\frac{1}{b}\right)\right] \tag{1}$$

$$P(V) = V\cdot I = \frac{V\cdot Ix}{1-\exp\left(\frac{-1}{b}\right)}\left[1-\exp\left(\frac{V}{b\cdot Vx}-\frac{1}{b}\right)\right] \tag{2}$$

$$\begin{aligned} Vx = {} & s\cdot\frac{E_i}{E_{in}}\cdot TCV\cdot(T-T_N)+s\cdot V\max \\ & -s\cdot\left(V_{\max}-V_{\min}\right)\cdot\exp\left(\frac{E_i}{E_{in}}\cdot\ln\left(\frac{V_{\max}-V_{oc}}{V_{\max}-V_{\min}}\right)\right) \end{aligned} \tag{3}$$

$$Ix = p\cdot\frac{E_i}{E_{in}}\cdot\left[I_{SC}+TCi\cdot(T-T_N)\right] \tag{4}$$

where

- P(V)= PV cell output power (V*I)
- I(V)= PV cell output current
- V = PV output voltage
- Isc = Short-circuit current at 25±C and 1000W/m2
- Voc = Open-circuit voltage at 25±C and 1000W/m2
- Vmax= Open-circuit voltage at 25±C and more than 1,200W/m2. Approx. 1.03*Voc
- Vmin= Open-circuit voltage at 25±C and less than 200W/m2. Approx. 0.85*Voc
- T= Solar panel temperature in ±C
- Ei= Effective solar irradiation in W/m2
- Tn= Standard test conditions nominal temperatures in C
- Ein= Standard test conditions nominal effective solar irradiation in W/m2
- Tci= Temperature coefficient of Isc in A/C
- Tcv= Temperature coefficient of Voc in V/C
- Ix= Short circuit current for any Ei and T.
- Vx= Open circuit voltage for any Ei and T
- s= Number of cells/modules connected in series
- p= Number of cells/modules connected in parallel
- b= Characteristic constant based in the I-V curve

The characteristic constant b is determined by iterating the equation described in (5).

$$while \left| b_{N+1} - b_N \right| \geq \varepsilon$$

$$b_{N+1} = \frac{V_{OP} - V_{OC}}{V_{OC} \cdot \ln\left(1 - \frac{I_{OP}}{I_{SC}} \cdot \left(1 - \exp\left(\frac{-1}{b_N}\right)\right)\right)} \tag{5}$$

Figures 2.9 and 2.10 shows the modeling of the voltage-current and power-voltage curve of a commercial model, Solarex SA-05, obtained from the proposed model and compared it to experimental measured values at STC [24]. These equations proved to have good accuracy when modeling a PV module.

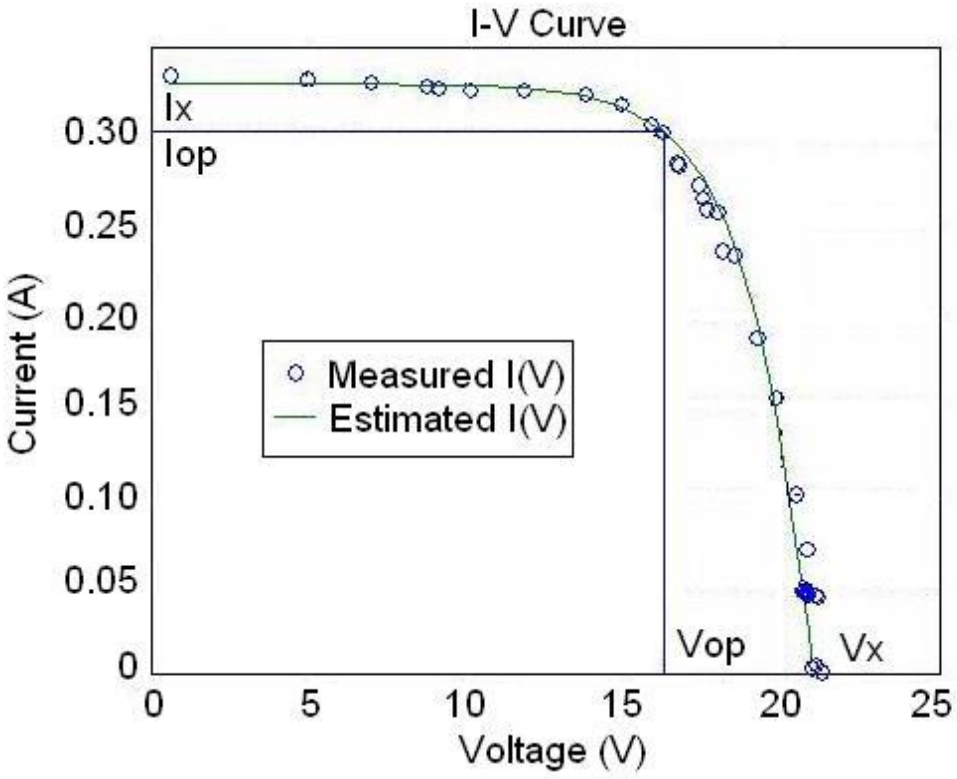

Fig 2.9: Experimental measures and estimation for the SA-05 I-V Curve [24]

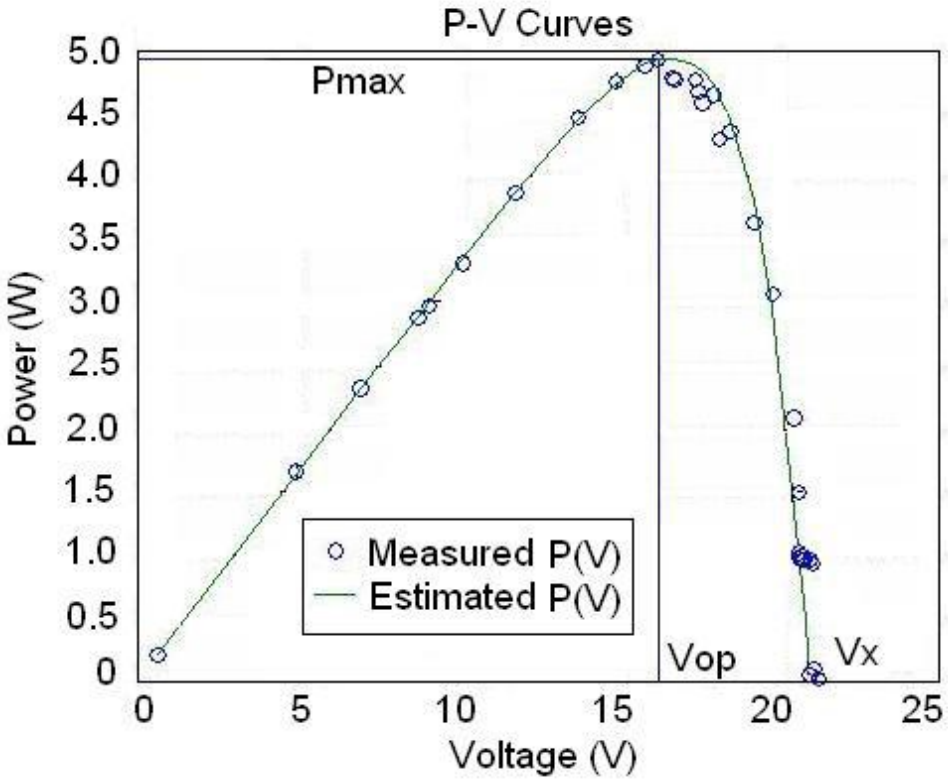

Fig 2.10: Experimental measures and estimation for the SA-05 P-V Curve [24]

2.5 Photovoltaic Cell's Maximum Power Point

Photovoltaic cells have only one operation point where it generates its maximum power, as observed in figure 2.11. This point is located at the knee of the power-voltage curve where the rate of change of power with respect to the voltage, dP/dV, is equal to zero. That point corresponds to a unique voltage, Vop, and a unique current value, Iop.

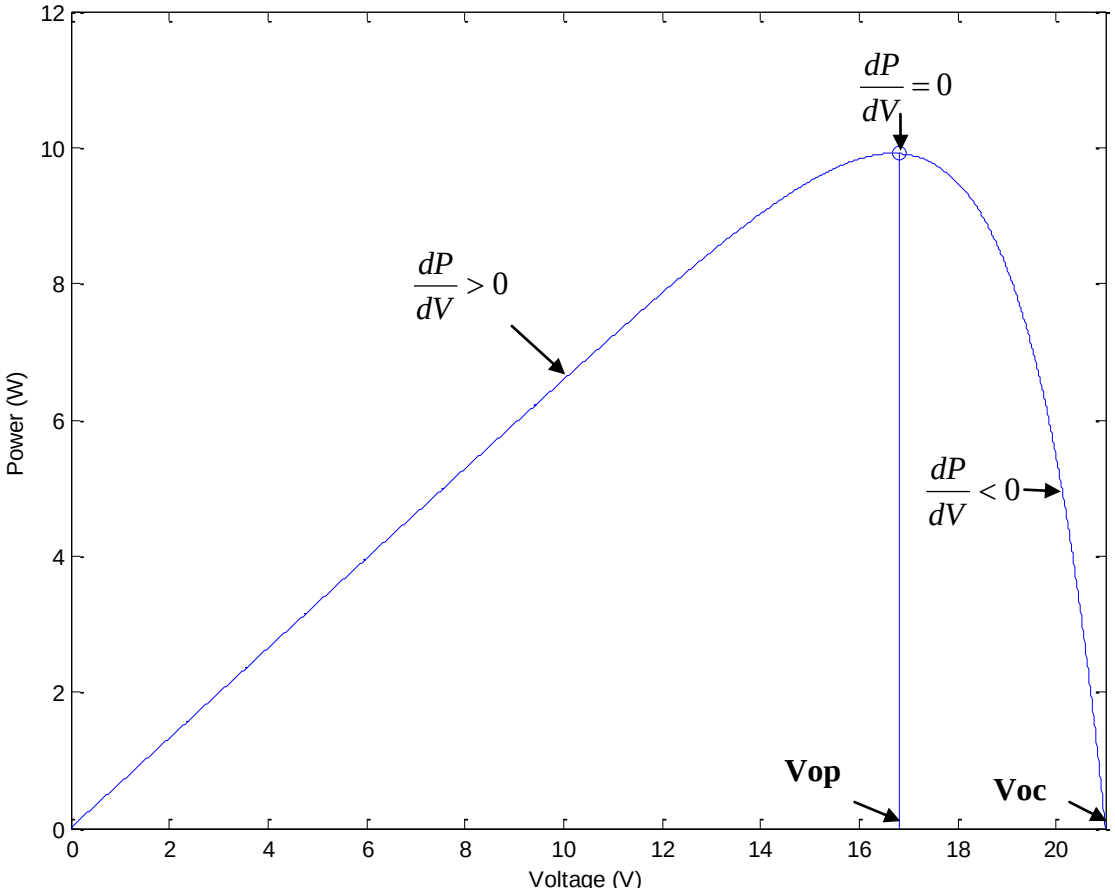

Figure 2.11: PV power versus voltage curve

The optimal voltage, Vop, can be found by solving the partial derivate of power with respect to voltage as shown in (6).

$$\frac{dP}{dV} = \frac{Ix - Ix \cdot \exp\left(\frac{V}{b \cdot Vx} - \frac{1}{b}\right)}{1 - \exp\left(\frac{-1}{b}\right)} - V \cdot \frac{-Ix \cdot \exp\left(\frac{V}{b \cdot Vx} - \frac{1}{b}\right)}{b \cdot Vx - b \cdot Vx \cdot \exp\left(\frac{-1}{b}\right)} = 0 \qquad (6)$$

A numerical solution to (6) is shown at (7).

$$Vop = real\left(b \cdot Vx\left(lambertw\left(-0.36787944 e^{\frac{1}{b}} \right) + 1 \right) \right) \tag{7}$$

where *lambertw* is defined to be the solution W(x) of the non linear equation $W(x)\exp(W(x)) = x$ and *real( )* is a function that extracts only the real part of a number. By substitution,

$$Iop = I(Vop) = \frac{Ix}{1 - \exp\left(\frac{-1}{b}\right)}\left[1 - \exp\left(\frac{Vop}{b \cdot Vx} - \frac{1}{b}\right)\right] \tag{8}$$

3 Fuel Cells Power System

In this section we are going to discuss the history of fuel cells, the basic concept of fuel cells, the advantages of the fuel cells as power systems and an electrical circuit model based on data obtained directly from the manufacturer's datasheet.

3.1 Introduction

Fuel cells are electrochemical devices that produce an electric current from the chemical reaction of two reactants, a fuel and an oxidant, in the presence of an electrolyte. Typical reactants used as fuel are hydrogen, hydrocarbons and alcohols. Typical oxidants are oxygen, chlorine and chlorine dioxide [56]. The electricity is produced when both reactants flow into the cell and a reaction occurs where an electrolyte remains within it. The electricity is produced by a process named catalysis. When the fuel reactant enters the cell, the protons and electrons are separated. Then the electrons are forced to travel through a circuit, producing an electric current. Then another catalytic process puts the electrons back in, recombine the protons with the electrons to form a waste product.

Fuel cells are very much like an electrochemical cell battery except that, in batteries, electrical energy is stored chemically inside the battery and, in fuel cells, electrical energy is produced chemically from external reactants sources [57].

Fuel cells are appealing because they offer high efficiency, low emissions of regulated pollutants [58] and, since fuel cells can produce electricity as long as fuel is supplied, it is a constant power supply which gives it an advantage when compared to other alternative energy technologies.

3.2 History

The principles of the fuel cell were discover and published by a German scientist in 1838 named Christian Friedrich [59]. In February 1839, based on Friedrich's work, scientist William Grove created the first fuel cell [60]. It was a phosphoric-acid fuel cell and was called “gas battery”. It was not until 1889 that Ludwig Mond called his experiment, a gas-battery using coal-derived “Mond-gas”, by the name of “fuel cell” that this name was used to name this technology. After Mond's fuel cell, a lot of research begun to be done to understand the principle and theory behind the chemical reactions of fuel cells. Scientist Friedrich Ostwald provided much of the understanding of the operation of a fuel cell and laid the groundwork for later researchers [61, 62].

The first commercial fuel cell was developed for the General Electric Company by Niedrach in the year 1958, using a modified version of the fuel cell also developed for the General Electric Company in 1955 by Thomas Grub that uses a sulphonated polystyrene ion-exchange membrane as the electrolyte. Niedrach developed a method to deposit platinum

onto the membrane which served as a catalyst for the chemical reactions of hydrogen and oxygen. This fuel cell was developed with NASA to be used to the Project Gemini [63].

Even though it was the first commercial fuel cell, it was not a practical fuel cell. It was not until a year later after its development, 1959, that the British engineer Francis Bacon, using a cell with nickel gauze electrodes and hydrogen and air as fuels, developed the first practical fuel cell. It was a 5kw stationary fuel cell system capable of powering a welding machine. This fuel cell was later licensed by Pratt and Whitney to be used in the US space program [64].

3.3 Fuel cell as a Power System

Due to its operation efficiency, good load response and wide size range, fuel cells has been used for a widely range of applications include utility applications [65], power generator for automotive field [66], and low power applications.

The advantage of its ability to produce power as long as fuel is supplied to the fuel cell makes it very useful as a power system since it is a constant, non intermittent power source. Its power will be available any time and ready to be used when needed. As a power system, it also offers excellent load performance, low emissions compared to fossil fuel and a wide range of sizes and high efficiencies [59].

3.3.1 Power Availability

Hydrogen fuel cell power comes from the chemical reaction of two reactants, hydrogen and oxygen. Hydrogen, in the universe, is the most abundant chemical element. It constitute almost 75% of the universe's elemental mass [68].Even though it's the most abundant chemical element in the universe, hydrogen, in its elemental gas form, is very rare in the Earth's atmosphere, 1 ppm by volume. Hydrogen is very abundant in Earth chemically combined. Chemically combined, hydrogen is the third most abundant element on Earth [69]. It is mostly found in chemical compounds such as water and hydrocarbons (methane, alcohols) [70]. Typically, hydrogen is extracted from methane, natural hydrocarbon gases or from water. Oxygen, in the universe, is the third most abundant chemical element in the universe [71]. Unlike hydrogen, oxygen is very abundant on Earth being the most abundant chemical in Earth. It's the second most common component of the earth's atmosphere. Oxygen may be obtained in is natural form from the Earth's atmosphere, being composed of 23.1% of its mass [72]. Also it may be extracted from compounds such as the air and water. Since fuel cells power availability will depend on the availability of those elements and since these two reactants are so abundant in Earth, technically fuel cell power availability is infinite.

3.3.2 Fuel Cell Electrical Characteristic

Fuel cell, like photovoltaic cells, has a non-linear relation between the voltage and the current. Figure 3.1 shows the typical voltage-current curve of the fuel cells at nominal conditions. It can be seen the nonlinear relation between voltage and current and that the current increases as the voltage decrease. Also can be noted that fuel cells have a point where voltage is maximum and current is minimum called open circuit voltage(Voc) and a point where the current is maximum and the voltage is minimum called short circuit current(Isc).

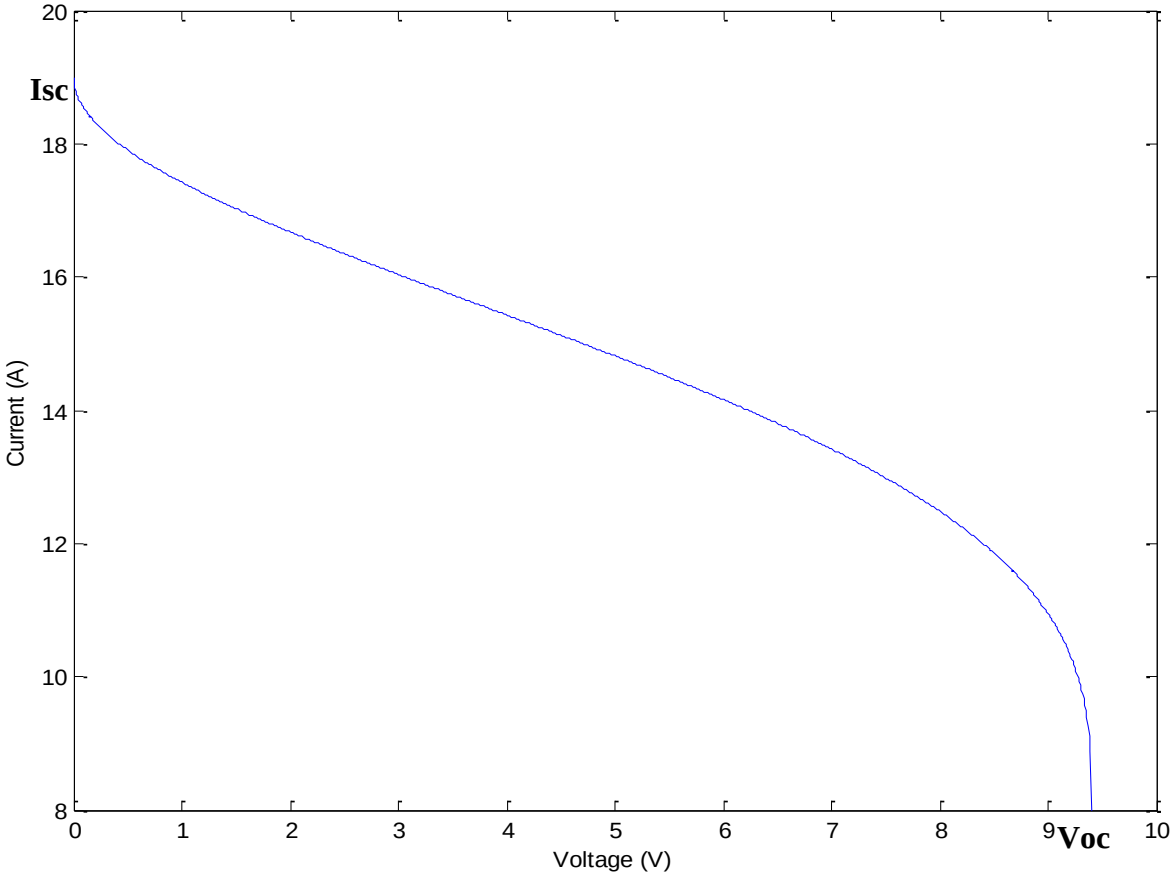

Fig 3.1: Fuel Cell's Voltage vs. Current

Since the voltage decrease as the current increase, there is a point where the product of voltage and current is a maximum. The point where the product of voltage and current is a maximum is called the maximum power point. The values of the voltage and current that their product gives a maximum value of power are called the optimal voltage, Vop, and current, Iop. Figure 3.2 shows the relation between power and voltage.

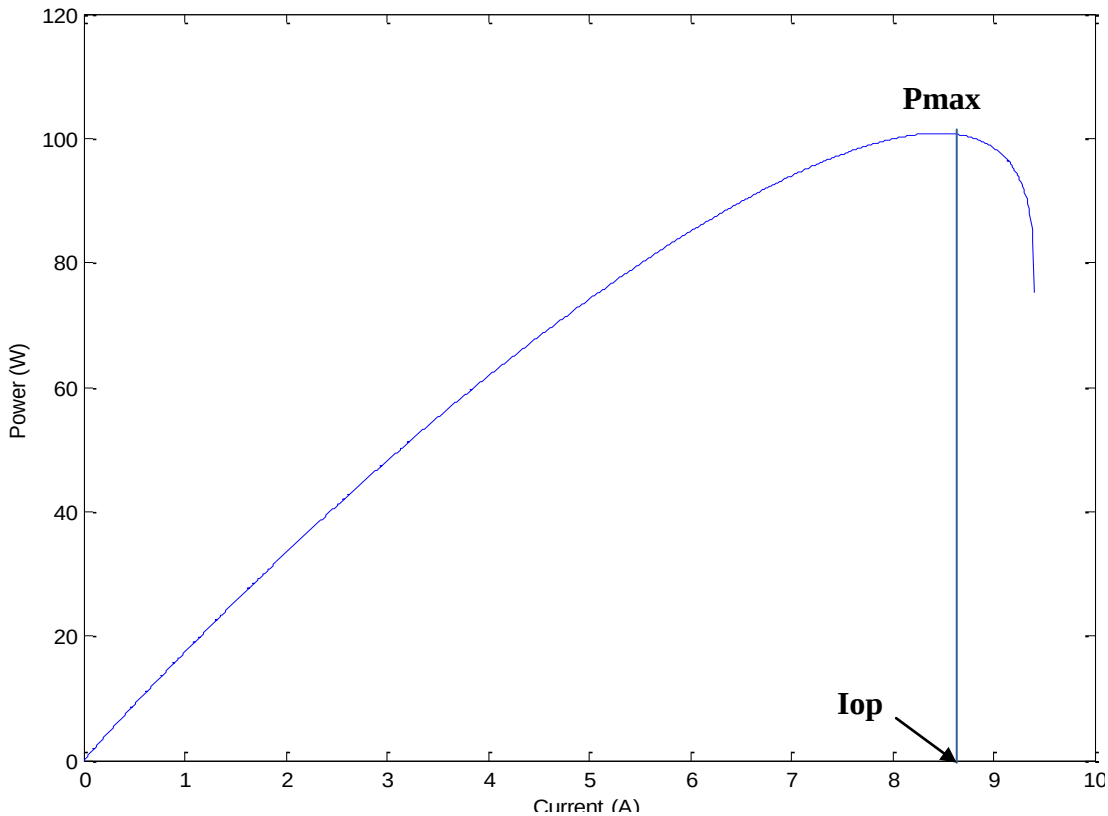

Fig 3.2: Fuel Cell's Power vs. Voltage

The maximum power point can only be achieved when the system is working at the optimal voltage and optimal current or, in other words, when the load, Rop, connected to the FC is equal to the division of its optimal voltage and optimal current.

Fuel Cell's voltage-current and power-voltage relations are typically affected the cell's operating temperature. Changes in temperatures drastically changes the fuel cell's open circuit voltage, short-circuit current and maximum power availability. Figure 3.3 shows the changes of the fuel cell V-I curve under different temperature values.

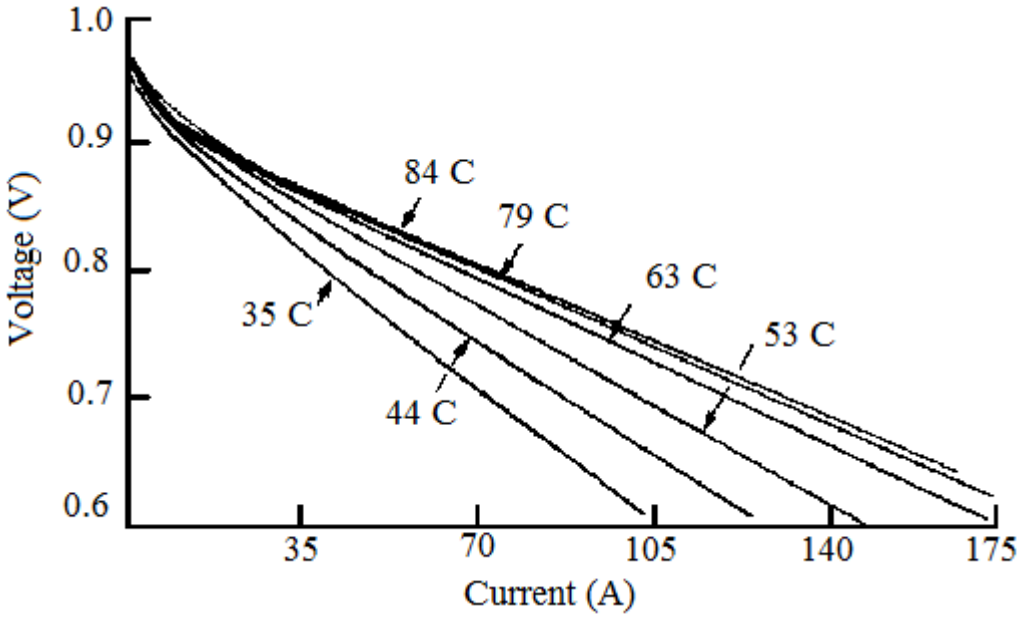

Fig 3.3: Relation between voltage and current under different temperatures [59]

Other important factors that affect the voltage-current curve and the power-voltage curve are the partial pressure of the reactants in the fuel cells and the reactants flow. Neither of these factors is going to be considered in the scope of this work.

3.4 Fuel Cell's Electrical Circuit Model

For this work, we are going to use an electrical circuit model given by [28]. Unlike other models, like [73,74 75 76], where complex computation are required, a lot of chemical knowledge are necessary , and the estimation of factors and variables in order to get a good approximation are required, this model uses factors and variables that are easily available or could be easily determined by the manufacturer's datasheet. The equations that represent the behavior of any fuel cell operating at normal conditions are the following [28]:

$$V_{FC} = V_L + (V_H - V_L) \cdot \left[\frac{\arccos\left(\frac{2 \cdot I}{I_H} - 1 \right)}{\pi} \right]^K \tag{9}$$

$$P = V_L \cdot I + I \cdot (V_H - V_L) \cdot \left[\frac{\arccos\left(\frac{2 \cdot I}{I_H} - 1 \right)}{\pi} \right]^K \tag{10}$$

$$k = \ln\left[\frac{V_{op} - V_L}{V_H - V_L} \right] \cdot \ln\left[\frac{\arccos\left(\frac{2 \cdot I_{op}}{I_H} - 1 \right)}{\pi} \right] \tag{11}$$

where

- V_{FC} is the fuel cell's output voltage in *V*
- V_L is the fuel cell's lowest voltage in *V*
- V_H is the fuel cell's highest voltage in *V*
- I is the fuel cell's output current in *A*
- I_H is the fuel cell's highest current in *A*
- K is the fuel cell's characteristic constant
- P is the fuel cell's output power in *W*
- V_{op} is the fuel cell's optimal voltage in *V*
- I_{op} is the fuel cell's optimal current in *A*

Figures 3.4 and 3.5 shows a comparison, which validates the accuracy of these equations, between data obtained from Tiscanelli's work [71] and the proposed equations. As it can be noted, the voltage-current and power-current curves generated by the equations used for this work showed to be very accurate when compared to the Tiscanelli experimental data.

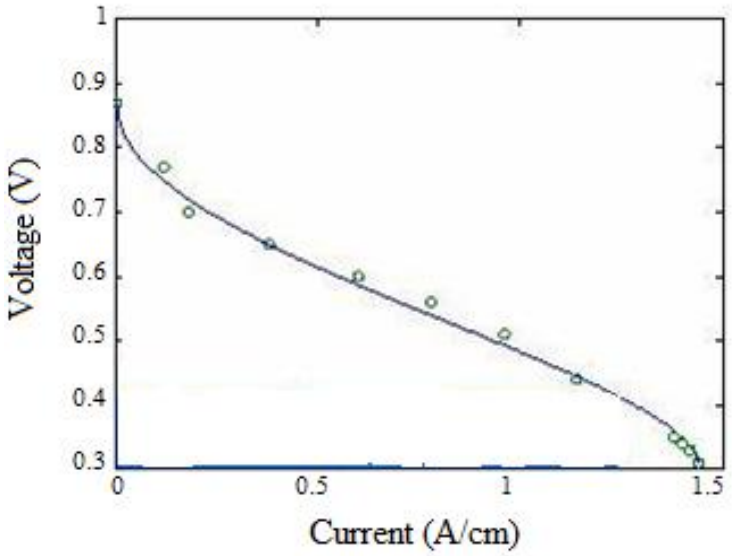

Fig 3.4: Tiscanelli's Experimental Data vs. Proposed Model I-V Curve [71]

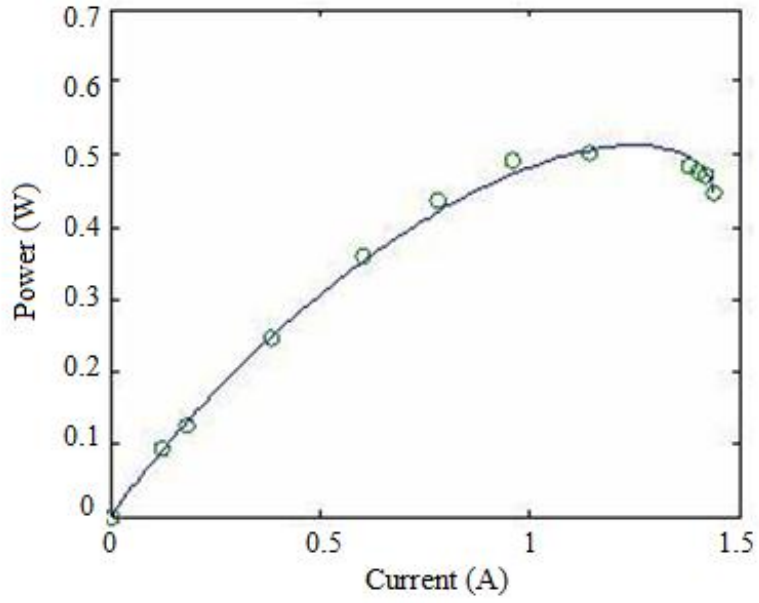

Fig 3.5: Tiscanelli's Experimenal Data vs. Proposed Model P-I Curve [71]

4 Sliding Mode Control

In this section the concept of sliding mode control, its use, and its abilities will be explained.

4.1 Basic Concept

Sliding mode control is a variable structure control where the dynamics of a non linear system are altered via the application of a high frequency switching control. In sliding mode control, the trajectories of the system are forced to reach a sliding manifold of surface, where it exhibit desirable features, in finite time and to stay on the manifold for all future time. It is achieved by suitable control strategy and non continuous control laws [84].

Sliding Mode Controllers consist of two phases: the reaching phase, where the trajectories of a system are forced to move toward to a desired sliding surface and reach it in finite time, and the sliding phase, where the trajectories of the systems are confined in the sliding surface and all the dynamics of the systems are represented by a reduce order system equals to the sliding surface.

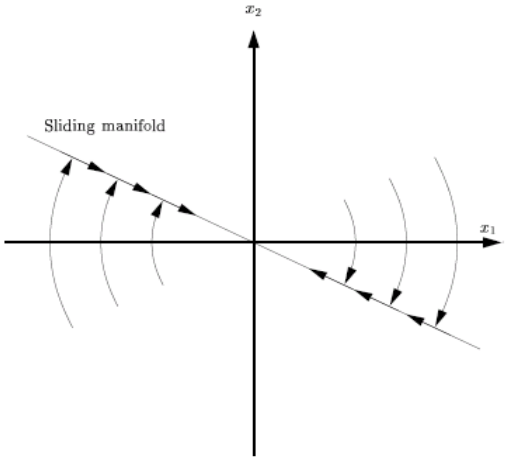

Fig 4.1: A Simple Idea of Sliding Mode Control

4.2 Designing a Control Law

To design a sliding mode control law, first we have to consider a non linear system defined by the following form:

$$\dot{x}_1 = x_2$$

$$\dot{x}_2 = f(x) + g(x) \cdot u(t)$$

where x(t) is state vector of dimension *n* and u(t) is a input vector of dimension *m* ,f(x) and g(x) are non linear functions.

A state feedback control law has to be designed to stabilize one state variable to a reference point by constraining the motion of the system to a sliding surface of the form

$S = k \cdot x(t) = \bar{x}$ where *k* is a vector of dimension p and $\bar{x}$ is a column matrix containing the reference point $\begin{bmatrix} \bar{x}_1 \\ 0 \end{bmatrix}$ of the state variables.

Taking as manifold $S = k \cdot \left(x_1 - \bar{x}_1 \right) + x_2 = 0$, the motion of the system is going to be governed by $\dot{x}_1 = -k \cdot \left(x_1 - \bar{x}_1 \right)$ that, by taking a value of *k* > 0, will tend to $\begin{bmatrix} \bar{x}_1 \\ 0 \end{bmatrix}$ as the time tends to infinite.

Stability of the manifold must be verified. To check for stability, a Lyapunov candidate of the form $V = \frac{1}{2} \cdot x^T \cdot a \cdot x$ must be positive definite, where *a* is an n x n square matrix, by selecting an appropriate control law of the form $u = -\beta(x) sign(s)$.

4.3 Applications

Sliding Mode Control is widely use for a lot of applications including control systems for DC/DC converters [72] [74], power supply, electric grid connections [73], motors speed regulator [74], position control system, among others.

Due to the nature of its high frequency switching control, SMC has seen a lot of applications in power electronics from controlling an on-off switch to acting as a pulse-width-modulator in dc/dc converters.

5 DC-DC Converters

In this section we are going to give brief information about the dc-dc converter, their basic configurations and how they work.

5.1 Introduction

DC- DC Converters are electronics devices that convert a dc voltage level to higher or a lower voltage level. In DC to DC converters, energy is periodically stored into and released from a magnetic field in an inductor or a transformer and, by adjusting the duty cycle of the switching device, the amount of power transferred can be controlled.

The three basic configurations are:

- Buck Converter- Reduce the input voltage to a lower voltage level
- Boost Converter- Increase the input voltage to a higher level
- Buck-Boost Converter- Increase or reduce the input voltage

The main advantage of using DC-DC converters over other type of voltage converters, such as linear regulators, is the high efficiency that can be achieved, as high as 95%.

5.2 DC-DC Converter Topologies

5.2.1 Buck Converter

5.2.1.1 Topology

A buck converter is a dc-dc converter that changes the input voltage to a lower voltage level. It is achieved by controlling the duty cycle of a control signal that is applied to the converter's switching device. Figure 5.1 shows the typical topology of a buck converter.

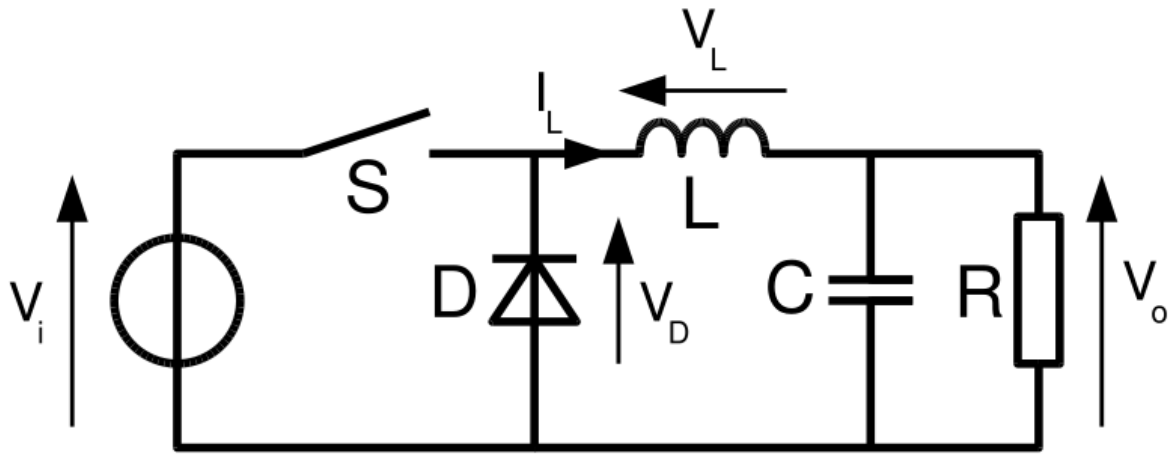

Fig 5.1: Typical Topology of a Buck Converter

A buck converter operates in two stages: the ON stage and the OFF stage. Those stages are equivalent to the states of the switching device. In the ON stage, the switching device is closed and the inductor is directly connected to the power source. In this state the inductor begins to charge. In the OFF stage, the switching device is open and the inductor is no longer connected to the power source. The inductor now begins to work as the power source supplying power to the load until the switching device closes again.

Besides having two stages, buck converters have two operating mode: continuous mode and discontinuous mode. In the continuous mode, the ON and OFF stages of the converter are in such a way that the current in the inductor never reaches zero. In the discontinuous mode, the ON and OFF stages of the converter are in such a way that the current in the inductor reaches zero.

The relationship between the output voltage with respect to the input voltage, in steady state and without losses, is the following:

- For Continuous Mode
  - $V_O = D \cdot V_I$ (12)
- For Discontinuous Mode
  - $V_O = V_I \frac{1}{\frac{2 \cdot L \cdot I_O}{D^2 \cdot T \cdot V_I} + 1}$ (13)

where *Vo* is the converter's output voltage, V_I is the converter's input voltage, *D* is the control signal's duty cycle, *L* is the inductor's inductance and *T* is the control signal's period.

5.2.1.2 State-Space Equations, Controllability and Observability

The differential equations of a buck converter for the continuous mode are the following:

$$\frac{di_L}{dt} = -\frac{1}{L}V_C + \frac{V_I}{L}u \tag{14}$$

$$\frac{dV_C}{dt} = \frac{1}{C}i_L - \frac{1}{RC}V_C \tag{15}$$

To establish the state-space equations for the buck converter we select the following state variables:

$X_1 = i_L$, $X_2 = V_C$

The state-space equations results as follows:

$$\dot{X} = \begin{bmatrix} 0 & -\frac{1}{L} \\ \frac{1}{C} & -\frac{1}{RC} \end{bmatrix} \begin{bmatrix} X_1 \\ X_2 \end{bmatrix} + \begin{bmatrix} \frac{Vi}{L} \\ 0 \end{bmatrix} \cdot u \tag{16}$$

$$y = \begin{bmatrix} 0 & 1 \end{bmatrix} X$$

Where

$$A = \begin{bmatrix} 0 & -\frac{1}{L} \\ \frac{1}{C} & -\frac{1}{RC} \end{bmatrix}, B = \begin{bmatrix} \frac{Vi}{L} \\ 0 \end{bmatrix}, C = \begin{bmatrix} 0 & 1 \end{bmatrix}$$

The controllability matrix is the following:

$$Cont = \begin{bmatrix} B & AB \end{bmatrix} = \begin{bmatrix} \frac{Vi}{L} & 0 \\ 0 & \frac{Vi}{LC} \end{bmatrix} \tag{17}$$

By inspection, the controllability matrix has rank 2 or full rank. By definition the buck converter is controllable.

The observability matrix is the following:

$$O = \begin{bmatrix} C \\ CA \end{bmatrix} = \begin{bmatrix} 0 & 1 \\ \frac{1}{L} & \frac{-1}{RC} \end{bmatrix} \tag{18}$$

By inspection, the observability matrix has a rank of 2 or full rank. By definition the buck converter is observable.

5.2.2 Boost Converter

5.2.2.1 Topology

A boost converter is a dc-dc converter that changes the input voltage to a higher voltage level. It is achieved by controlling the duty cycle of a control signal that is applied to the converter's switching device. Fig 5.2 shows the typical topology of a boost converter.

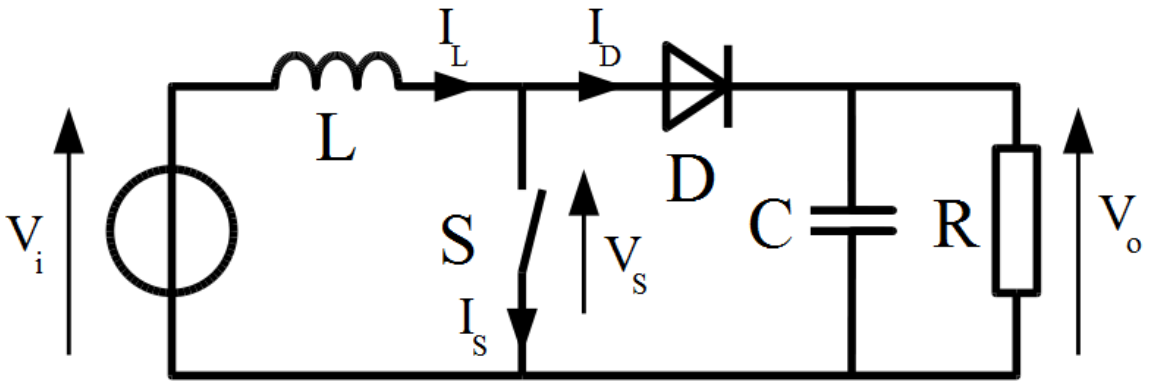

Fig 5.2: Typical Topology of a Boost Converter

A boost converter operates in two stages: the ON stage and the OFF stage. Those states are equivalent to the states of the switching device. In the ON stage, the switching device is closed and the inductor is directly connected to ground. In this state the inductor begins to charge. In the OFF stage, the switching device is open and the inductor is no longer connected to ground but to the load. The inductor now begins to work as the power source supplying power to the load and, being in series with the main power source, increasing the voltage level until the switching device closes again.

Besides having two stages, boost converters have two operating mode: continuous mode and discontinuous mode. In the continuous mode the, ON and OFF stages of the converter are in such a way that the current in the inductor never reaches zero. In the discontinuous mode, the ON and OFF stages of the converter are in such a way that the current in the inductor reaches zero.

The relationship between the output voltage with respect to the input voltage, in steady state and without losses, is the following:

- For Continuous Mode
  - $V_O = \frac{1}{1-D} \cdot V_I$ (19)
- For Discontinuous Mode
  - $V_O = 1 + \frac{D^2 \cdot T \cdot V_I}{2 \cdot L \cdot I_O}$ (20)

where *Vo* is the converter's output voltage, V_I is the converter's input voltage, *D* is the control signal's duty cycle, *L* is the inductor's inductance, I_o is the output current and *T* is the control signal's period.

5.2.2.2 State-Space Equations, Controllability and Observability

The differential equations of a boost converter for the continuous mode are the following:

$$\frac{di_L}{dt} = \frac{V_I}{L} + \frac{V_C}{L} - \frac{V_C}{L}u \tag{21}$$

$$\frac{dV_C}{dt} = \frac{1}{C}i_L - \frac{1}{RC}V_C - \frac{i_L}{c}u \tag{22}$$

To establish the state-space equations for the boost converter we select the following state variables:

$X_1 = i_L > 0$, $X_2 = V_C \geq V_i$

The state-space equations results as follows:

$$\dot{X} = \begin{bmatrix} 0 & -\frac{1}{L} \\ \frac{1}{C} & -\frac{1}{RC} \end{bmatrix} \begin{bmatrix} X_1 \\ X_2 \end{bmatrix} + \begin{bmatrix} \frac{-X_2}{L} \\ \frac{-X_1}{C} \end{bmatrix} U + \begin{bmatrix} \frac{1}{L} \\ 0 \end{bmatrix} V_I \tag{23}$$

$$y = \begin{bmatrix} 0 & 1 \end{bmatrix} X$$

Where

$$f(x) = \begin{bmatrix} \frac{-X_2 + V_I}{L} \\ \frac{X_1}{C} - \frac{X_2}{RC} \end{bmatrix}, g(x) = \begin{bmatrix} \frac{-X_2}{L} \\ \frac{-X_1}{C} \end{bmatrix}, \text{h(x)} = X_2$$

For the system to be controllable, a matrix, G , must have full rank.

$$G = [g \quad [f, g]] \tag{24}$$

Where $[f, g] = \frac{\partial g}{\partial x} f(x) - \frac{\partial f}{\partial x} g(x)$

$$G = \begin{bmatrix} \frac{-X_2}{L} & -\frac{2X_1}{LC} + \frac{X_2}{RCL} \\ \frac{-X_1}{C} & \frac{X_1}{RC^2} + \frac{2X_2}{LC} + \frac{V_I}{L} \end{bmatrix}$$

The rank of matrix G is 2. In other words, it has full rank. By definition, the boost converter is controllable.

For the system to be locally observable, the matrix O must have full rank.

$$O = \frac{\partial}{\partial x} \begin{bmatrix} h \\ l_f h \end{bmatrix} = \begin{bmatrix} 0 & 1 \\ \frac{1}{C} & \frac{-1}{RC} \end{bmatrix}$$

(25)

Where $l_f h = \frac{\partial h}{\partial f} \cdot f(x)$

$$O = \begin{bmatrix} 0 & 1 \\ \frac{1}{C} & \frac{-1}{RC} \end{bmatrix}$$

Matrix O has a rank of 2 or full rank, then the boost converter is locally observable.

5.2.3 Buck-Boost Converter

5.2.3.1 Topology

A buck-boost converter is a dc-dc converter that changes the input voltage to a higher or a lower voltage level, while inverting the polarity. It is achieved by controlling the duty cycle of a control signal that is applied to the converter's switching device. Depending on the duty cycle value it will act as a buck converter or as a boost converter. Fig 5.3 shows the typical topology of a buck-boost converter.

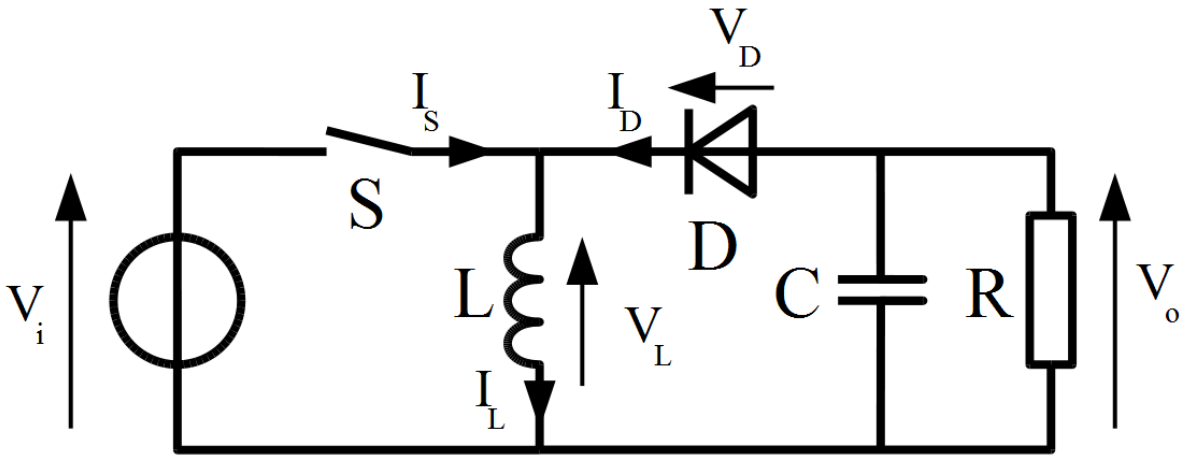

Fig 5.3: Typical Topology of a Buck-Boost Converter

A buck-boost converter operates in two stages: the ON stage and the OFF stage. Those states are equivalent to the states of the switching device. In the ON stage, the switching device is closed and the inductor is directly connected to power source. In this state the inductor begins to charge. In the OFF stage, the switching device is open and the inductor is no longer connected to power source but to the load. The inductor now begins to work as

the power source supplying power to the load and the capacitor until the switching device closes again. Depending in the duty cycle the converter increase or decrease the input voltage value.

Besides having two stages, buck-boost converters have two operating mode: continuous mode and discontinuous mode. In the continuous mode the, ON and OFF stages of the converter are in such a way that the current in the inductor never reaches zero. In the discontinuous mode, the ON and OFF stages of the converter are in such a way that the current in the inductor reaches zero.

The relationship between the output voltage with respect to the input voltage, in steady state and without losses, is the following:

- For Continuous Mode
  - $V_O = \frac{-D}{1-D} \cdot V_I$ (26)
- For Discontinuous Mode
  - $V_O = -\frac{D^2 \cdot T \cdot V_I}{2 \cdot L \cdot I_O}$ (27)

where *Vo* is the converter's output voltage, V_I is the converter's input voltage, *D* is the control signal's duty cycle, *L* is the inductor's inductance, I_o is the output current and *T* is the control signal's period.

5.2.3.2 State-Space Equations, Controllability and Observability

The differential equations of a buck-boost converter for the continuous mode are the following:

$$\frac{di_L}{dt} = \frac{V_I}{L}u + \frac{V_C}{L} - \frac{V_C}{L}u \tag{28}$$

$$\frac{dV_C}{dt} = \frac{1}{C}i_L \cdot u - \frac{1}{RC}V_C - \frac{i_L}{c} \tag{29}$$

To establish the state-space equations for the buck-boost converter we select the following state variables:

$X_1 = i_L$, $X_2 = V_C$

The state-space equations results as follows:

$$\dot{X} = \begin{bmatrix} 0 & \frac{1}{L} \\ -\frac{1}{C} & -\frac{1}{RC} \end{bmatrix} \begin{bmatrix} X_1 \\ X_2 \end{bmatrix} + \begin{bmatrix} \frac{V_I - X_2}{L} \\ \frac{X_1}{C} \end{bmatrix} U \tag{30}$$

$$y = \begin{bmatrix} 0 & 1 \end{bmatrix} X$$

Where

$$f(x) = \begin{bmatrix} \frac{-X_2}{L} \\ \frac{-X_1}{C} - \frac{X_2}{RC} \end{bmatrix}, g(x) = \begin{bmatrix} \frac{V_I - X_2}{L} \\ \frac{X_1}{C} \end{bmatrix}, \text{h(x)} = X_2$$

For the system to be controllable, a matrix, G, must have full rank .

$$G = [g \quad [f, g]] \tag{24}$$

Where $[f, g] = \frac{\partial g}{\partial x} f(x) - \frac{\partial f}{\partial x} g(x)$

$$G = \begin{bmatrix} \frac{-X_2 + V_I}{L} & -\frac{2X_1}{LC} + \frac{X_2}{RCL} \\ \frac{X_1}{C} & \frac{X_1}{R} + \frac{V_I}{LC} \end{bmatrix}$$

Matrix G has a rank of 2 or full rank so the system is controllable from everywhere.

For the system to be locally observable, the matrix O must have full rank.

$$O = \frac{\partial}{\partial x} \begin{bmatrix} h \\ l_f h \end{bmatrix} \tag{25}$$

Where $l_f h = \frac{\partial h}{\partial f} \cdot f(x)$

$$O = \begin{bmatrix} 0 & 1 \\ -\frac{1}{C} & \frac{-1}{RC} \end{bmatrix}$$

Matrix O has a rank of 2 or full rank, then the buck-boost converter is locally observable.

6 Hybrids Renewable Energy Power System

In this chapter, a brief introduction to the basic concepts and typical problems of the hybrid renewable energy power systems is going to be given. The hybrid renewable energy power system scheme we used will be introduced and fully explained. Control strategies used will be discussed and explained

6.1 Introduction

The use of hybrid renewable energy power systems have been increasing in the last years due to factors like the need of generating cleaner electricity to reduce the greenhouse gases that creates global warming [81, 82], the increment in the cost of electricity generated by fossil fuels [83] and its ability to be installed in remote places where the electric grid cannot reach or is not cost-efficient to be connected to them.

HRPES are systems composed of one or more different renewable energy power systems interconnected to serve as typical power systems. Typical combined renewable energy systems are wind/solar systems and solar/fuel cell systems. For this work we are going to be focused on solar/fuel cell hybrid systems. Batteries are also used for energy storage.

The use of two or more combined renewable energy system has the advantage of decreasing the possibility of having intervals of time where there is insufficient power to satisfy the load demand.

HREPS suffers from several problems when it is connected to a load. Problems like poor power quality, low power output due to load mismatching, unregulated load voltage and no-power intervals of time are among the most critical ones. Due to these problems, a control strategy should be developed to eliminate or reduce the impact of them. Control strategies such as maximum power point trackers, voltage regulators circuits, load-matching circuits and power regulator controllers has been applied successfully to reduce and eliminate the problems that affects the hybrid power systems.

6.2 Composition and Scheme of HREPS

The proposed hybrid renewable energy power system is composed of a solar cell module, a fuel cell, two buck dc-dc converters and two sliding mode based controller. A DC/AC inverter is also used but it's not the scope of this work to show how it works. Also a battery bank is also implemented into the system. Figure 6.1 shows the scheme of the HREPS.

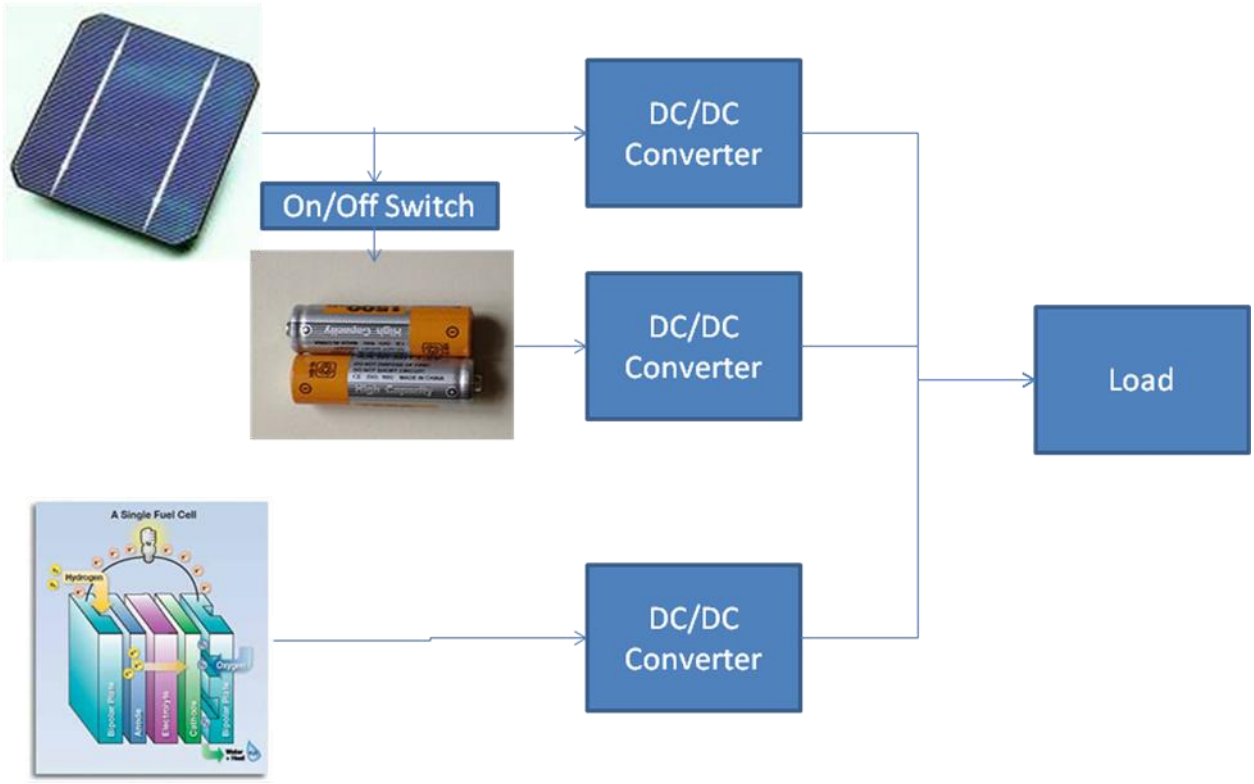

Fig 6.1: HREPS Proposed Scheme

The photovoltaic cell is our first system. It is connected to a buck dc-dc converter. A sliding mode based controller is in charge of controlling the power output of the photovoltaic cell. The fuel cell is our second system. It is connected to a buck dc-dc converter. A sliding mode based controller is in charge of controlling the power output of the fuel cell only when auxiliary power is required. Both systems are connected through an inverter for AC loads and directly for DC load. A battery is added as a third system and is connected through an on/off charger controller switch to the photovoltaic cell and to the load through a dc/dc converter.

6.2.1 Photovoltaic Cell

Our system will have as its primary system a photovoltaic cell. For simulations matters, equations of the photovoltaic cell, as presented in chapter 2 of this work, are going to be used. Several commercial models are implemented and connected in arrays to increase their power output.

6.2.2 Fuel Cell

Our system will have as its secondary/auxiliary system a fuel cell. For simulations matters, equations of a typical fuel cell, as presented in chapter 3 of this work, are going to be used. Several commercial models, with different power levels, are implemented.

6.2.3 Batteries

Our system will have, as its third system, batteries to supply extra power when the system demands more power than could be generated by the other two systems such as when there is no Sun's energy. The battery model used is the model implemented by Simulinks. See appendix C1 for the battery model information.

6.2.4 Sliding Mode Controller

Our HREPS consist of two sliding mode- based independent controllers that must produce a control signal capable of driving the switching device inside the buck converters

and force the system to operate at desired conditions. Both controllers will work along but in different ways.

6.2.4.1 Sliding Mode Based Control for Primary DC-DC converter

The control structure for the primary dc-dc converter must be capable of two things, regulate the output voltage to a reference voltage and to deliver its maximum power when load regulation cannot be achieved. Due to the energy conservation law, voltage regulation and maximum power point tracker can only be achieve when the system is connected to a unique resistive load that satisfy the Ohms' Power law described by equation (33).

$$R = \frac{V_{REF\ MAX}^{\ 2}}{P_{\max}} \tag{33}$$

where V_{REFMAX} is the maximum reference voltage that is desired at the load, for DC power is simply the voltage level and for AC power is the signal amplitude, and P_{MAX} is the maximum power available. Besides that specific value, both operation modes cannot be achieved, with sliding mode control or by any other type of control, by simply using one dc-dc converter. Due to it, it will operate at one mode at a time. One operation mode must be in charge of regulating the dc-dc converter's output voltage to a reference value and a second operation mode should force the system to operate at maximum power mode without considering

voltage regulation. The controller must be capable of automatically switch from one operation to the other without manual intervention.

The first operation mode is voltage regulation mode. Voltage regulation, in the electrical engineer aspect, is the ability of a system to maintain the output voltage to a reference value under any changes in the load or power demand.

Voltage regulation is necessary because of the following reasons:

1) Photovoltaic and Fuel cell's output voltage varies with the load. So as load is changing also the output voltage is changing affecting the normal operation of the devices connected to the dc-dc converter.
2) Without voltage regulation at dc voltage level, the need of another control strategy is going to be needed to regulate the AC voltage of the inverter to a usable voltage level.

This operation mode will be operating when the load's power demand is equal or less than the maximum power available by the solar cell or , by Ohm's law, when

$$R \geq \frac{V_{REFMAX}^{\ 2}}{P_{\max}}$$

For voltage regulation, the DC/DC converter should have the following behaviour:

$$\begin{cases} On & V_{REF} - V_{LOAD} > 0 \\ Off & V_{REF} - V_{LOAD} \leq 0 \end{cases}$$

Knowing how it should behave the switching device, in order to achieve this operating mode; we will need a controller that behaves the following way:

$$u = \begin{cases} 1 & V_{REF} - V_{LOAD} > 0 \\ 0 & V_{REF} - V_{LOAD} \leq 0 \end{cases}$$

where *1* is the logical value that gives a high voltage output that is capable of saturating the switching device and *0* is the logical value that gives a low voltage that is capable of turning off the switching device.

The second operation mode is the Maximum Power operation mode. The maximum power operation mode is the operating point where the photovoltaic cell produces its maximum power. While operating at this mode no voltage regulation is possible. This operation mode will be achieved when the load's power demand, for the reference load voltage level, is equal or more than the maximum power available by the solar cell or , by Ohm's law, when

$$R \leq \frac{V_{REFMAX}^{\ 2}}{P_{\max}}$$

For maximum power, the second operating should behave like the following:

$$\begin{cases} On & V_{PV} - V_{OP} > 0 \\ Off & V_{PV} - V_{OP} \leq 0 \end{cases}$$

Knowing how should behave the switching device; we will need a controller that behaves the following way:

$$u = \begin{cases} 1 & V_{PV} - V_{OP} > 0 \\ 0 & V_{PV} - V_{OP} \leq 0 \end{cases}$$

where *1* is the logical value that gives a high voltage output capable of saturating the switching device and *0* is the logical value that gives a low voltage capable of turning off the switching device

To automatically switch between the two operation modes a control law composed of the two operation modes control law must be designed. The control law must behave the following way:

$$u = \begin{cases} 1 & (V_{PV} - V_{OP}) and (V_{REF} - V_{LOAD}) > 0 \\ 0 & (V_{PV} - V_{OP}) or (V_{REF} - V_{LOAD}) \leq 0 \end{cases}$$

A control law that guarantees us that our controller will behave in the required way is given by the following equation (34):

$$u = \frac{1}{4}\left[\left(1 + sign\left(\mathrm{V_{REF}} - \mathrm{V_{LOAD}}\right)\right) \cdot \left(1 + sign\left(\mathrm{V_{PV}} - \mathrm{V_{OP}}\right)\right)\right] \qquad (34)$$

This control law will guarantees us the following:

- Will operate in only one operation mode at a given time.
- Will automatically switch between operation modes.

Figure 6.2 shows the typical behavior of the power of a PV cell versus resistance load with the operation modes of the primary controller. As seen in the figure, if the system is not forced to operate at the maximum power point after the optimal resistance, Rop, is reached, the power generated by the PV will begin to drop as the resistance value decrease.

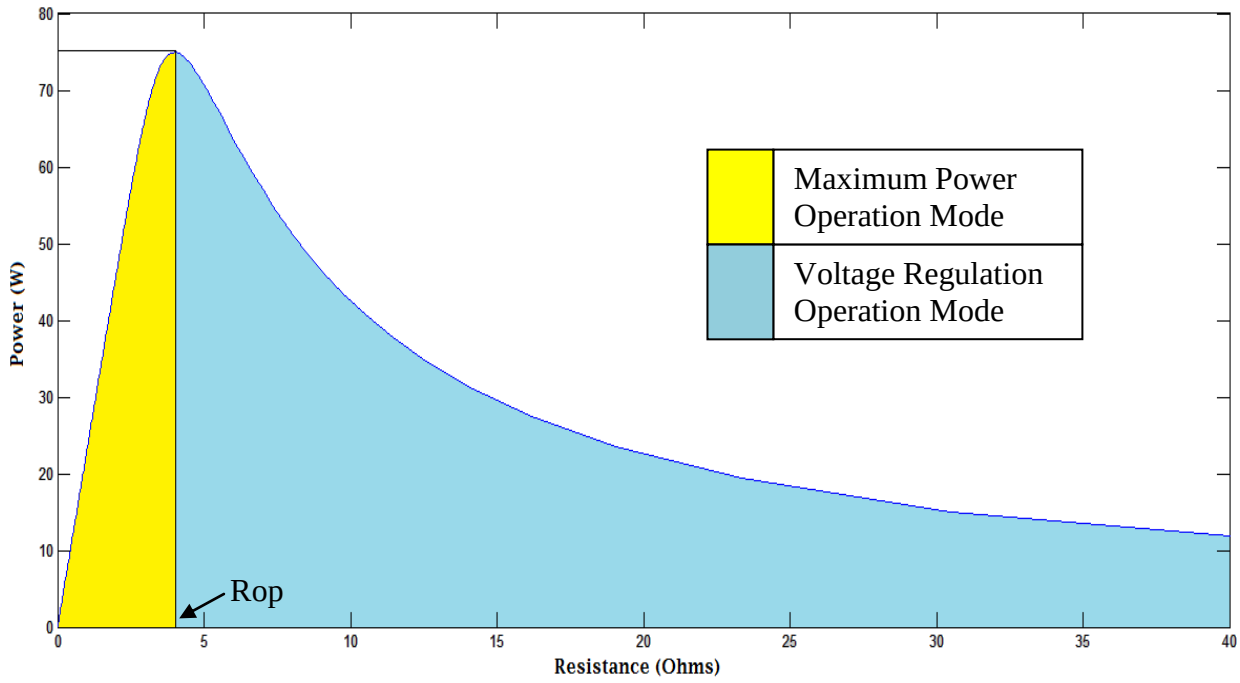

Fig 6.2: Behavior of primary controller's operation mode in PV Power-Resistance Graph

6.2.4.2 Sliding Mode Based Control for Secondary DC-DC Converter

The control structure for a secondary dc-dc converter must be capable of automatically activating when the primary dc-dc converter cannot supply enough power to maintain a regulated voltage at the load and, to lock the system to operate at its maximum power point, once it's reached, for all future time regardless the load voltage regulation. The auxiliary controller consists of two operating modes: the active-normal mode and the active-maximum power mode.

The first operating mode is the active mode. This operation mode corresponds to the activation of the auxiliary dc-dc converter. This operating mode is responsible of maintaining the regulated voltage at the load whenever the primary controller is working at the maximum-power operating mode or cannot regulated it.

This operating mode should behave the following way:

$$\begin{cases} On & (V_{PV} - V_{OP}) and (V_{REF} - V_{LOAD}) > 0 \\ Off & (V_{PV} - V_{OP}) or (V_{REF} - V_{LOAD}) \leq 0 \end{cases}$$

Knowing how should behave the switching device, in order to achieve this operating mode; we will need a controller that behaves the following way:

$$u = \begin{cases} 1 & (V_{PV} - V_{OP}) and (V_{REF} - V_{LOAD}) > 0 \\ 0 & (V_{PV} - V_{OP}) or (V_{REF} - V_{LOAD}) \leq 0 \end{cases}$$

where *1* is the logical value that gives a high voltage output that is capable of saturating the switching device and *0* is the logical value that gives a low voltage that is capable of turning off the switching device.

The second operating mode is the active-maximum power mode. This operating mode is responsible of forcing the fuel cell, or the auxiliary system used, to operate at its maximum power when maximum power is reached.

The second operating mode have the following two operation state or behaviour:

$$\begin{cases} On & V_{AUX} - V_{OPAUX} > 0 \\ Off & V_{AUX} - V_{OPAUX} \leq 0 \end{cases}$$

where V_{AUX} is the output voltage of the auxiliary renewable energy system, and VOPAUX is the optimal voltage of the auxiliary renewable energy system.

Knowing how should behave the switching device; we will need a controller that behaves the following way:

$$u = \begin{cases} 1 & V_{AUX} - V_{OPAUX} > 0 \\ 0 & V_{AUX} - V_{OPAUX} \leq 0 \end{cases}$$

where *1* is the logical value that gives a high voltage output that is capable of saturating the switching device and *0* is the logical value that gives a low voltage that is capable of turning off the switching device.

To automatically switch between the two operation modes a control law composed of the two operation modes control law must be designed. The control law must behave the following way:

$$u = \begin{cases} 1 & (V_{PV} - V_{OP}) and (V_{REF} - V_{LOAD}) and (V_{AUX} - V_{OPAUX}) > 0 \\ 0 & (V_{PV} - V_{OP}) or (V_{REF} - V_{LOAD}) or (V_{AUX} - V_{OPAUX}) \leq 0 \end{cases}$$

A control law that will meet the required criteria is shown in the following:

$$u = \frac{1}{8}\left[\begin{array}{l} (1 + sign(V_{REF} - V_{LOAD})) \cdot (1 + sign(V_{PV} - V_{OP})) \\ \cdot (1 + sign(V_{AUX} - V_{OPAUX})) \end{array}\right]$$

A control law that guarantees us that our controller will behave in the required way is given by the following equation (35):

$$u = \frac{1}{8}\left[\begin{array}{l}\left(1+sign\left(V_{REF}-V_{LOAD}\right)\right)\cdot\left(1+sign\left(V_{PV}-V_{OP}\right)\right)\\ \cdot\left(1+sign\left(V_{AUX}-V_{OPAUX}\right)\right)\end{array}\right] \quad (35)$$

This control law guarantees us the following:

- Will operate in only one operation mode at a given time.
- Will automatically switch between operation modes.

Figure 6.3 shows the typical graph of the power of a PV cell versus resistance load with the operation modes of the auxiliary controller with respect to the primary controller. As seen in the figure, if the system is not forced to operate at the maximum power point after the resistance value is reached, the power generated by the PV will begin to drop as the resistance value decrease.

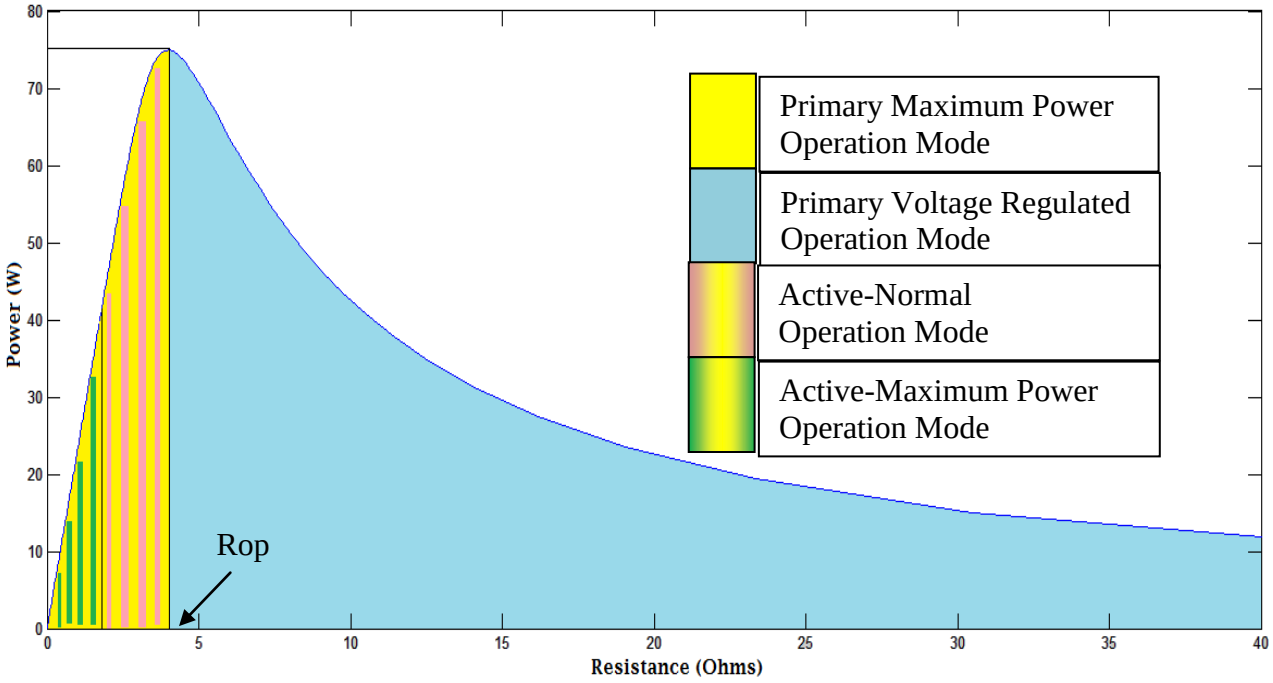

Fig 6.3: Behavior of both controllers' operation mode in PV Power-Resistance Graph

6.2.4.3 Sliding Mode Based Controller for Battery Bank System

A battery bank system will be used to supply power when the system is not able to satisfy the demand. The main reason to include a battery bank is that it can let you choose a lower power fuel cell system because it can be of help at night when the PV system is not generating any power and the FC is working alone. Two control strategies are needed for a battery bank. One is to stop the battery bank from forcing the secondary system to operate and the other is to control the power distribution from the battery.

To use a battery bank, the following conditions must be satisfied:

1) The battery bank should only be charge using PV power. The reason for that is to reduce the use of hydrogen from the fuel cell.
2) The battery bank voltage should be higher than the load's reference voltage but lower than the PV optimal voltage.
3) The battery bank should stop recharging when the PV voltage is near its optimal value. This is to prevent the need of activating the secondary system.

The first controller should charge the battery when the PV voltage is higher than a reference value. If lower then it should be disconnected. It should behave like the following:

$$\begin{cases} On & V_{PV} - \left(V_{OP} + V_{off}\right) > 0 \\ Off & V_{PV} - \left(V_{OP} + V_{off}\right) \leq 0 \end{cases}$$

where V_{PV} is the output voltage of the PV, V_{OP} is the PV's optimal voltage and V_{OFF} is the voltage difference between the optimal voltage and the PV voltage in which the switch should turn off.

Knowing how should behave the switching device, in order to achieve this operating mode, we will need a controller that behaves the following way:

$$u = \begin{cases} 1 & V_{PV} - \left(V_{OP} + V_{off}\right) > 0 \\ 0 & V_{PV} - \left(V_{OP} + V_{off}\right) \leq 0 \end{cases}$$

where *1* is the logical value that gives a high voltage output capable of saturating the switching device and *0* is the logical value that gives a low voltage capable of turning off the switching device

A control law that guarantees us this operation is defined in the next equation:

$$\mathrm{u} = \frac{1}{2} \cdot \left[1 + sign\left(V_{PV} - \left(V_{OP} + V_{off}\right)\right)\right] \tag{36}$$

This control law will also guarantee us conditions one and three are satisfied.

In order to supply additional power when both systems are not able to do so, a second control law must be implemented to extract the necessary power from the battery bank. The switching device connected to the battery bank must behave the following way:

$$\begin{cases} On & \left(V_{FC} - V_{OPFC}\right) and \left(V_{REF} - V_{LOAD}\right) > 0 \\ Off & \left(V_{FC} - V_{OPFC}\right) or \left(V_{REF} - V_{LOAD}\right) \leq 0 \end{cases}$$

where V_{FC} is the fuel cell's voltage, V_{OPFC} is the fuel cell's optimal voltage, V_{REF} is the reference voltage level wanted in the load and V_{LOAD} is the voltage at the load.

Knowing how should behave the switching device, in order to achieve this operating mode, we will need a controller that behaves the following way:

$$u = \begin{cases} 1 & (V_{FC} - V_{OPFC}) and (V_{REF} - V_{LOAD}) > 0 \\ 0 & (V_{FC} - V_{OPFC}) or (V_{REF} - V_{LOAD}) \leq 0 \end{cases}$$

where *1* is the logical value that gives a high voltage output capable of saturating the switching device and *0* is the logical value that gives a low voltage capable of turning off the switching device.

A control law that guarantees us that our controller will behave in the required way is given by the following equation (37):

$$\mathrm{u} = \frac{1}{4}\left[\left(1 + sign\left(V_{FC} - V_{OPFC}\right)\right) \cdot \left(1 + sign\left(V_{REF} - V_{LOAD}\right)\right)\right] \quad (37)$$

This control law will guarantee us that the battery bank will be operating only when the two other energy system cannot meet the power demand of the load.

6.2.5 DC- DC Converters

- Topology : Buck Converter
    - The proposed dc-dc converter for our system is the buck converter. The reason for this selection is that most solar cells and fuel cells used for power generation have open circuit voltages and optimal voltage higher than typical inverters or batteries voltages (6,12,24 VDC). Since there is no need to elevate that voltage the buck converter is the better option. A buck-boost converter could also be used as a second choice with the sliding mode control designed.

- Switching Device: Mosfet
    - As for switching device, Mosfet are going to be used. Mosfet offers low input current, low resistance when conducting and high switching speed.

6.2.6 DC Load, DC-AC Inverter and AC Load

For the simulations, dc and ac loads will be composed of resistors, inductors, dc motors, ac motors, capacitors and/or batteries. A 12, 24 or 48VDC/120VAC inverter will be used to produce AC voltage from the DC voltage.

7 HREPS Simulation

In this section the simulation and results of our proposed design are shown. All simulations were done using Matlab TM and Matlab/Simulink TM. This section will include the model of the photovoltaic cells, the model of the fuel cell, the model of the buck converter, the model of the inverter. Simulations are going to be presented for HREPS composed of one, two and three energy system. Also the HREPS will be simulated under different environmental and load conditions to prove its ability to operate under any circumstance.

7.1 Simulation Models

7.1.1 HREPS Simulation Model

As seen in fig 6.1 in chapter 6, our HREPS is composed of two renewable energy power sources, solar cells and fuel cell, three dc-dc converters, four sliding mode controllers and the load. As for the simulation model, the model, with all system interconnected, used to simulate our proposed scheme is shown in figure 7.1. It's composed of a solar cell system, a fuel cell system, four sliding mode controllers, three dc-dc buck converters, battery bank, a capacitor to reduce fast transitions in the voltage at the load, and resistive loads.

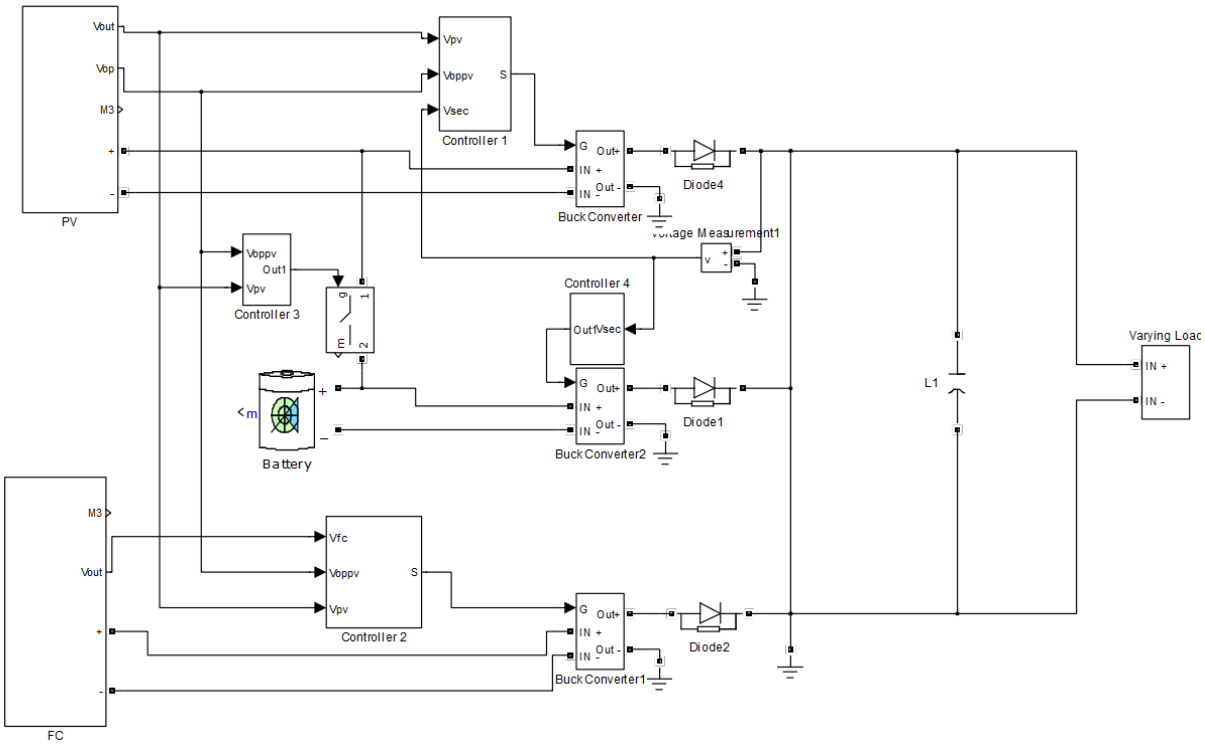

Fig 7.1: Simulation Model of proposed HREPS

7.1.1.1 Photovoltaic Cells Model

For the simulation of photovoltaic cells we used the model found in chapter 2. In chapter 2 the photovoltaic cells are modeled as a current source, which depends on irradiation and temperature, and a capacitor connected in parallel. Figure 7.2 shows the equivalent electrical model of the proposed photovoltaic module:

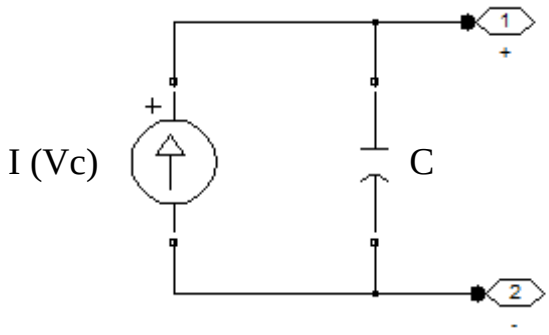

Fig 7.2: Equivalent Electrical Model of proposed PV cell

were I (Vc) is the output current of the PV and C is the capacitance value that simulates the time delay it takes the photovoltaic to reach any voltage level. The simulation model used to simulate the electrical model of the solar cell is shown in figure 7.3.

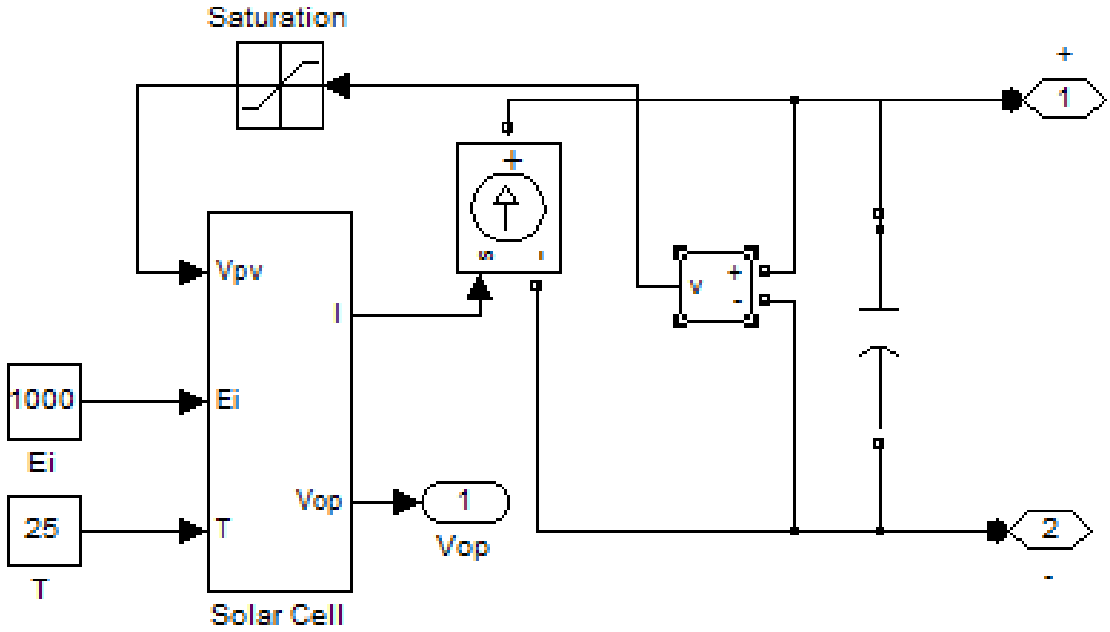

Fig 7.3: Equivalent Simulink Photovoltaic Cell Model

The PV cell model is composed of a subsystem called solar cell, a signal controlled current source, a voltage measurement to measure the voltage at the capacitor and feed it back to the solar cell subsystem, two blocks, *Ei* and *T* corresponding to the effective irradiance and the temperature, and a capacitor. The solar cell subsystem composition is shown in figure 7.4.

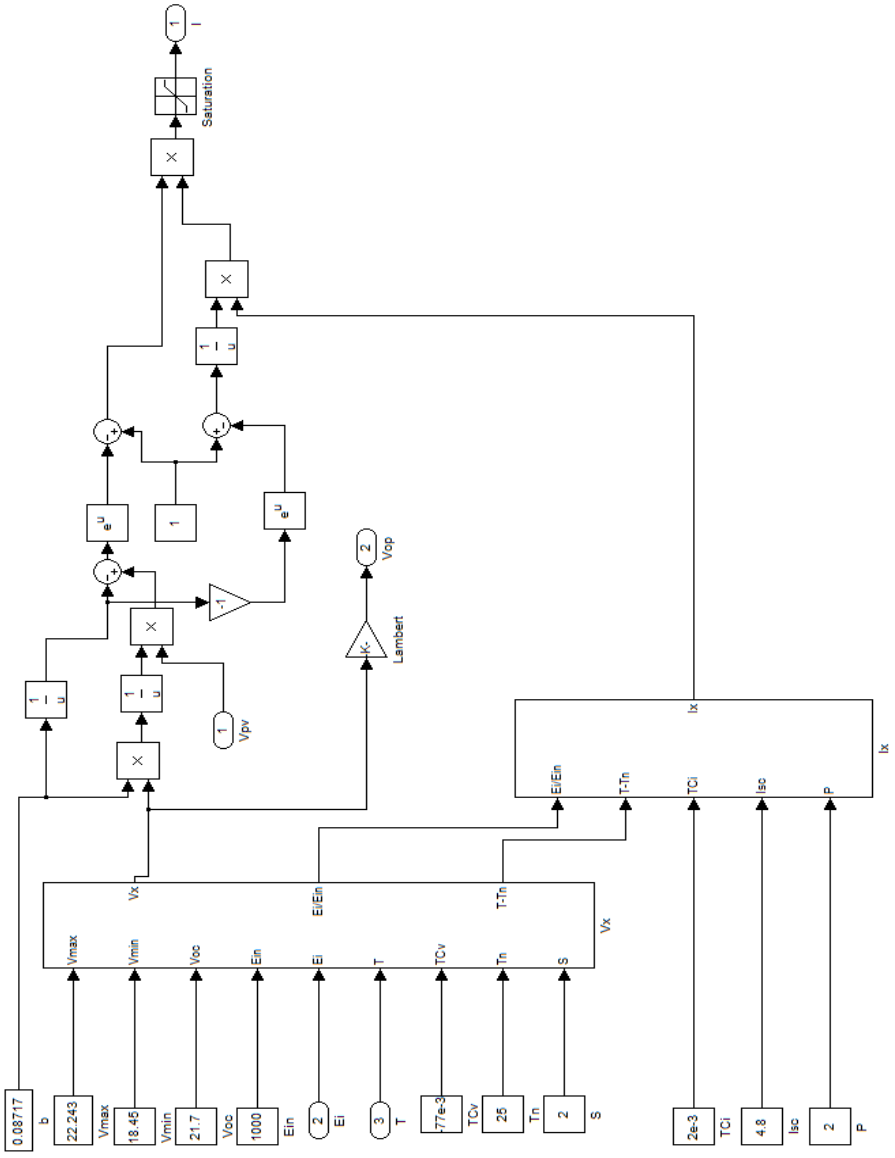

Fig 7.4: Solar Cell Subsystem Composition

7.1.1.2 Fuel Cell Model

For the simulation of fuel cells we used the model discussed in chapter 3. In chapter 3the fuel cells are modeled as a voltage source, an inductor connected in series and a capacitor connected in parallel. Figure 7.5 shows the equivalent electrical model of the proposed fuel cell:

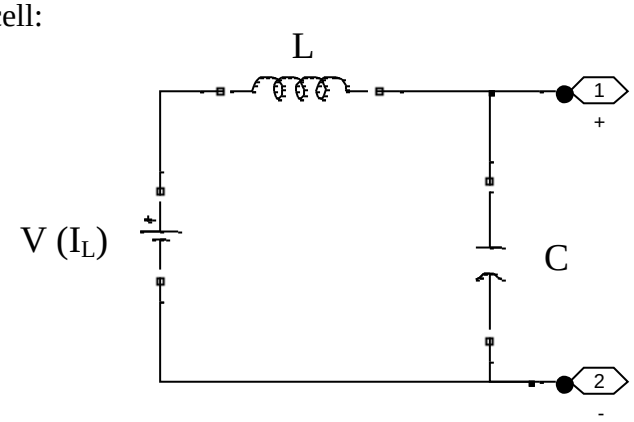

Fig 7.5: Equivalent Electrical Model of proposed Fuel Cell System

were $V(I_L)$ is the FC voltage, L and C are the inductance and capacitance value that simulates the time delay it takes the fuel cell to reach any voltage level. The simulation model used to simulate the electrical model of the fuel cell is shown in figure 7.6.

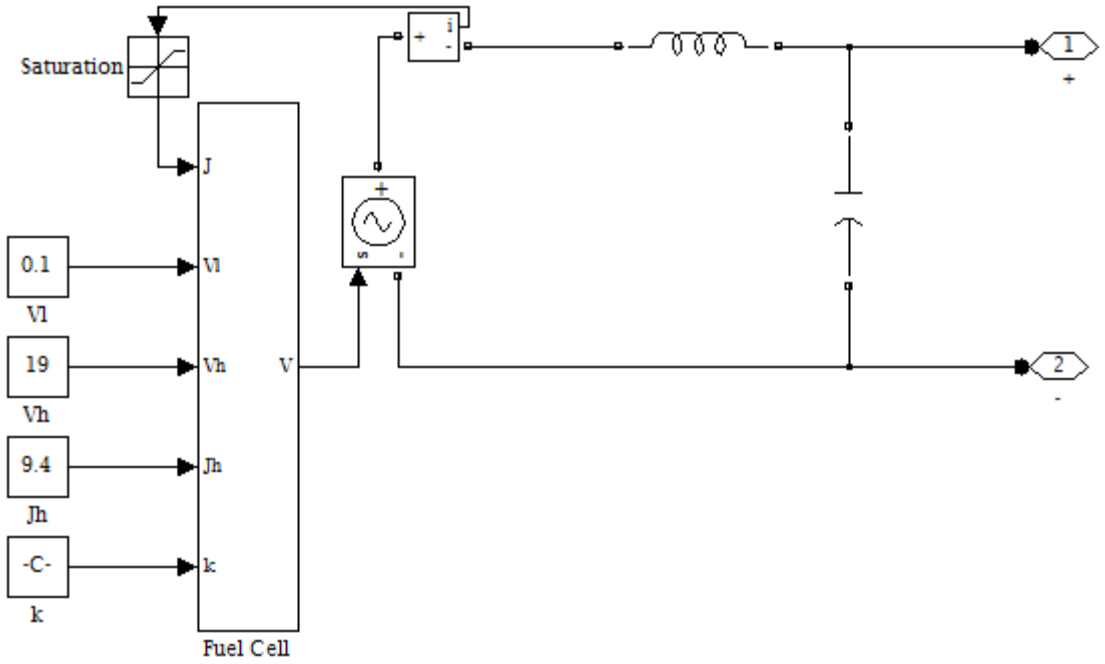

Fig 7.6: Equivalent Simulink Fuel Cell Model

The fuel cell model is composed of a subsystem called fuel cell, responsible of calculating the equations presented at chapter 3, a signal controlled voltage source, a current measurement to measure the current at the inductor and feed it back to the fuel cell subsystem, four blocks, corresponding to the high and low currents and voltages, an inductor and a capacitor. The fuel cell subsystem composition is shown in figure 7.7.

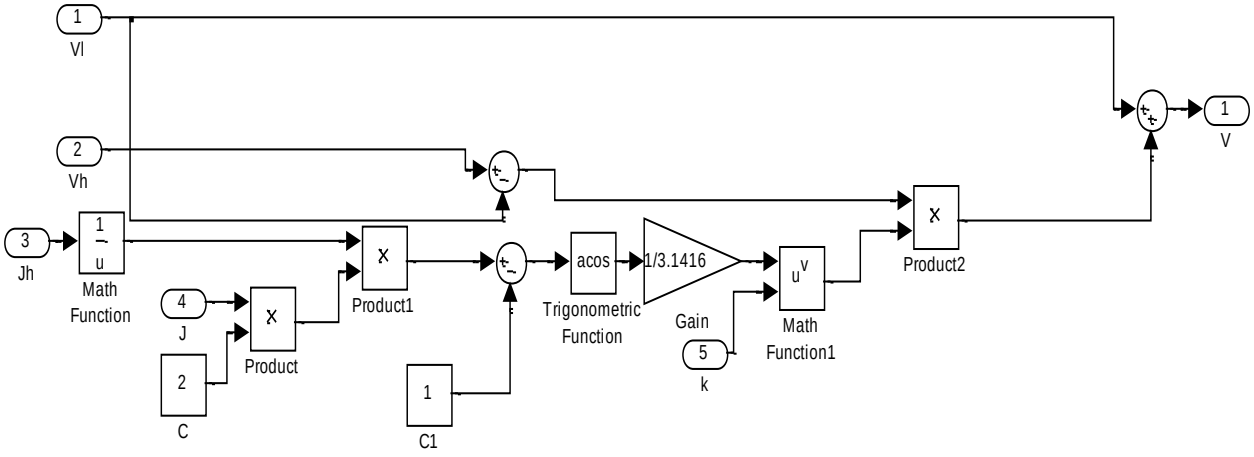

Fig7.7: Fuel Cell Subsystem Composition

7.1.1.3 Sliding Mode Controller Model for Photovoltaic

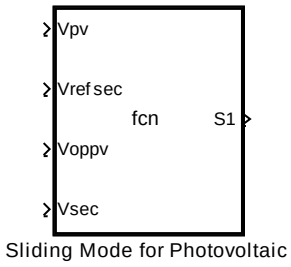

Fig 7.8: Sliding Mode controller block for Photovoltaic

The sliding mode controller for photovoltaic was simulated using simulink blocks interconnected in such a way that execute the proposed control laws. The composition of this block is shown in figure 7.9. The block has four inputs and one output. Vpv is the photovoltaic cell's output voltage, Voppv correspond to the photovoltaic cell's optimal voltage, Vrefsec corresponds to the reference voltage at the output of the dc-dc converter,

Vsec is the voltage at the output of the dc-dc converter and S is the output signal of the controller.

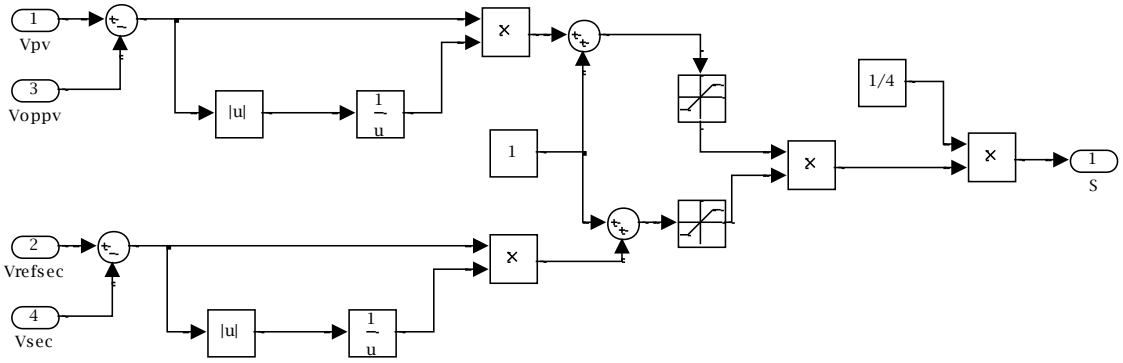

Fig 7.9: Sliding Mode Controller for PV Block Model Composition

7.1.1.4 Sliding Mode Controller for Secondary System

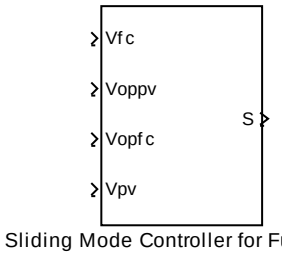

Fig 7.9: Sliding Mode controller block for Secondary System

The sliding mode controller for fuel cell was simulated using simulink blocks interconnected in such a way that execute the proposed control laws. The composition of this block is shown in figure 7.10. The block has four inputs and one output. Vfc is the fuel cell's output voltage, Voppv correspond to the photovoltaic cell's optimal voltage, Vopfc

corresponds to the optimal voltage of the fuel cell, Vpv is the output voltage of the photovoltaic cell and S is the output signal of the controller.

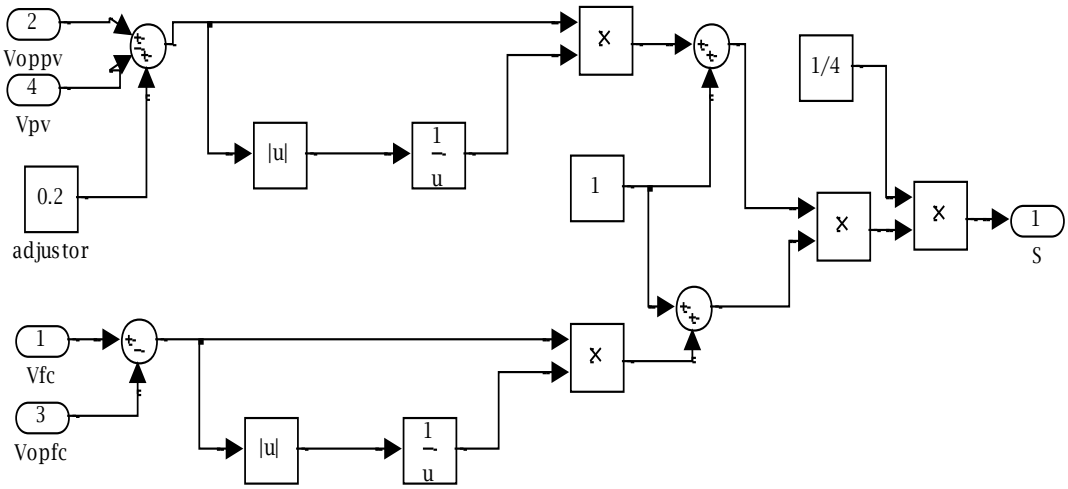

Fig 7.10: Sliding Mode Controller for FC Block Model Composition

7.1.1.5 DC-DC Converter Simulation Block

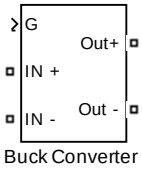

Fig 7.11: DC-DC Converter Block

The DC-DC converter was simulated using the simulink's power system toolbox. The Buck converter topology was used for the simulations. Fig 7.12 shows the simulation elements used to simulate our buck converter.

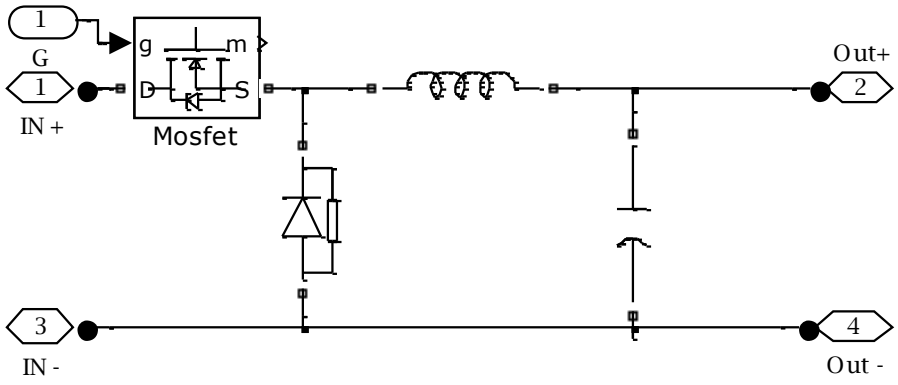

Fig 7.12: DC-DC Converter Model Composition

Our buck converter is switched using a mosfet device. The buck converter simulation block contains 3 inputs and two outputs:

- IN+ = Primary positive input of the buck converter
- IN- = Primary negative input of the buck converter
- Out+ = Secondary positive output of the buck converter
- Out- = Secondary negative output of the buck converter
- G = Mosfet's gate input

7.2 Simulation Results

7.2.1 Optimal Voltage Equation Accuracy

To test the accuracy of our optimal voltage equation, estimations obtained by our equation were compared to the manufactures datasheet, as seen in table 7.1, under standard test conditions and to the values obtained by the photovoltaic model under 600W/m^2 and 35^{o}C, as seen in table 7.2. Error percent for both conditions are low validating the ability of the equation of obtaining a very approximate value.

PV Model	Vop Datasheet	Vop Estimated	Error %	Pmax Datasheet	Pmax Estimated	Error %
Siemens SP75	17.0	17.5937	3.49	74.8	74.815	0.02
Shell SQ80	17.5	18.156	3.74	80.15	80.44	0.36
SLK60M6	30.6	30.762	0.53	209.92	209.777	0.068
Solarex SX-5	16.5	16.673	1.05	4.455	4.449	0.135
SolarexSX-10	16.8	17.098	1.774	9.912	9.8989	0.132

Table 7.1: Comparison between estimated optimal values versus datasheet values at STC

PV Model	Vop Model	Vop Estimated	Error %	Pmax Model	Pmax Estimated	Error %
Siemens SP75	16.5	16.7014	1.22	42.8609	42.7958	0.15
Shell SQ80	17.54	17.7189	2.00	47.33	47.2972	0.06
SLK60M6	29.71	29.8098	0.33	122.4382	122.3257	0.09
Solarex SX-5	13.1	13.3509	1.91	2.1579	2.1519	0.27
Solarex SX-10	15.87	16.17	1.89	5.6419	5.6342	0.13

Table 7.2: Comparison of estimated optimal values versus PV model optimal values at 600W/m^2 and 35^{o}C

7.2.2 HREPS Simulations Results for One Renewable Energy Systems - DC Load

Simulations are presented in the next subsections showing the behavior of a Renewable energy system composed of just one power system. In the simulations is shown the two operation modes of the primary controller and how it improves the behavior of the PV system when comparing it to the response of the system connected directly to the load.

7.2.2.1 Voltage Regulation Operating Mode

In this subsection we are going to simulate our system to test the ability of our proposed controller to regulate the load's voltage to a reference voltage level. This sub section also shows simulations on how the proposed controller behaves under certain load conditions. Comparisons with a directly connected system are also shown.

For the voltage regulation operating mode simulations, we used the following specifications:

- Siemens SP75 Solar Module (See AppendixA1 for specs)
- DC-DC Buck converter
- Solar Irradiance : 1000W/m^2
- Temperature: 25^oC
- Desired Voltage Level: 12VDC

As established before, to operate in Voltage-Regulation Mode the following relation must be satisfied:

$$R \geq \frac{V_{REFMAX}^{\ 2}}{P_{\max}} \Rightarrow R \geq \frac{12^2}{74.8} \Rightarrow R \geq 1.925$$

Figure 7.13 shows the simulation of a PV module with our proposed controller under different resistance values where it should exhibit voltage regulation. The simulation was conducted by connecting a PV module, through a controlled buck converter, to a resistive load and the same PV module directly to the resistive load. The resistive load was varied the following way:

Time (s)	Resistance (ohms)
0.01	20
0.02	10
0.03	5
0.04	2.5

Table 7.3: Variation of resistance for One Renewable energy DC system inVRM

As seen in the figure, the load voltage without a controller varies dramatically with each variation of the load creating unregulated voltage and power irregularities. With our controller, the load voltage kept regulated at the desired fixed value for each variation of the load.

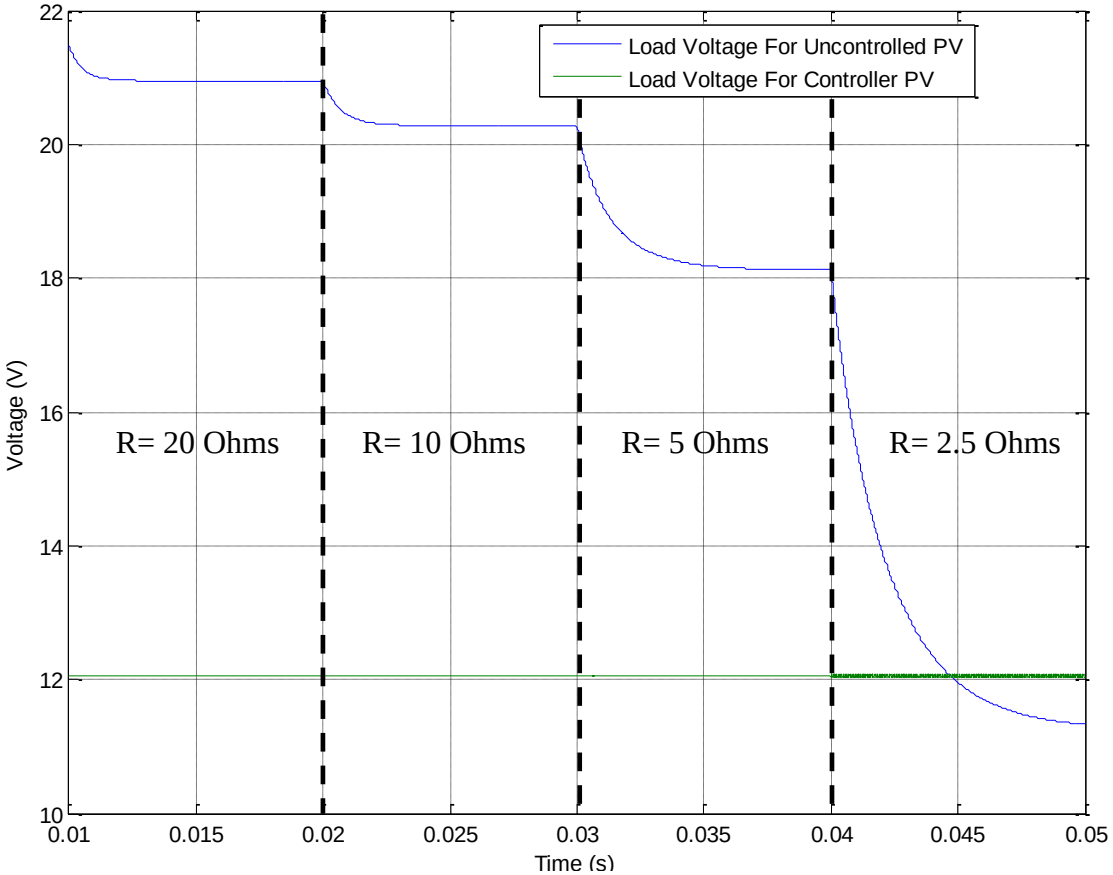

Fig 7.13: Controlled vs. Uncontrolled Load Voltage for PV Cell in VRM

In figure 7.14 is shown how the controller's duty cycle behave and respond to changes in the load. It can be seen that, as the load's power demand increase, the duty cycle increases and will continue to increase until it reaches to one. In other words, the photovoltaic module voltage, if not controlled, eventually is going to be equal to the load's voltage.

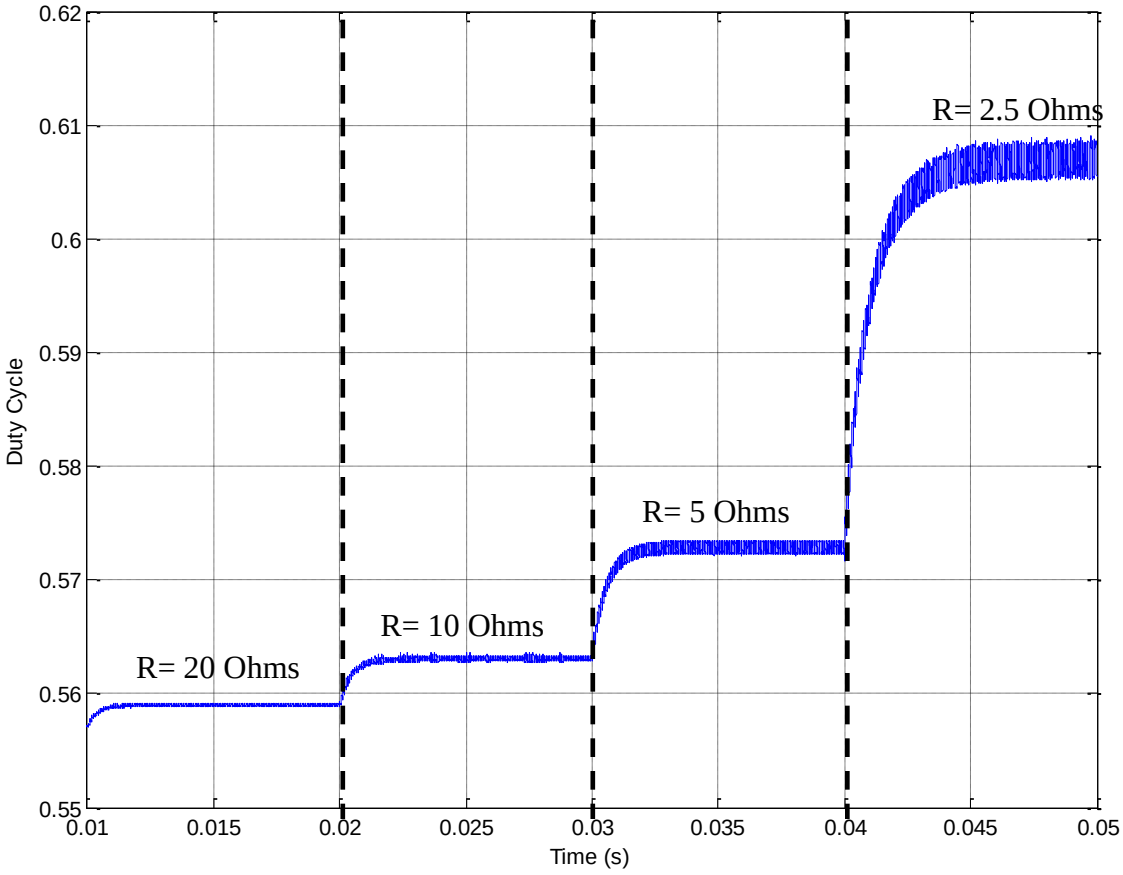

Fig 7.14: Duty Cycle Behavior of a PV Cell in Voltage Regulation Operation Mode

7.2.2.2 Maximum Power Operating Mode

In this subsection we are going to simulate our system to test the ability of our proposed controller to force the system to operate at its maximum power. This sub section also shows simulations on how the proposed controller behaves under certain load conditions. Comparisons with a directly connected system are also shown.

For this operating mode simulation, we used the following specifications:

- Primary System: Siemens SP75 Solar Module (See Appendix A1 for specs)
- DC-DC Buck converter
- Solar Irradiance : 1000W/m^2
- Temperature: 25^oC
- Desired Voltage Level: 12VDC

As established before, to operate in Maximum Power Mode-Active Mode the following relation must be satisfied:

$$R \leq \frac{V_{REFMAX}^{\ 2}}{P_{\max}} \Rightarrow R \leq \frac{12^2}{74.8} \Rightarrow R \leq 1.925$$

When operating at load conditions where its value is less than 1.925, our controller must force our system to operate at its maximum power without considering voltage regulation.

Figure 7.15 shows the simulation of a PV module with our proposed controller under different resistance values where it should operate at maximum power mode. The simulation was conducted by connecting a PV module, through a controlled buck converter, to a resistive load and the same PV module directly to the resistive load. The resistive load was varied the following way:

Time (s)	Resistance (Ohms)
0.01	1.8
0.02	1.6
0.03	1.4
0.04	1.2

Table 7.4: Variation of resistance for One Renewable energy DC system in MPM

As seen in the figure, both controlled and uncontrolled load voltage varies significantly with each load variation creating unregulated voltage. It's also noted that the controlled load voltage variations are not as much as without the controller meaning that a higher power is produced with the controlled PV than with the uncontrolled PV.

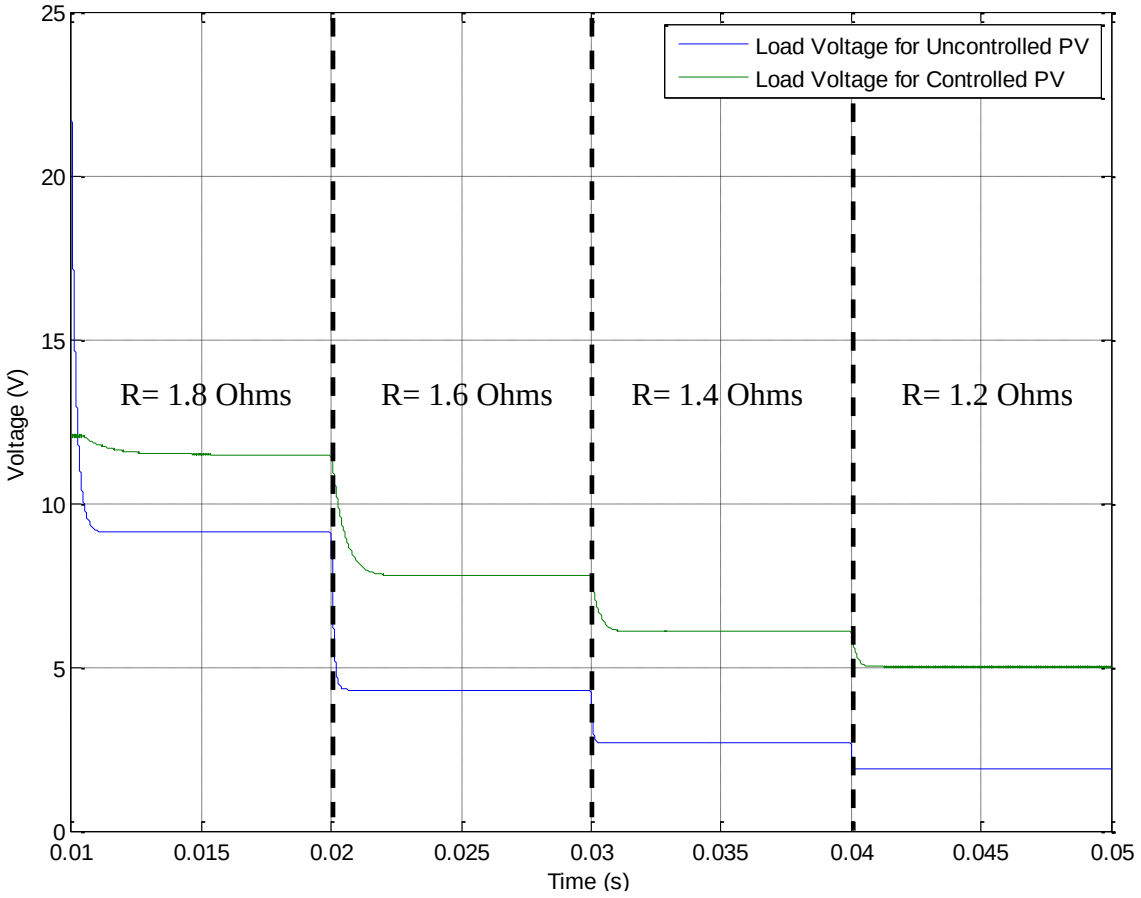

Fig 7.15: Comparison of Load Voltage for a Controlled and Uncontrolled System

Figure 7.16 shows the comparison of the output voltage of the PV with and without the controller. It is noted that the output voltage of the controlled PV module is forced to operate at its optimal voltage guarantying a maximum power operation. Without the controller the PV voltage pass the voltage where it exhibits its maximum power and keep falling to other voltage values where the power is not a maximum.

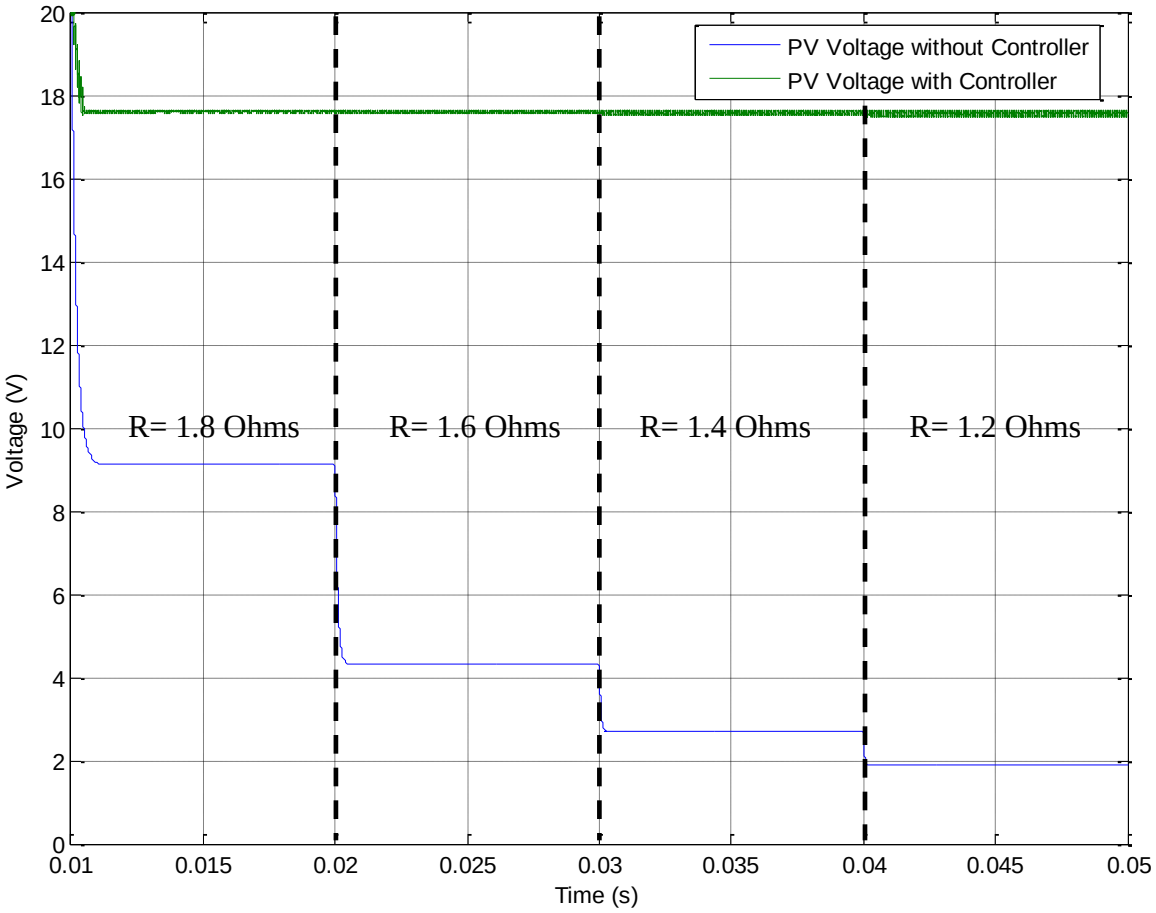

Fig 7.16: Comparison of PV Output Voltage for a Controlled and Uncontrolled System

Figure 7.17 shows a comparison of the power produced by the PV system connected to the varying load through our controller and the power produced by a PV system when connected directly to the same varying load. As shown, our controller forces the PV system to operate at is maximum power for any variation of the load while connected directly, the power generated is lower and decrease every time the load value decrease.

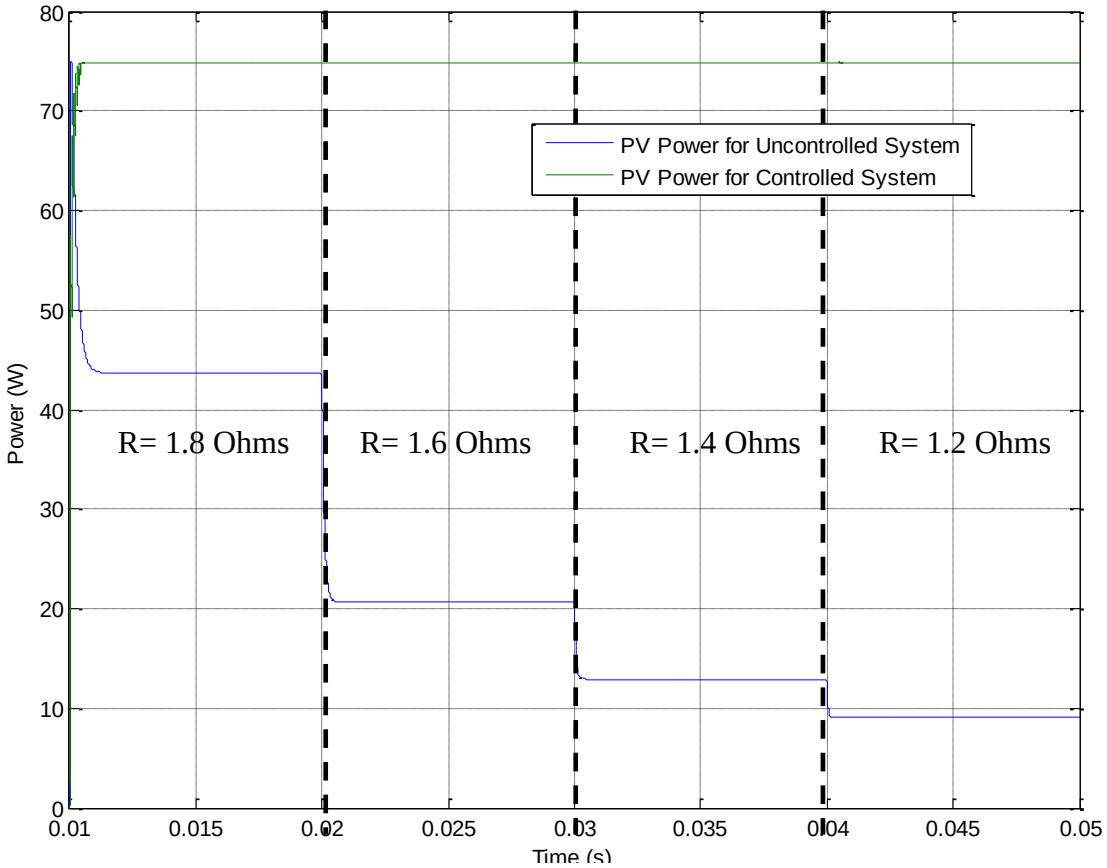

Fig 7.17: Comparison of Load Power for a Controlled and Uncontrolled System

7.2.3 HPRES Simulations Results For One Renewable Energy Systems Operation Modes- AC Load

Simulations are presented in the next subsections validating our controller ability to operate at each operating modes when the load's voltage is AC.

7.2.3.1 Voltage Regulation Operating Mode

In this subsection simulations are presented to test the ability of our proposed controller to regulate the load's voltage to a reference voltage level under AC load voltage. This sub section also shows simulations on how the proposed controller behaves under certain load conditions.

For the voltage regulation operating mode simulations, we used the following things:

- Siemens SP75 Solar Module (See AppendixA1for specs)
- DC-DC Buck converter
- Solar Irradiance : 1000W/m^2
- Temperature: 25^{o}C
- Desired Voltage Level: 120 VAC_{RMS} @60Hz(12VDC at the inverter's input)

As established before, to operate in Voltage-Regulation Mode the following relation must be satisfied:

$$R \geq \frac{V_{REFMAX}{}^2}{P_{\max}} \Rightarrow R \geq \frac{170^2}{74.8} \Rightarrow R \geq 386.36$$

Figure 7.18 shows the simulation of a PV module with our proposed controller under different resistance values where it should exhibit voltage regulation. The simulation was conducted by connecting only the PV module, through a controlled buck converter, to a 12VDC/120VAC Inverter to a resistive load. The load vas varied the following way:

Time (s)	Resistance (Ohms)
0.01	450
0.02	440
0.03	430
0.04	420

Table 7.5: Variation of resistance for One Renewable energy AC system in VRM

As shown, the load voltage kept regulated at the reference value for each variation of the load to ensure that the output AC voltage level is 120VAC and validating the ability of our controller to operate successfully under variation of the load and the voltage. Our controller was able to keep a constant DC voltage at the output of the DC/DC converter with a varying input.

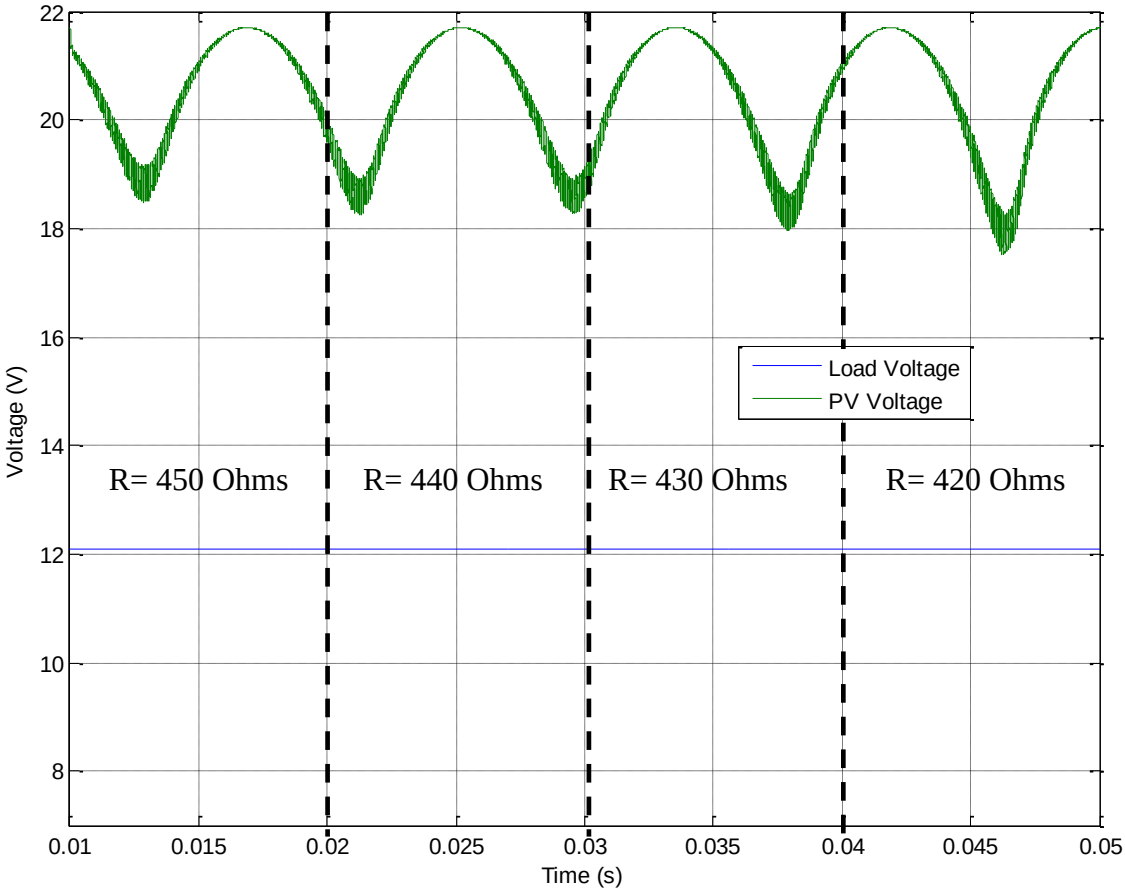

Fig 7.18: Behavior of the Voltages under AC Voltage Regulation Operation Mode

In figure 7.19 is shown how the PV output power behaves to changes in the load. As shown in the figure, our controller was able to adjust to each variation of the load and with the variation of the voltage to provide the required power for each instant of time validating the ability of our controller to operate under dynamic conditions.

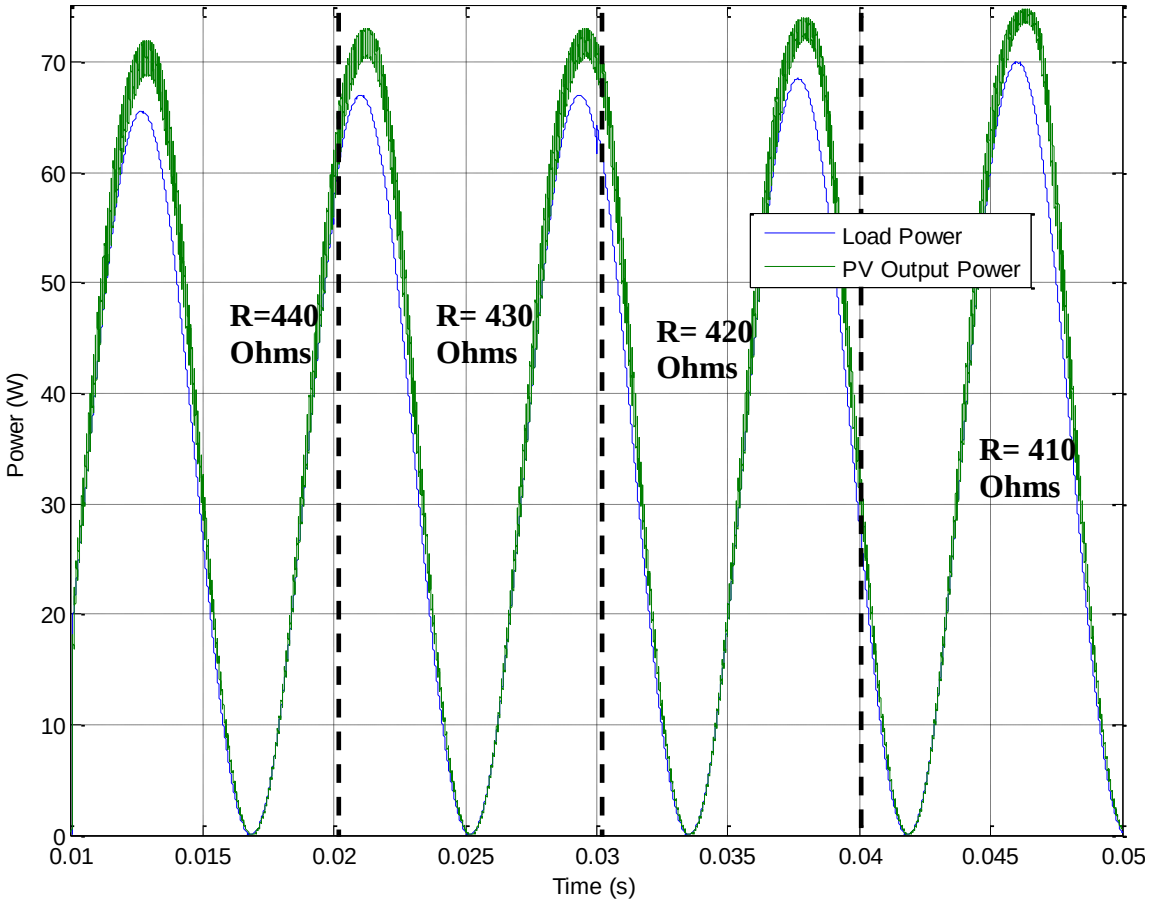

Fig 7.19: Behavior of Power under AC Voltage Regulation Operation Mode

7.2.3.2 Maximum Power Operating Mode

In this subsection simulations are presented to test the ability of our proposed controller to operate at its maximum power whenever it is required to. This sub section also shows simulations on how the proposed controller behaves under certain load conditions.

For these operating mode simulations, we used the following things:

- Primary System: Siemens SP75 Solar Module (See AppendixA1 for specs)
- DC-DC Buck converter
- Solar Irradiance : 1000W/m^2
- Temperature: 25^oC
- Desired Voltage Level: 120VAC_{RMS}@60Hz

As established before, to operate in Maximum Power Mode-Active Mode the following relation must be satisfied:

$$R \leq \frac{V_{REFMAX}{}^2}{P_{\max}} \Rightarrow R \leq \frac{170^2}{74.8} \Rightarrow R \leq 386.36$$

When operating at load conditions where its value is less than 386.36, our controller must force our system to operate at its maximum power without considering voltage regulation.

Figure 7.20 shows the simulation of a PV module with our proposed controller under different resistance values where it should exhibit maximum power. The simulation was conducted by connecting only the PV module, through a controlled buck converter and a inverter, to a resistive load. The resistive load was varied the following way:

Time (s)	Resistance (Ohms)
0.01	300
0.02	280
0.03	260
0.04	240

Table 7.6: Variation of resistance for One Renewable energy AC system in MPM

As can be seen, our controller was able to maintain the regulation of the load voltage until it reach a point e power where the power demanded is higher that the PV maximum power. When that point is reached our system switch to maximum power mode where the load voltage gets unregulated and the PV voltage is fixed at the optimal voltage, as it can be seen.

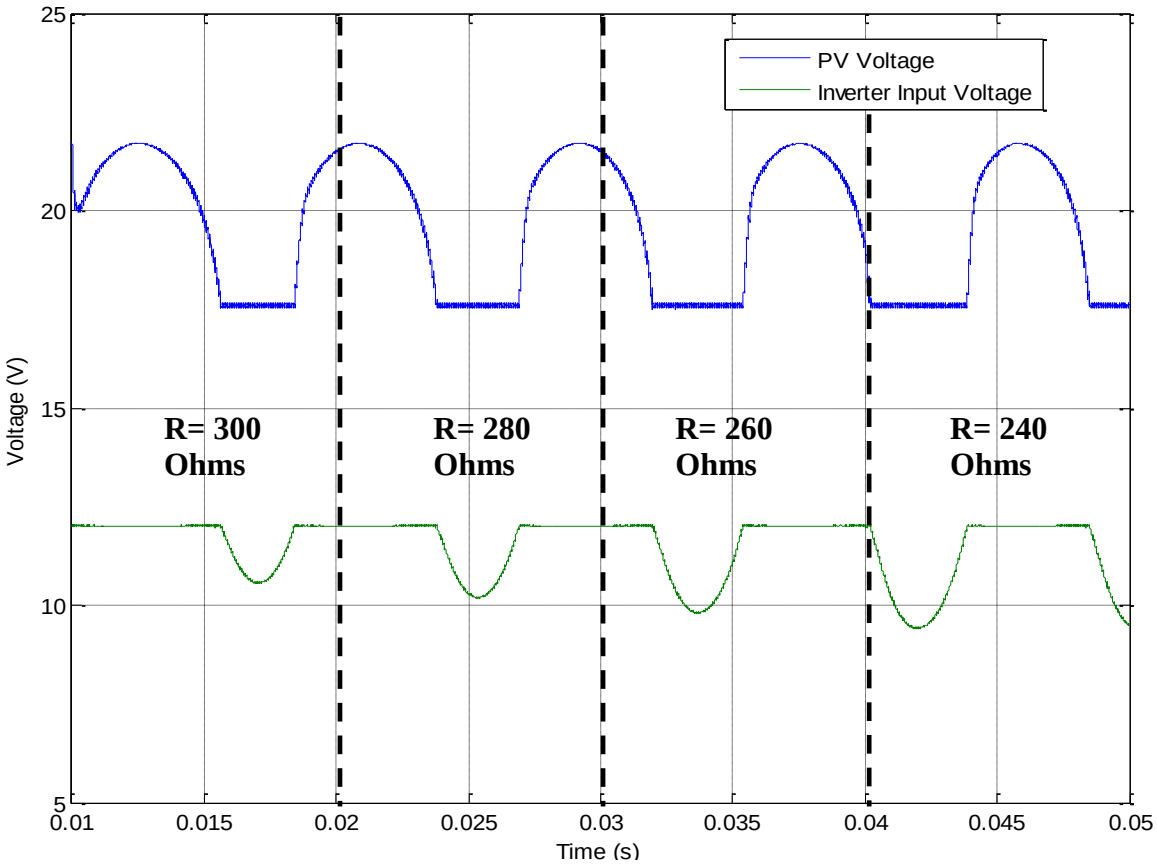

Fig 7.20: Behavior of the Voltages under AC Maximum Power Mode

Figure 7.21 shows the behavior of the power produced by the PV module and the load power. As it can be seen, the PV module produces the power required until it reaches its maximum power and it stays there until the power required drops below the maximum power value validating the ability of our controller in forcing the system to operate at its maximum power when it reaches it.

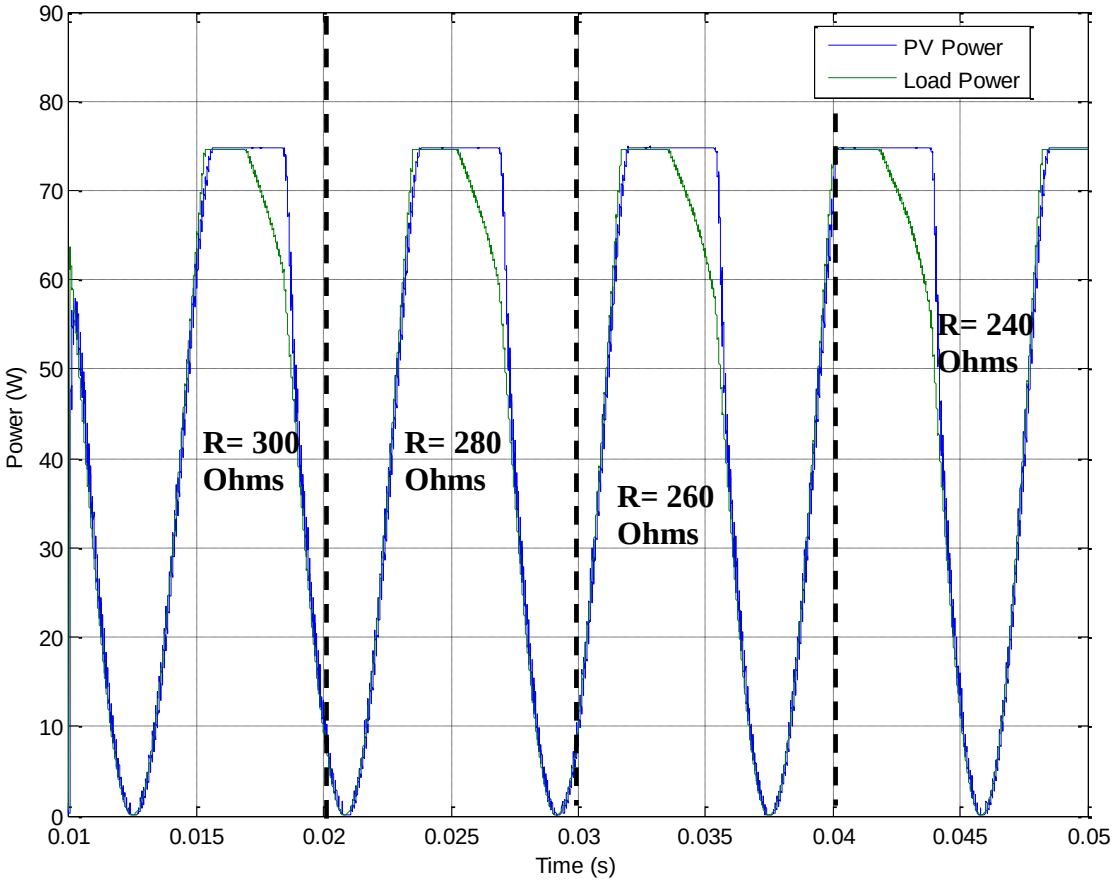

Fig 7.21: Behavior of Power under AC Maximum Power Mode

7.2.4 HPRES Simulations Results for Two Renewable Energy Systems - DC Load

Simulations were done to prove the efficacy of our proposed control system in achieving the proposed operations modes when two renewable energy systems are interconnected. Simulations are shown in the following sub sections validating the abilities of our control scheme.

7.2.4.1 Voltage Regulation/Off-State Operating Mode

In this subsection simulations are presented validating the ability of our proposed controller to regulate the load's voltage to a reference voltage level with auxiliary system connected. Simulations are also presented to show the behavior of our system under certain load conditions.

For the voltage regulation operating mode simulations, we used the following things:

- Siemens SP75 Solar Module (See Appendix A1for specs)
- Horizon H100 Fuel Cell (See Appendix B1 for specs)
- DC-DC Buck converter
- Solar Irradiance : 1000W/m^2
- Temperature: 25^oC
- Desired Voltage Level: 12VDC

As established before, to operate in Voltage-Regulation Mode the following relation must be satisfied:

$$R \geq \frac{V_{REFMAX}^{\ 2}}{P_{\max}} \Rightarrow R \geq \frac{12^2}{74.8} \Rightarrow R \geq 1.925$$

Figure 7.22 shows the simulation of a PV module with our proposed controller under different resistance values where it should exhibit voltage regulation. The simulation was conducted by connecting only the PV module, through a controlled buck converter, to a resistive load and a fuel cell, through a controlled buck converter. The load was varied the following way:

Time (s)	Resistance (Ohms)
0.00	40
0.01	20
0.02	10
0.03	5
0.04	2.5

Table 7.7: Variation of resistance for Two Renewable energy DC system in VRM

The FC is not operating in this mode so its voltage will be equal to its open circuit voltage, as shown in the figure. We can see that our controller was able to regulate the dc voltage, which goes into the inverter, to the reference value validating the ability of our controller to regulate the voltage and controlling the power generation of two systems.

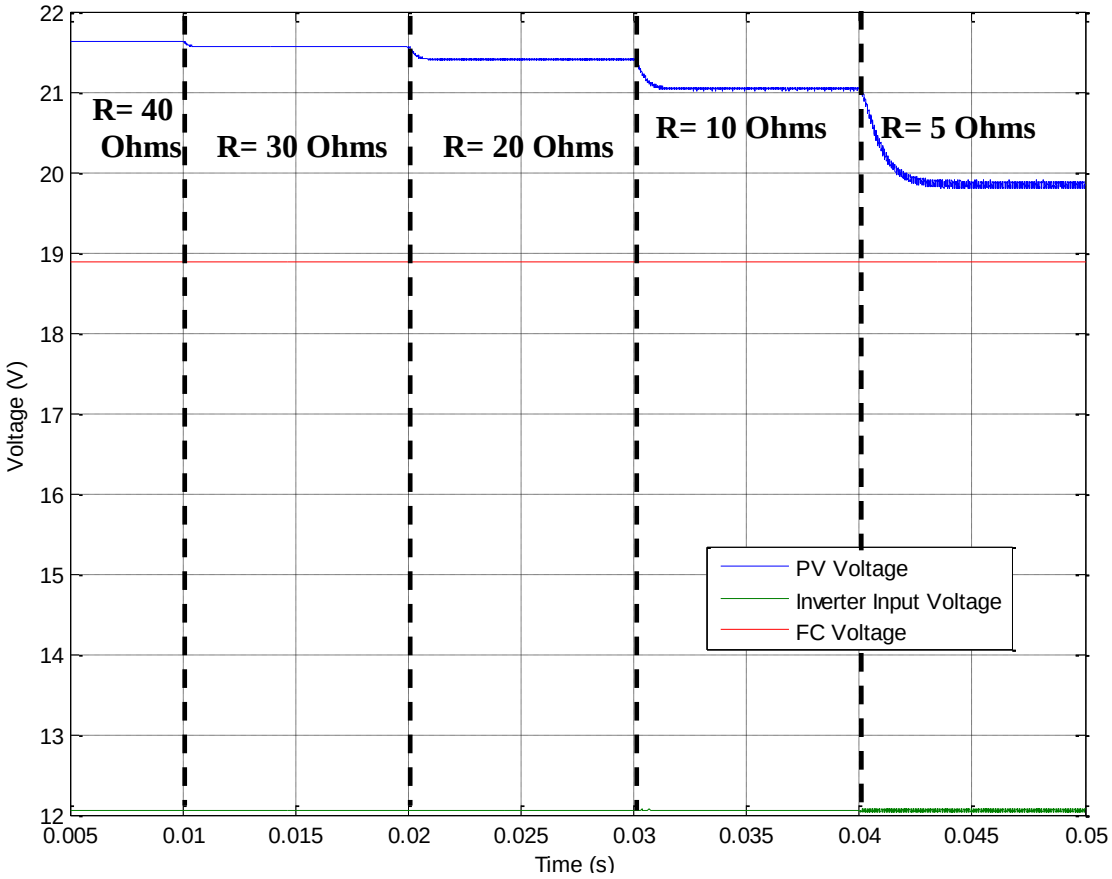

Fig 7.22: Voltages Behaviors for Two Renewable Energy System under VRM

Fig 7.23 shows the power generation of each system. As noted the power generated by the FC is zero since the primary system can provide all the necessary power. We can also see that for each variation of the load, the power also increase validating the ability of our controller to extract the necessary amount of power to supply the load.

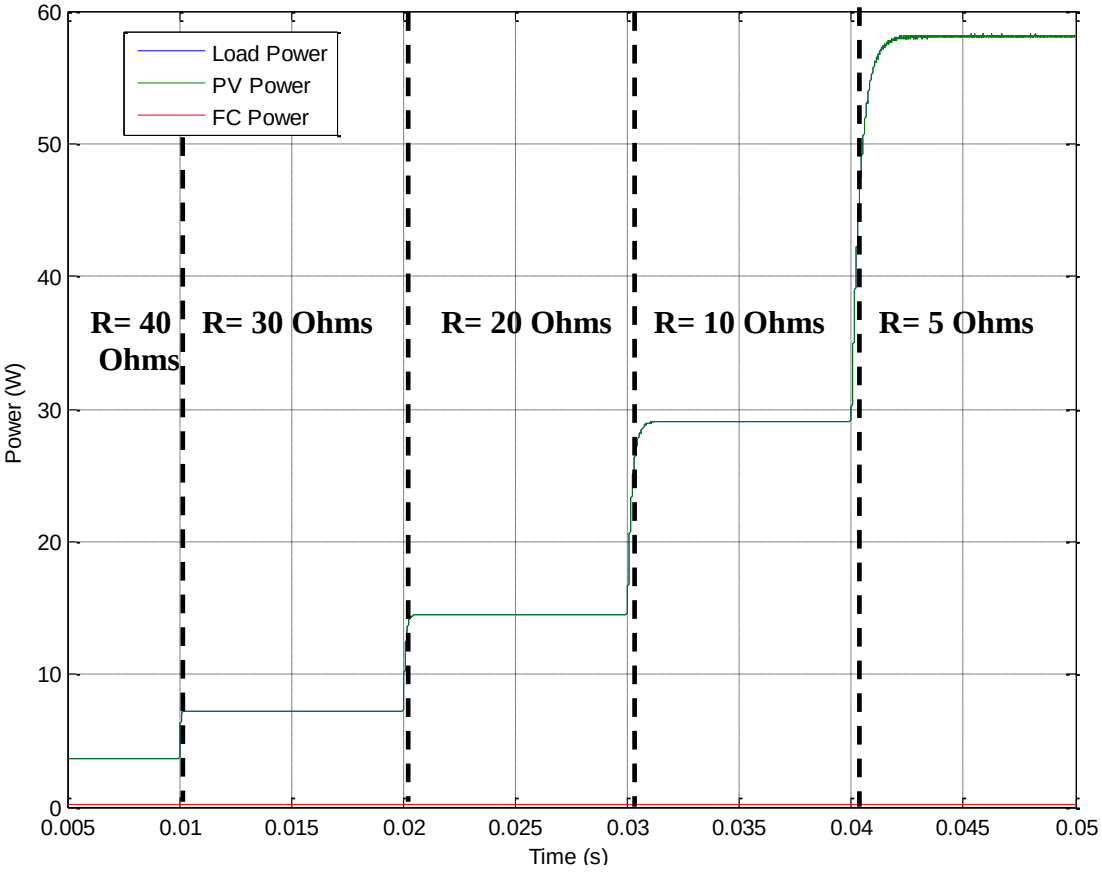

Fig 7.23: Power Behaviors for Two Renewable Energy System under VRM

7.2.4.2 Maximum Power /Active Mode Operating Mode

In this subsection simulations are presented validating the ability of our proposed controllers to regulate the load's voltage to the reference voltage level by extracting the additional power from the auxiliary system. Simulations are also presented to show the behavior of our system under certain load conditions.

For these operating mode simulations, we used the following things:

- Primary System: Siemens SP75 Solar Module (See Appendix A1 for specs)
- Secondary System: Horizon H-100 Fuel Cell (See Appendix B1 for Specs)
- DC-DC Buck converter
- Solar Irradiance : 1000W/m^2
- Temperature: 25^{o}C
- Desired Voltage Level: 12VDC

As established before, to operate in Maximum Power Mode-Active Mode the following relation must be satisfied:

$$R \leq \frac{V_{REFMAX}{}^2}{P_{\max}} \Rightarrow R \leq \frac{12^2}{74.8} \Rightarrow R \leq 1.925$$

When operating at load conditions where its value is less than 1.925, our controller must force our system to operate at its maximum power without considering voltage regulation.

Figure 7.24 shows the simulation of a PV and FC with our proposed controller under different resistance values where it should exhibit maximum power operation mode for the primary controller and active mode for the secondary controller. The simulation was conducted by connecting only the PV module, through a controlled buck converter, to a resistive load. The load was varied the following way:

Time (s)	Resistance (Ohms)
0.01	1.8
0.02	1.6
0.03	1.4
0.04	1.2

Table 7.8: Variation of load for Two Renewable Energy DC systems in MRM/AM

As shown, the load voltage is regulated at the reference value and did not show significant variation regarding the variation of the load validating the ability of our controllers in regulating the voltage to a reference value given disturbances or variations in the load. Also can be seen that our controller forced the primary system to operate at its optimal voltage and turned on the second system to provide the necessary extra current required validating the ability of our controllers to automatically adjust to the required operating mode.

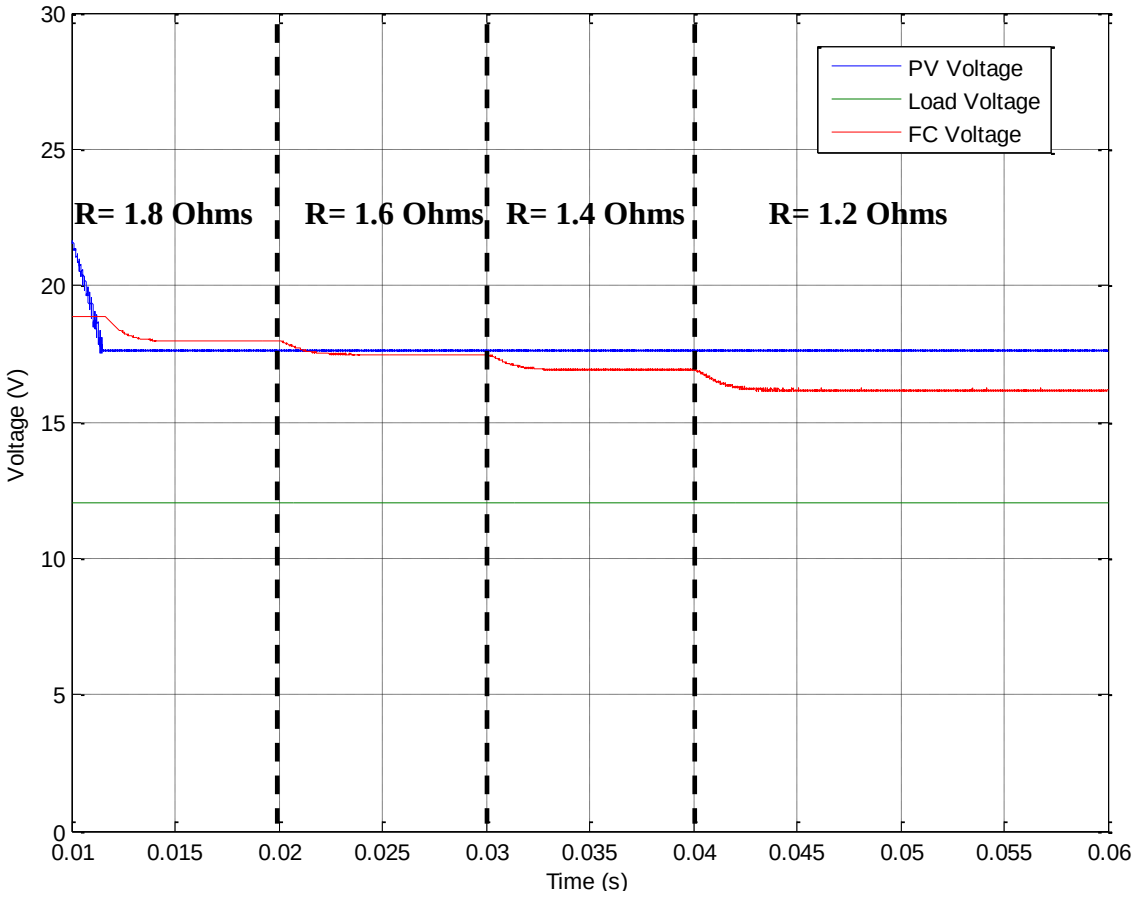

Fig 7.24: Voltages Behaviors for Two Renewable Energy System under VRM/AM

Figure 7. 25 show the behavior of the power generation of the systems. As it can be seen the primary system is operating at maximum power and the secondary system is providing the necessary power required to keep the system working at the required voltage. This simulation validates the ability of our system to control the power generation of two renewable energy systems.

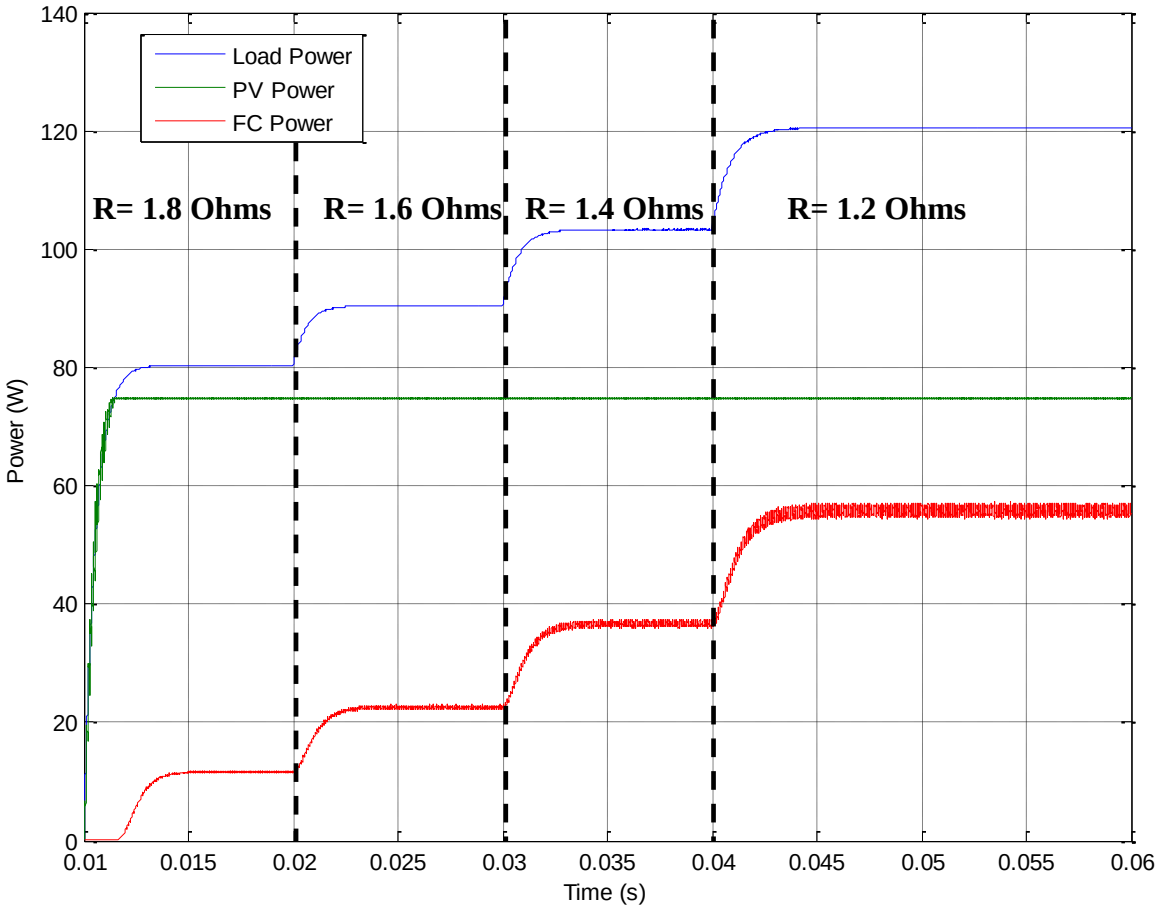

Fig 7.25: Voltages Behaviors for Two Renewable Energy System under VRM/AM

7.2.4.3 Switching from Operating Modes- DC Load

In this subsection, simulations are presented to validate the ability of our proposed controller to automatically switch from the operation modes. This sub section also shows simulations, as a stand-alone system, on how the proposed controller behaves under changes in the load conditions.

For these operating mode simulations, we used the following things:

- Primary System: Siemens SP75 Solar Module (See Appendix A1for specs)
- Secondary System: Horizon H-100 Fuel Cell (See Appendix B1 for Specs)
- DC-DC Buck converter
- Solar Irradiance : 1000W/m^2
- Temperature: 25^oC
- Desired Voltage Level: 12VDC

In order to force the system to change from one operating mode to another, the load has to be varied from value higher than $\frac{V_{REFMAX}^{\ 2}}{P_{\max}}$ to a value lower than $\frac{V_{REFMAX}^{\ 2}}{P_{\max}}$. For this simulation we varied the load as shown in table 7.9:

Resistance (Ohms)	Time(ms)
20	10
10	20
5	30
2.5	40
1.125	50
0.5625	60
0.28125	70
0.1406	80

Table 7.9: Resistive Load Variation for Simulation of Operating Mode Switching

In figure 7.26 is shown the behavior of the voltage of the load and the two renewable systems for each variation of the load. As can be seen, for load values higher than $\frac{V_{REFMAX}{}^2}{P_{\max}}$,the fuel cell system was not activated, so its output voltage is its open circuit voltage. As for the photovoltaic cell, the voltage was dropping down for each load variation until it gets to the optimal voltage value and stays there for all the time being. That point is where the primary system changes from its first operation mode to its second mode or, in other words, where the load value is smaller than $\frac{V_{REFMAX}{}^2}{P_{\max}}$. It can also be seen that once the primary system switch to its second operation mode, the secondary system gets activated and begin operating at its primary mode. From there it can be seen that its voltage start to drop and eventually it'll get to its optimal voltage point. As for the load voltage, the value stayed constant and regulated for each variation of the load.

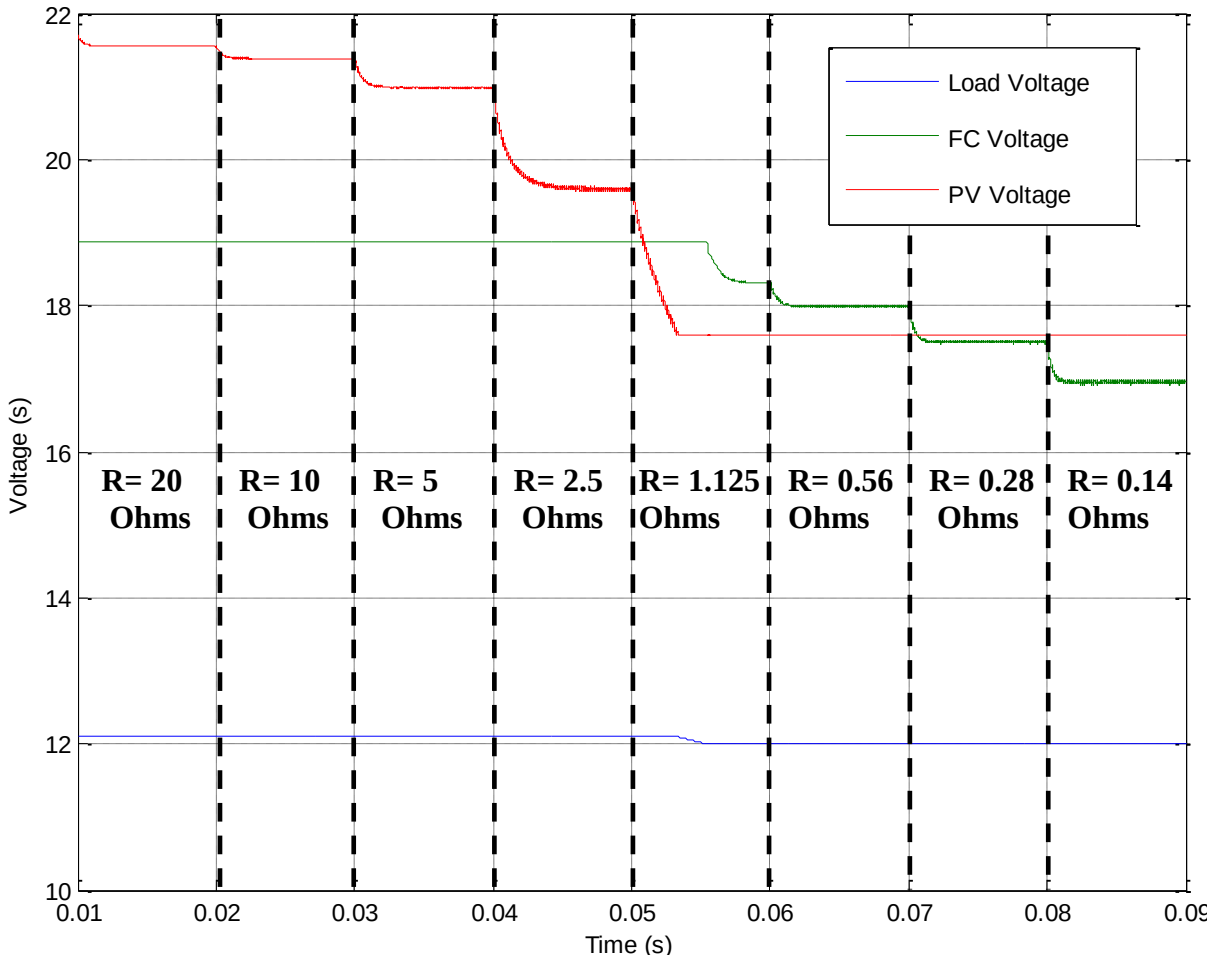

Fig 7.26: Voltage Behaviors of proposed system under Changing of Operation Mode

Figure 7.27 shows the behavior of the power generated by each system. As can be seen the first system to be activated is the PV, the primary system, and is not until it reaches its maximum power that the FC, the secondary system, gets activated. This simulation validates the ability of our system to automatically switch from operation modes as the load a condition varies.

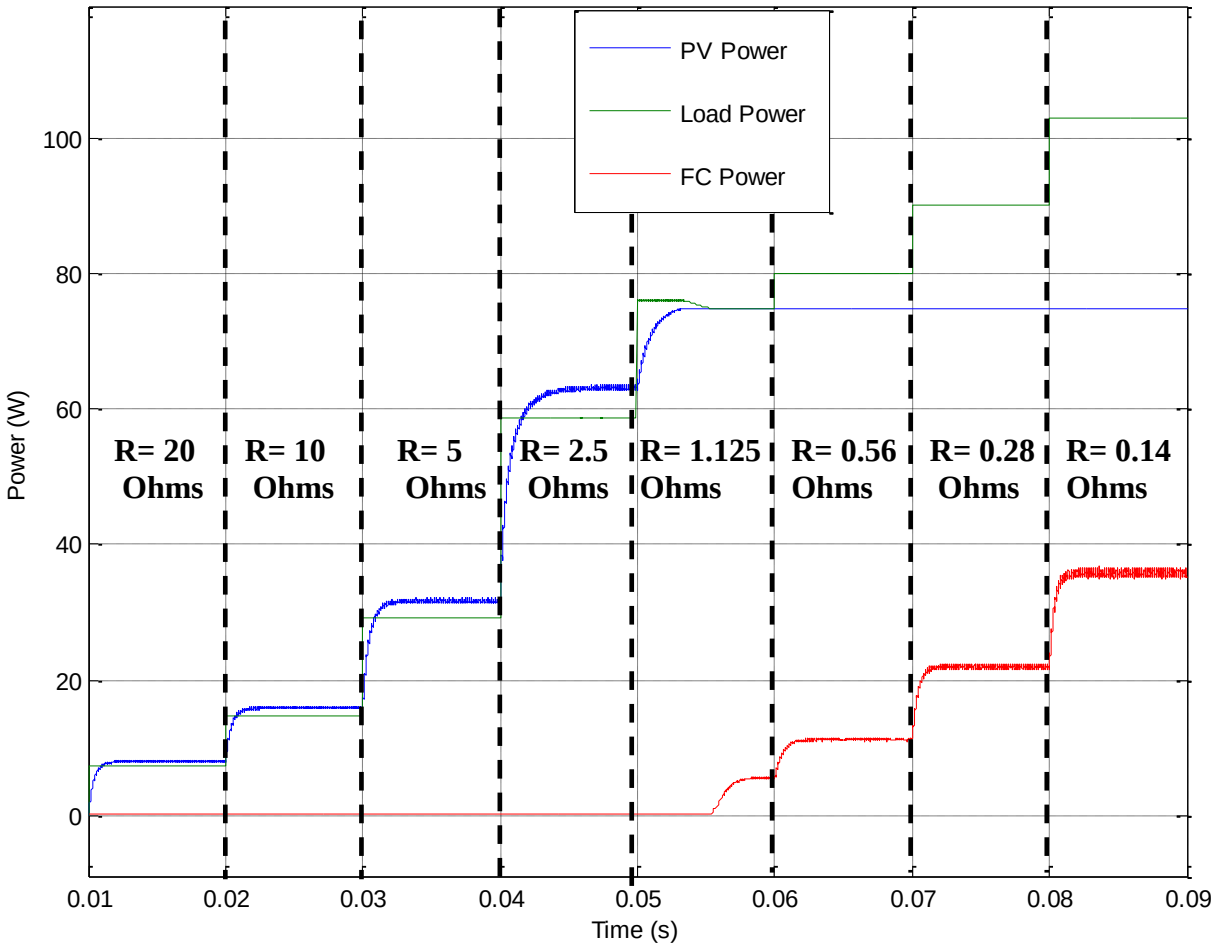

Fig 7.27: Power Behaviors of Proposed System under Changing of Operation Modes

7.2.5 HPRES Simulations Results for Two Renewable Energy Systems - AC Load

Simulations were done to prove the efficacy of our proposed model in achieving the proposed operations modes. Simulations are shown in the following sub sections validating the abilities of our control scheme.

7.2.5.1 Voltage Regulation/ Off-State Operating Mode

In this subsection we are going to simulate our system to test the ability of our proposed controller to regulate the load's voltage to a reference voltage level with auxiliary system connected. This sub section also shows simulations on how the proposed controller behaves under certain load conditions.

For the voltage regulation operating mode simulations, we used the following things:

- Siemens SP75 Solar Module (See Appendix A1 for specs)
- Horizon H100 Fuel Cell (See Appendix B1 for specs)
- DC-DC Buck converter
- Solar Irradiance : 1000W/m^2
- Temperature: 25^oC
- Desired Voltage Level: 120VAC@60Hz (12VDC at the input of the inverter)

As established before, to operate in Voltage-Regulation Mode the following relation must be satisfied:

$$R \geq \frac{V_{REFMAX}^{\ 2}}{P_{\max}} \Rightarrow R \geq \frac{170^2}{74.8} \Rightarrow R \geq 386.36$$

Figure 7.28 shows the simulation of a PV module with our proposed controller under different resistance values where it should exhibit voltage regulation. The simulation was conducted by connecting only the PV module, through a controlled buck converter, to a 12VDC/120VAC Inverter to a resistive load. The load vas varied the following way:

Time (s)	Resistance (Ohms)
0.01	450
0.02	440
0.03	430
0.04	420

Table 7.10: Variation of resistance for Two Renewable energy AC system in VRM

As shown, the load voltage kept regulated at the reference value for each variation of the load to ensure that the output AC voltage level is 120VAC and validating the ability of our controller to operate successfully under variation of the load and the voltage. Our controller was able to keep a constant DC voltage at the output of the DC/DC converter with a varying input.

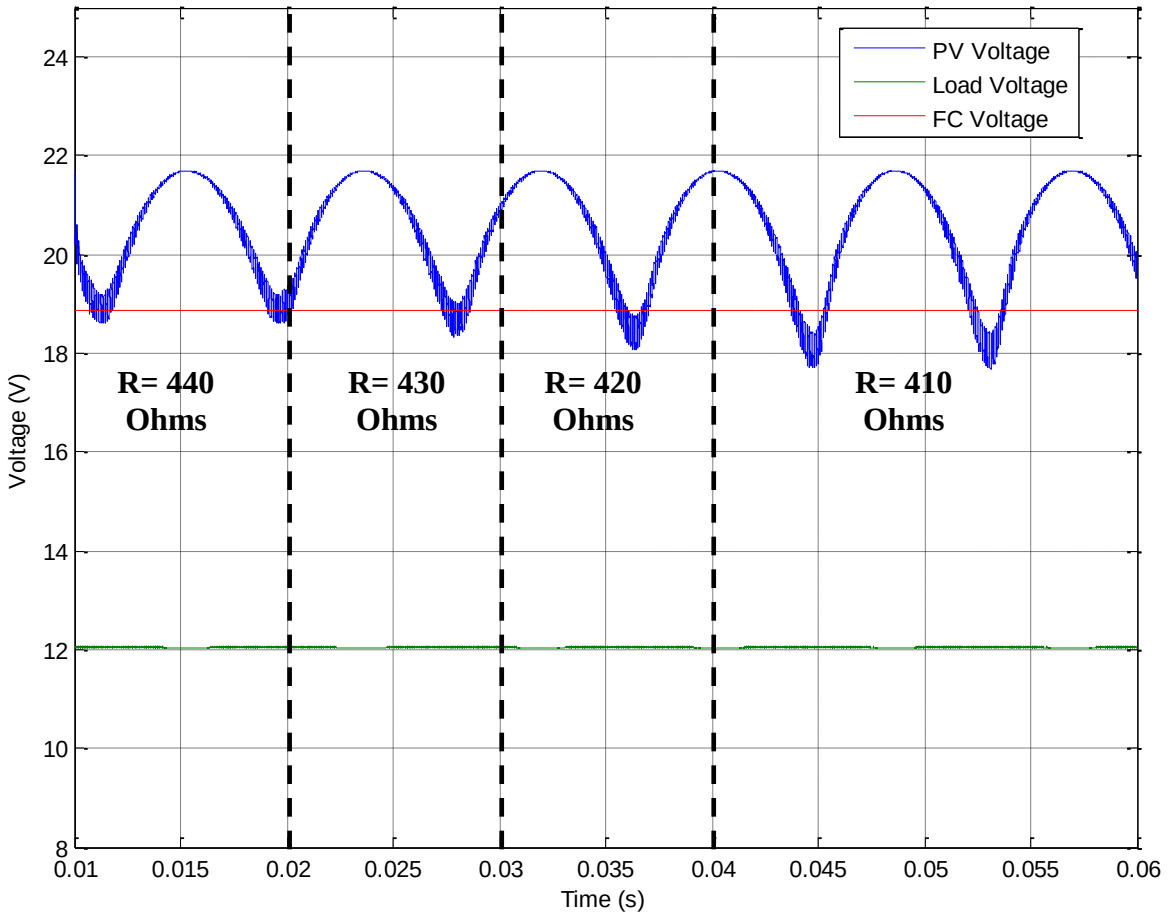

Fig 7.28: Voltages Dynamics for two systems under AC VRM/OFF

In figure 7.29 is shown how the PV output power behaves to changes in the load. As shown in the figure, our controller was able to adjust the power generation for each variation of the load and with the variation of the voltage to provide the required power for each instant of time validating the ability of our controller to operate under dynamic conditions.

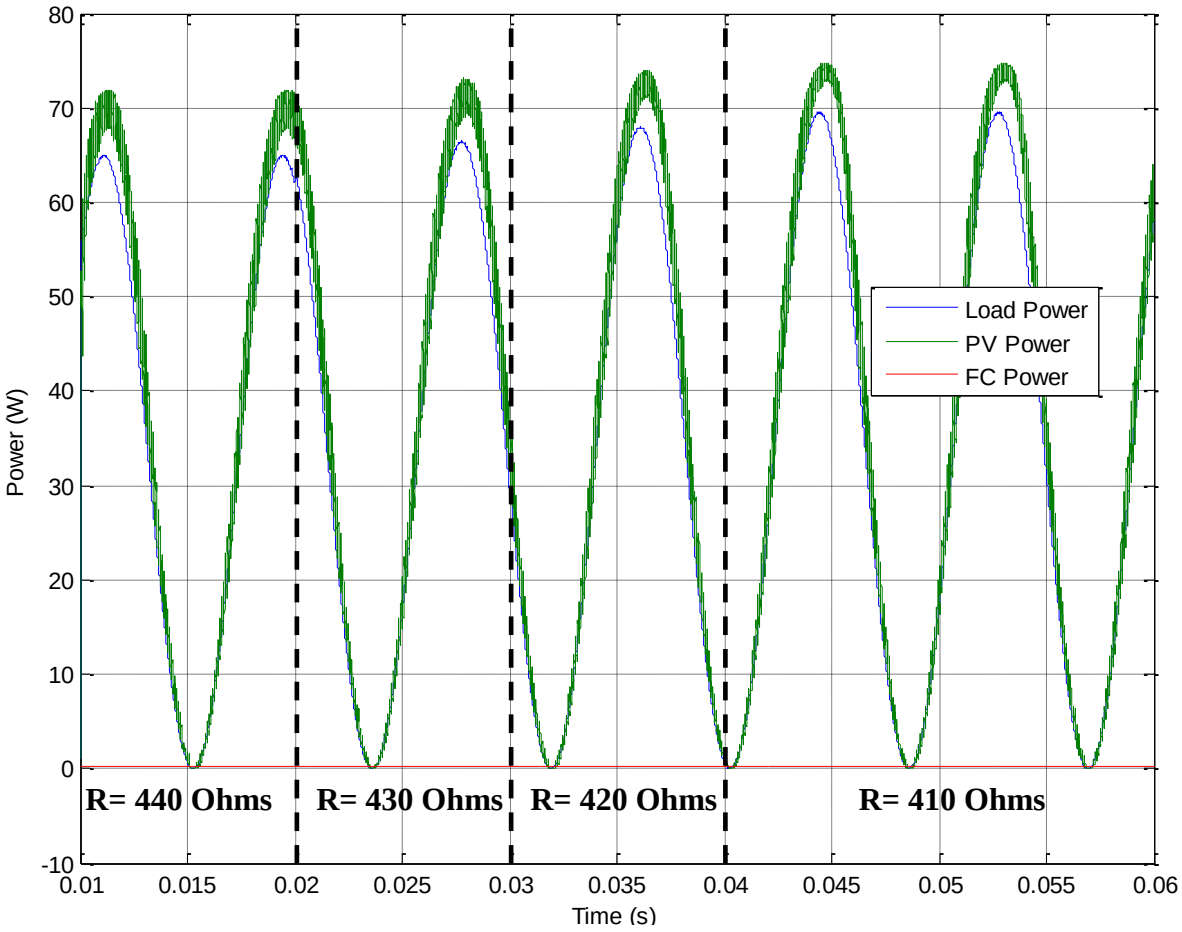

Fig 7.29: Power Generation Dynamics for two systems under AC VRM/OFF

7.2.5.2 Maximum Power/ Active Mode Operating Mode

In this subsection we are going to simulate our system to test the ability of our proposed controller to force the PV system to operate at its maximum. This sub section also shows simulations on how the proposed controller behaves under certain load conditions.

For these operating mode simulations, we used the following things:

- Primary System: Siemens SP75 Solar Module (See Appendix A1 for specs)
- Secondary System: Horizon H-100 Fuel Cell (See Appendix B1 for Specs)
- DC-DC Buck converter
- Solar Irradiance : 1000W/m^2
- Temperature: 25^oC
- Desired Voltage Level: 120VAC

As established before, to operate in Maximum Power Mode-Active Mode the following relation must be satisfied:

$$R \leq \frac{V_{REFMAX}{}^2}{P_{\max}} \Rightarrow R \leq \frac{170^2}{74.8} \Rightarrow R \leq 386.36$$

When operating at load conditions where its value is less than 1.925, our controller must force our system to operate at its maximum power without considering voltage regulation.

Figure 7.30 the behavior of the voltage of our PV/FC system under varying load conditions. The simulation was conducted by connecting only the PV module, through a controlled buck converter, to a resistive load. The resistive load was varied the following way:

Time (s)	Resistance (Ohms)
0.01	300
0.02	280
0.03	260
0.04	240

Table 7.11: Variation of Load for Two Renewable energy AC system in MPM/AM

As seen in the figure, since the power demanded by the load is varying as the voltage at the load varies; the primary controller will operate at the maximum power mode for low power time intervals, when the power demanded is higher than the power that can be supplied from the primary system. When that point is reached, the secondary system start to operate in its active mode supplying the necessary extra power to keep the load voltage regulated at the reference value.

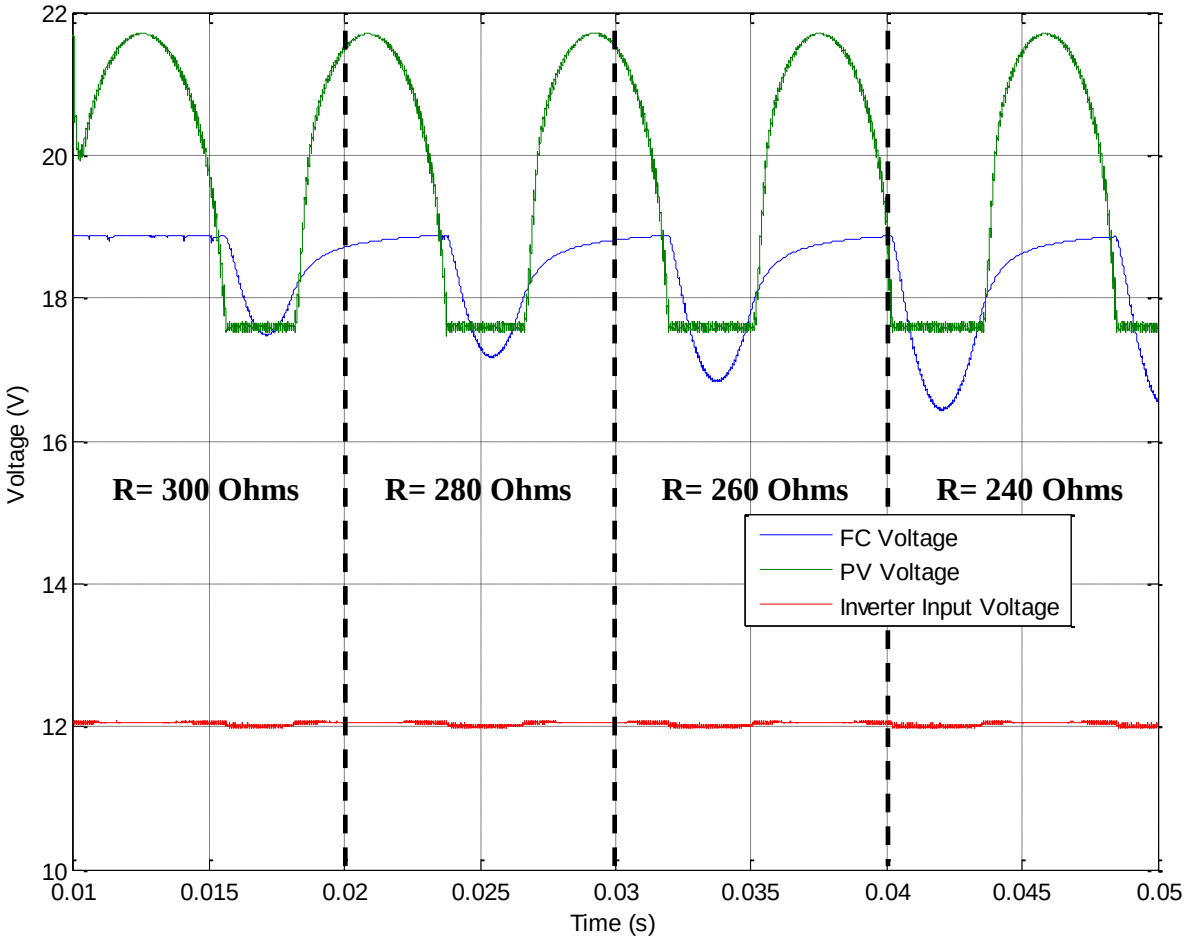

Fig 7.30: Behaviors of Voltage under Maximum Power/Active Mode Operation Mode

Figure 7. 31 show the behavior of the power generation of the systems. As it can be seen the primary system is operating at maximum power and the secondary system is providing the necessary power required to keep the system working at the required voltage. This simulation validates the ability of our system to control the power generation of two renewable energy systems.

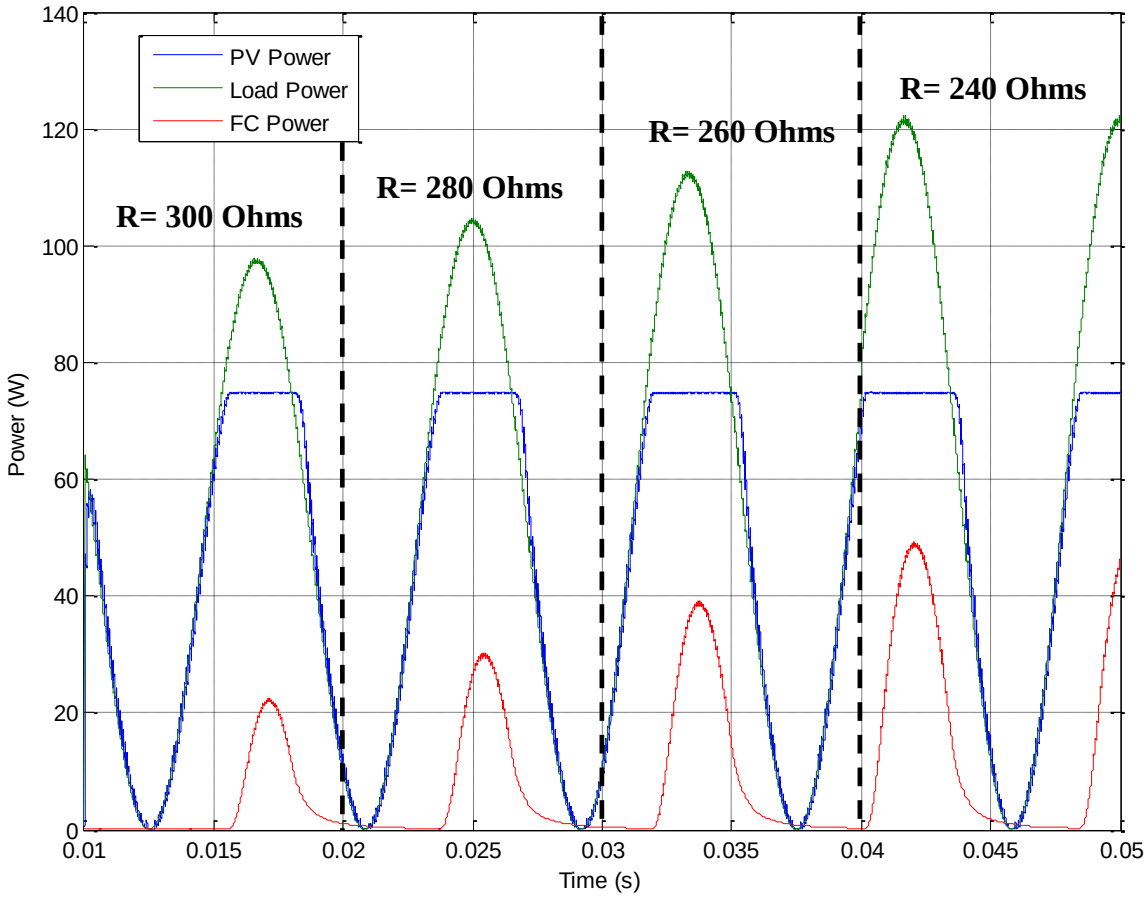

Fig 7.31: Behaviors of Power under Maximum Power/Active Mode Operation Mode

7.2.6 HPRES Simulations Results under Variations of Solar Irradiation and Temperature

Simulations are presented to show the ability of our control strategy to estimate the maximum power point, regulate the load voltage to the reference value when operating at Voltage Regulation Mode and dynamically follow the optimal voltage to guarantee a maximum power operation when operating at the Maximum Power Mode.

Figure 7.32 shows the variation of the solar irradiance, in W/m^2, used for the simulation. The solar irradiance was varied back and forth from 600 W/m^2 to 1000 W/m^2 at a frequency of 60 hertz.

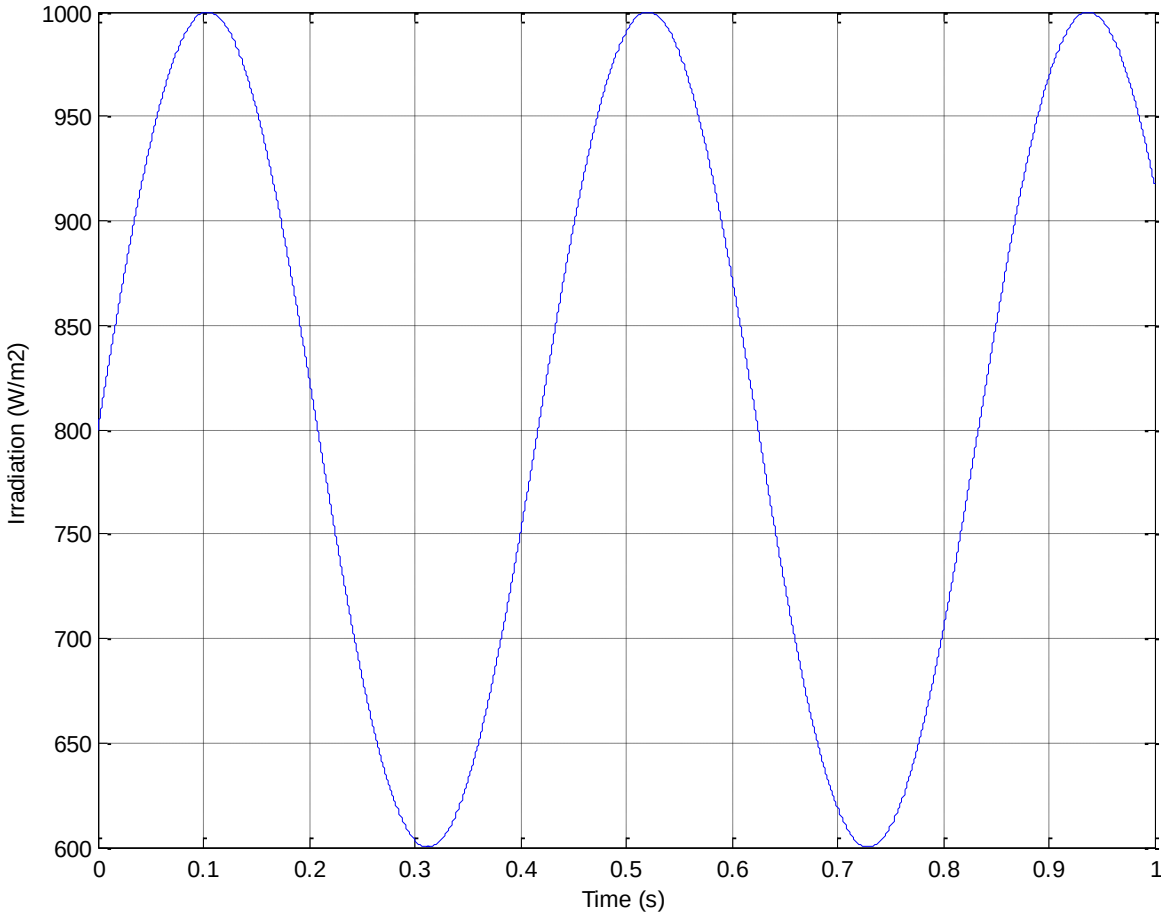

Fig 7.32: Variation of the Solar Irradiance in W/m^2

Figure 7.33 shows the variation of the temperature, in ^{O}C, used for the simulation. The temperature was varied back-and-forth from 25^{o}C to 45^{O}C at a frequency of 60 hertz.

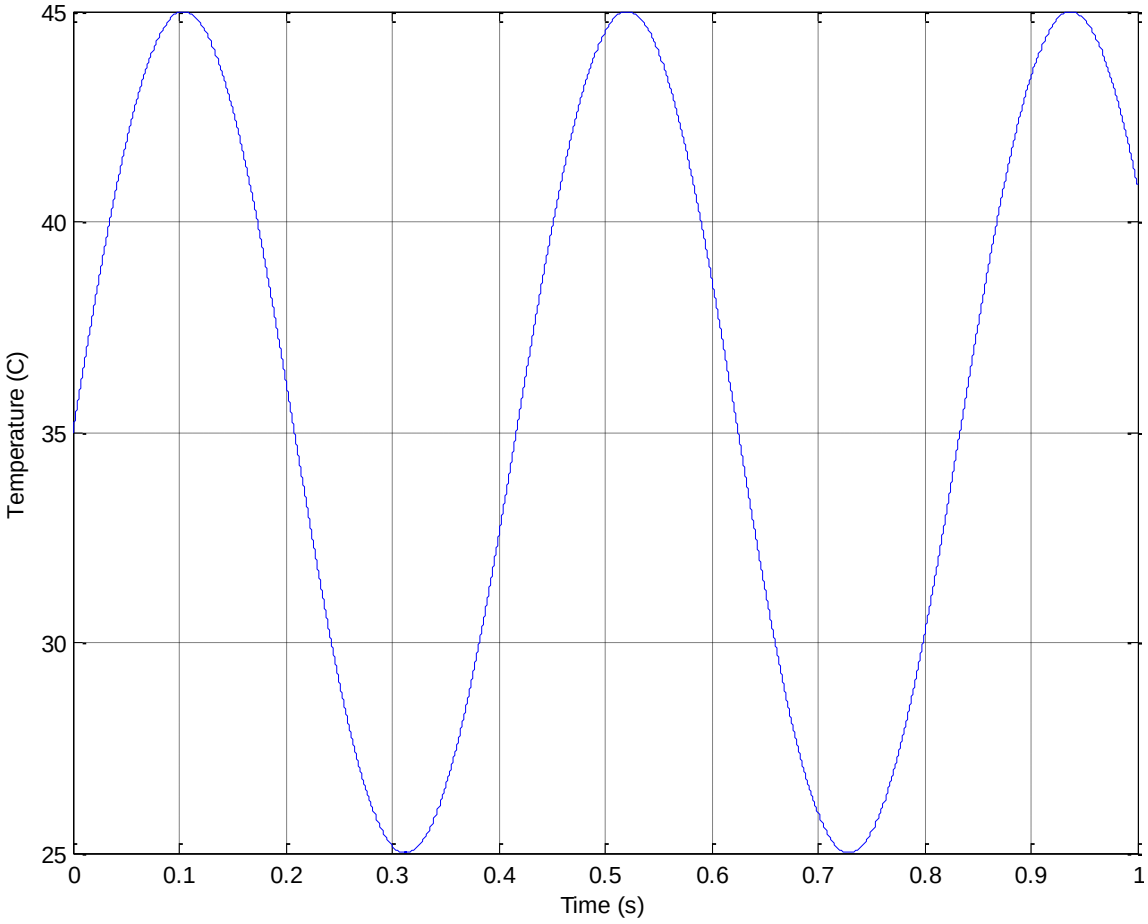

Fig 7.33: Variation of the Temperature in ^{O}C

7.2.6.1 One RES under Variations of Solar Irradiation and Temperature

In this subsection we are going to simulate our system to test the ability of our proposed controller to regulate the load voltage to the reference value and to automatically change its operation mode to the maximum power mode when the conditions are required. Only one system is used for this simulation.

For the voltage regulation operating mode simulations, we used the following specifications:

- Siemens SP75 Solar Module (See Appendix A1for specs)
- DC-DC Buck converter
- Desired Voltage Level: 12VDC
- Load: 2.5 Ohms Resistance

Figure 7.34 shows the dynamics of the optimal voltage and the dynamics of the PV output voltage for our controlled system and a not controlled system. As shown our controller was capable of estimating the optimal voltage and automatically adjusts itself to follow that voltage when Maximum Power operating mode is required. When compared to the non controlled system, it can be seen that our system stays closer to the optimal voltage while the uncontrolled system keeps increasing and decreasing.

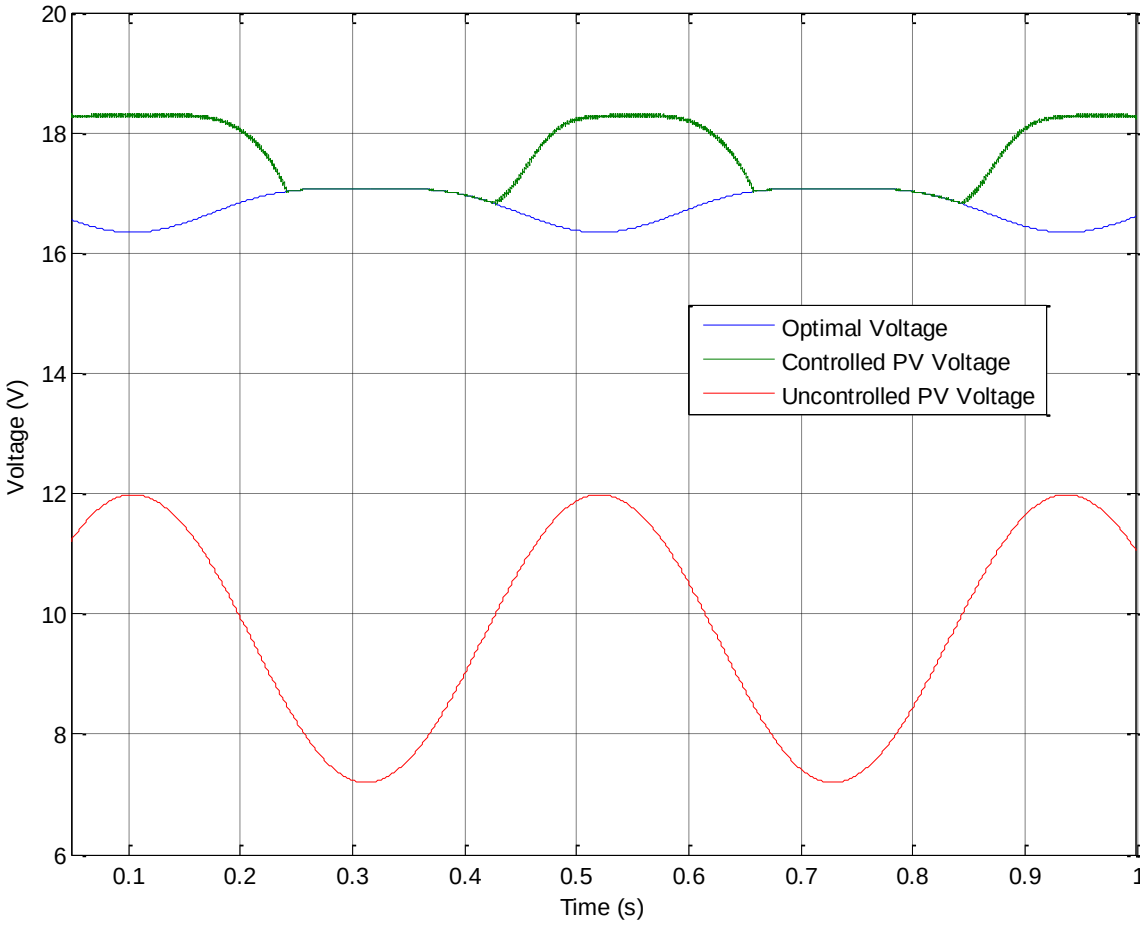

Fig 7.34: Optimal Voltage and PV Voltage Dynamics for Simulation Conditions

Figure 7.35 shows the dynamics of the load voltage from our controlled system and for an uncontrolled system under the same simulation conditions. As can be seen, while the power demand is lower than the available power, the voltage is regulated at the reference value until the power available is not enough, then the voltage regulation cannot be achieved and the PV output voltage follows the optimal voltage value guaranteeing maximum power operation mode.

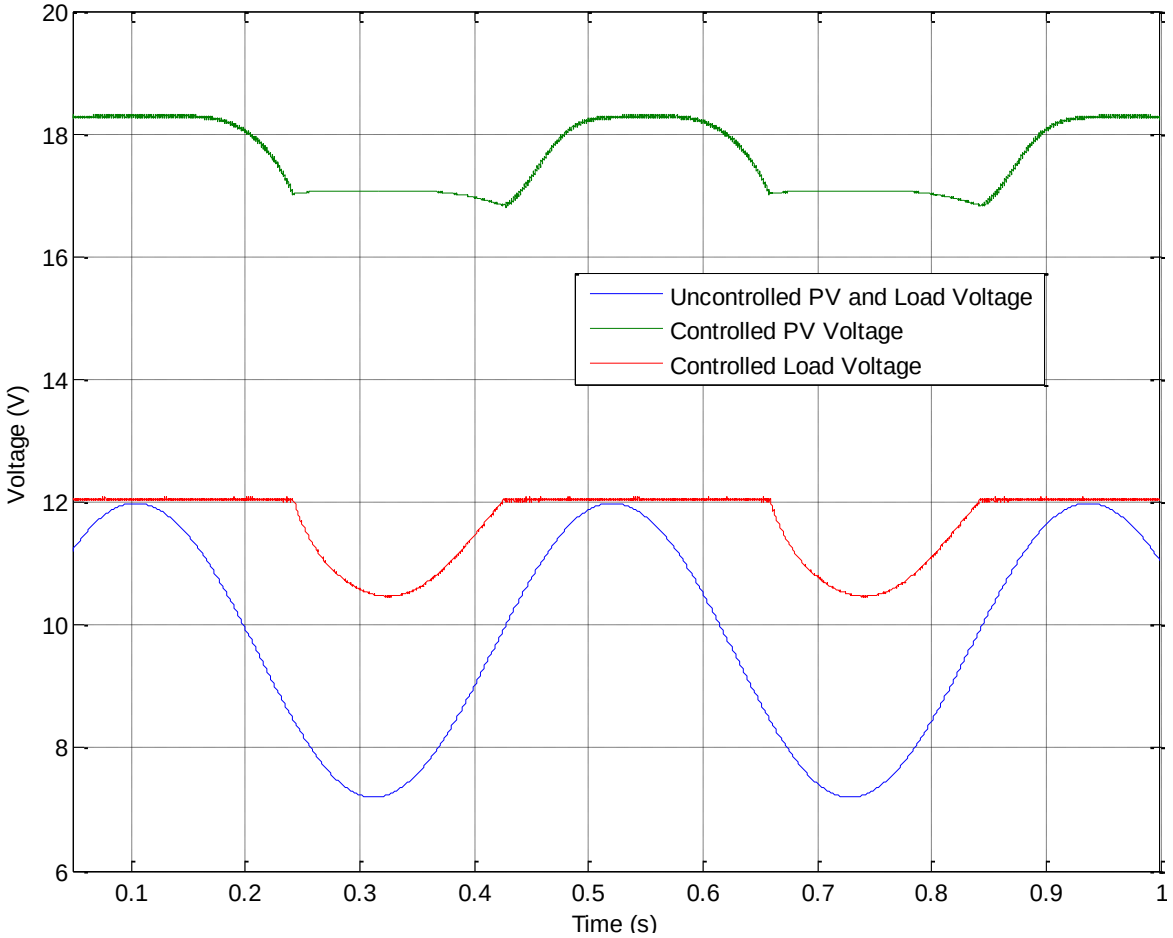

Fig 7.35: Load Voltages Dynamics for a Controlled and Uncontrolled System

Figure 7.36 shows the dynamics of the power generated by our controlled PV system and an uncontrolled system. As seen, the power generated by our controlled is more stable than without a controller. Also is noted that the power output by our controller is higher than the power output of an uncontrolled system validating the ability of our controller in increasing the efficiency of the system.

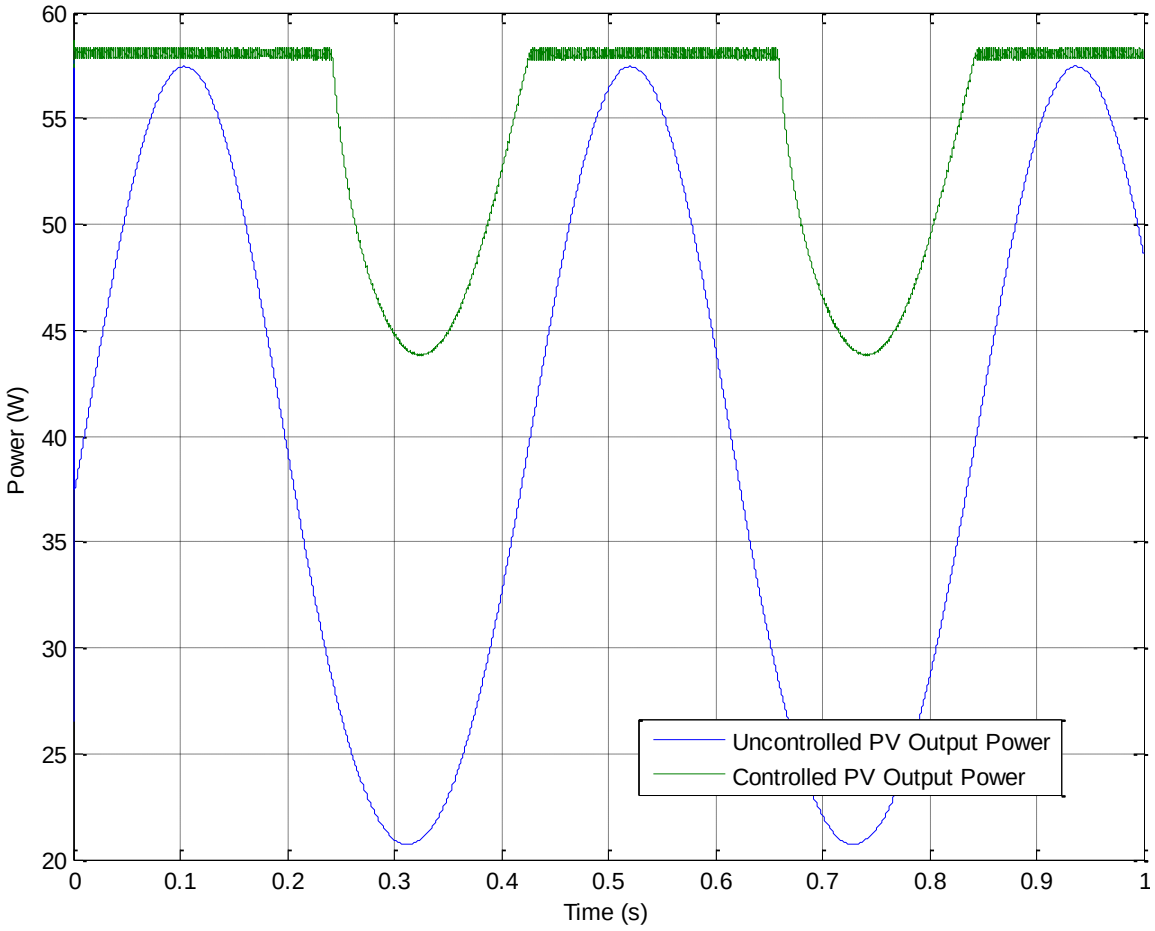

Fig 7.36: Power Dynamics for a Controlled and Uncontrolled System

7.2.6.2 Two RES under Variations of Solar Irradiation and Temperature

In this section simulation are presented validating the ability of our system to adjust the power generation to achieve voltage regulation under variations of certain environmental conditions.

For the voltage regulation operating mode simulations, we used the following specifications:

- Siemens SP75 Solar Module (See Appendix A1 for specs)
- Secondary System: Horizon H-100 Fuel Cell (See Appendix B1 for Specs)
- DC-DC Buck converter
- Desired Voltage Level: 12VDC
- Load: 2.5 Ohms Resistance

Figure 7.37 shows the dynamics of the PV optimal voltage and the dynamics of the PV and fuel cell output voltage. As shown our controller was capable of estimating the optimal voltage and automatically adjusts itself to follow that voltage when Maximum Power operating mode is required and extract the necessary power from the secondary system to achieve voltage regulation.

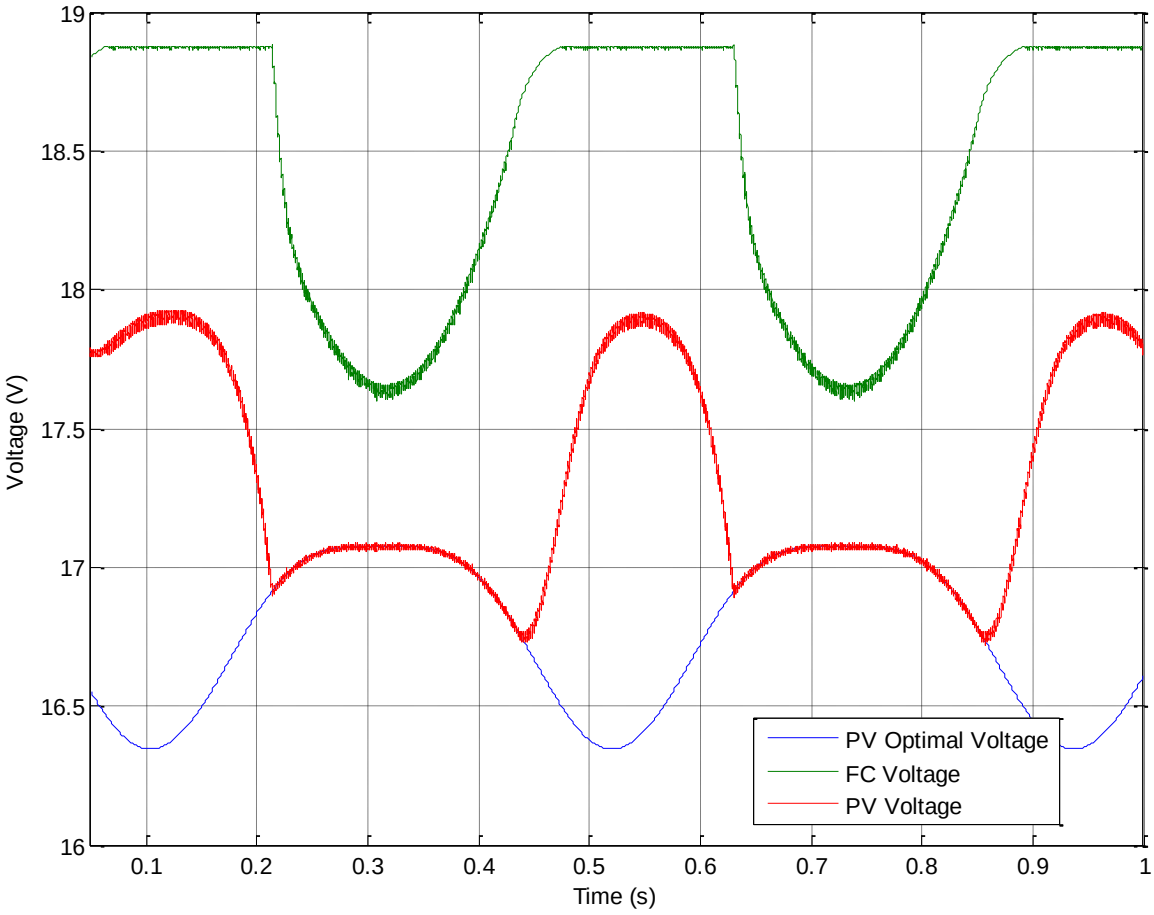

Fig 7.37: Optimal Voltage, PV and FC Voltage Dynamics for Simulation Conditions

As seen in the figure 7.38, since the power demanded by the load is varying as the voltage at the load varies; the primary controller will operate at the maximum power mode for small time intervals, when the power demanded is higher than the power that can be supplied from the primary system. When that point is reached, the secondary system start to operate in its active mode supplying the necessary extra power to keep the load voltage regulated at the reference value.

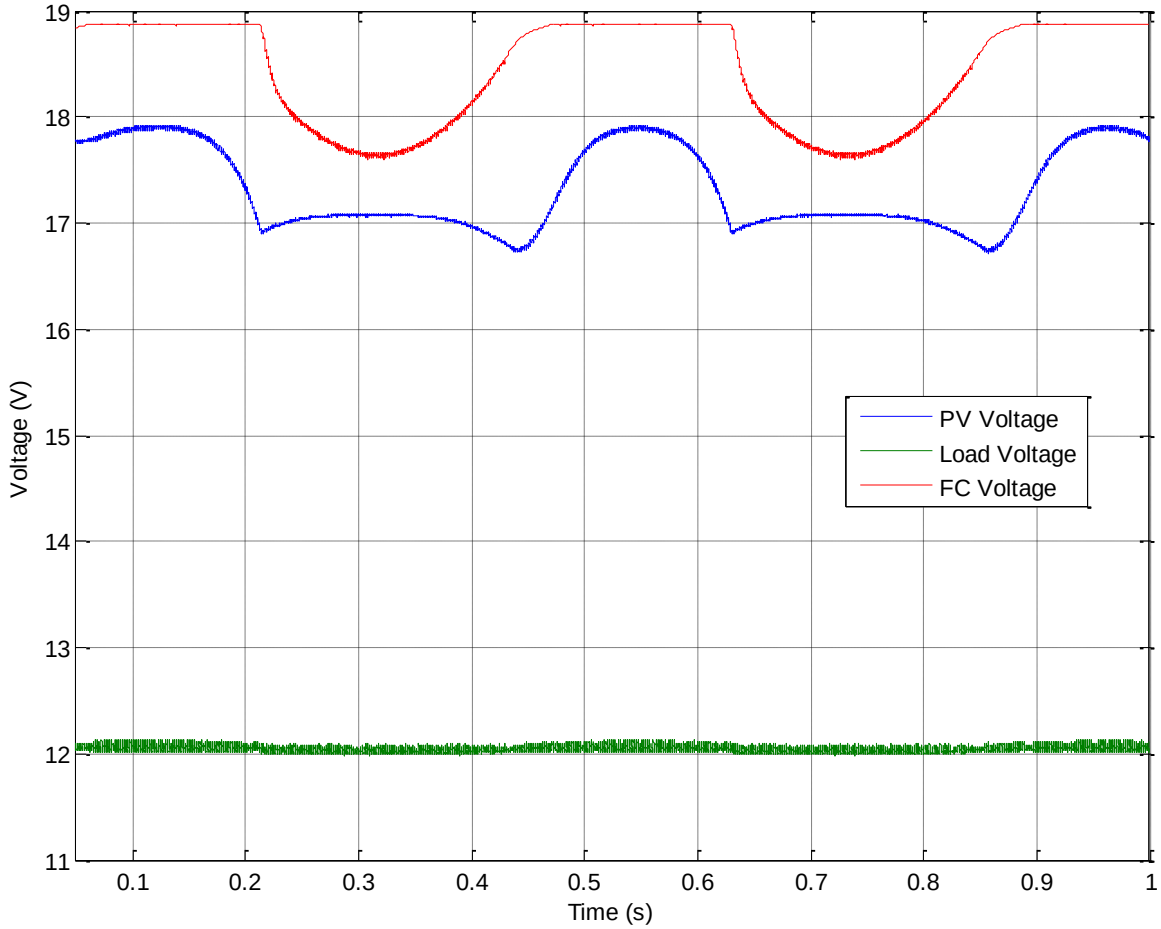

Fig 7.38: Load Voltages Dynamics for the Simulation Conditions

Figure 7.39 shows the dynamics of the power generated by our RES. As it can be seen the primary system is operating at maximum power and the secondary system is providing the necessary power required to keep the system working at the required voltage. This simulation validates the ability of our system to control the power generation of two renewable energy systems.

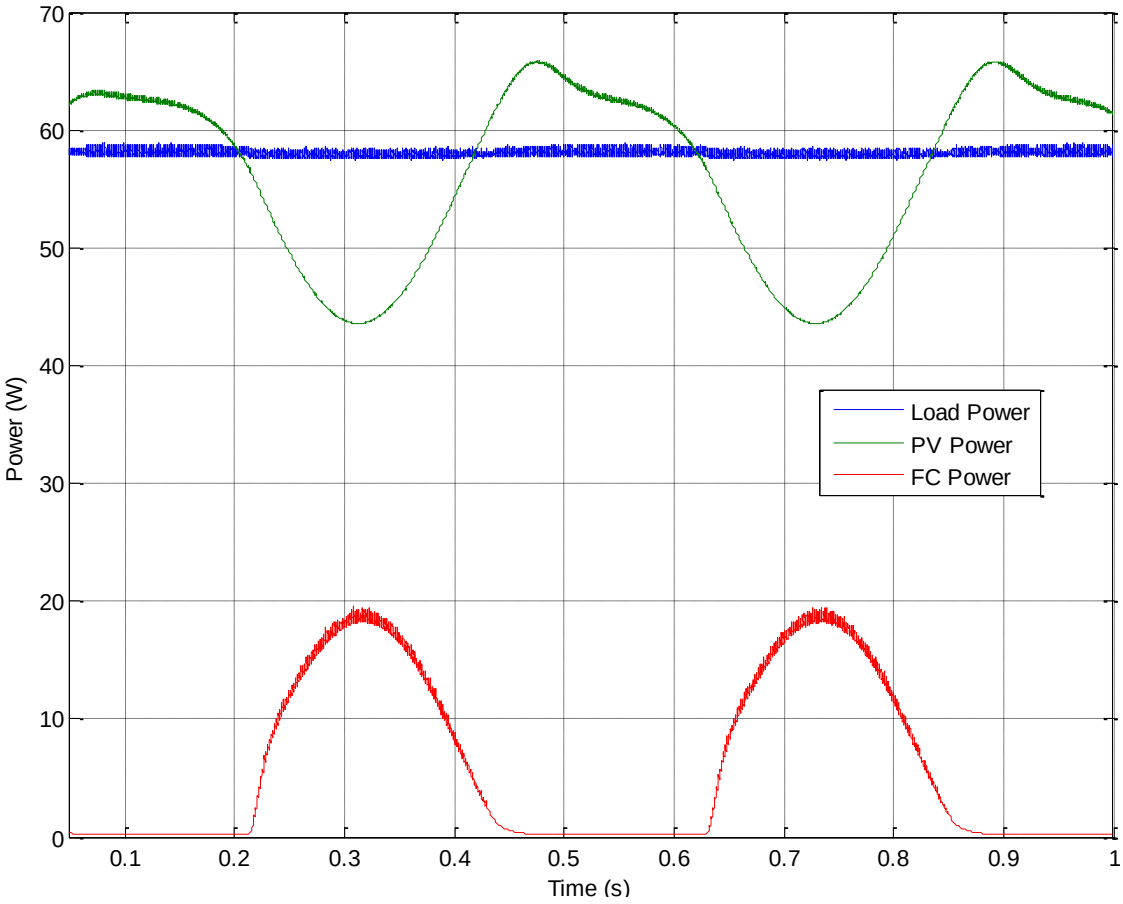

Fig 7.39: Power Dynamics for a Controlled and Uncontrolled System

7.2.7 Residential Applications with HREPS with Two RES and Battery Bank

In this subsection simulations are presented to validate the ability of our controller in delivering power under varying environmental conditions and under AC load by controlling the behavior of each system individually.

To simulate a house load, an average power demand of 1.5kW will be used. To simulate a demand of 1.5kW a resistance with the following value is going to be used:

$$R = \frac{V_{LOAD}{}^{2}}{P} = \frac{120^2}{1500} = 9.6\Omega$$

The solar irradiation will be varied the following way:

Time (s)	**Solar Irradiation (W/m^2)**
0.05	600
0.10	1000
0.15	400
0.20	200
0.25	10

Table7.12: Variation of the solar irradiation

For the system composition, we used the following specifications:

- 1200W Siemens SP75 Solar Module (See Appendix A1 for specs)
- Secondary System: Horizon H-1000 Fuel Cell (See Appendix B2 for Specs)
- DC-DC Buck converter
- Inverter 24VDC/120VAC
- Desired Voltage Level: 120VAC
- Battery Bank 48 VDC

Figure 7.40 shows the behavior of the PV and FC voltages and the load voltage. As can be seen from the figure, the PV voltage was varying with any variation in the irradiance. It's also noted that the FC also reach its optimal voltage at a given time. Even though both systems were working at its maximum power modes, the voltage regulation was not lost because the batteries provide the additional power necessary to obtain regulation. This simulation validates the ability of our control system to generate the required power to satisfy the load demand by controlling the power generated by three sources in a hierarchical way extracting the maximum power available by a system before extracting from the next power source.

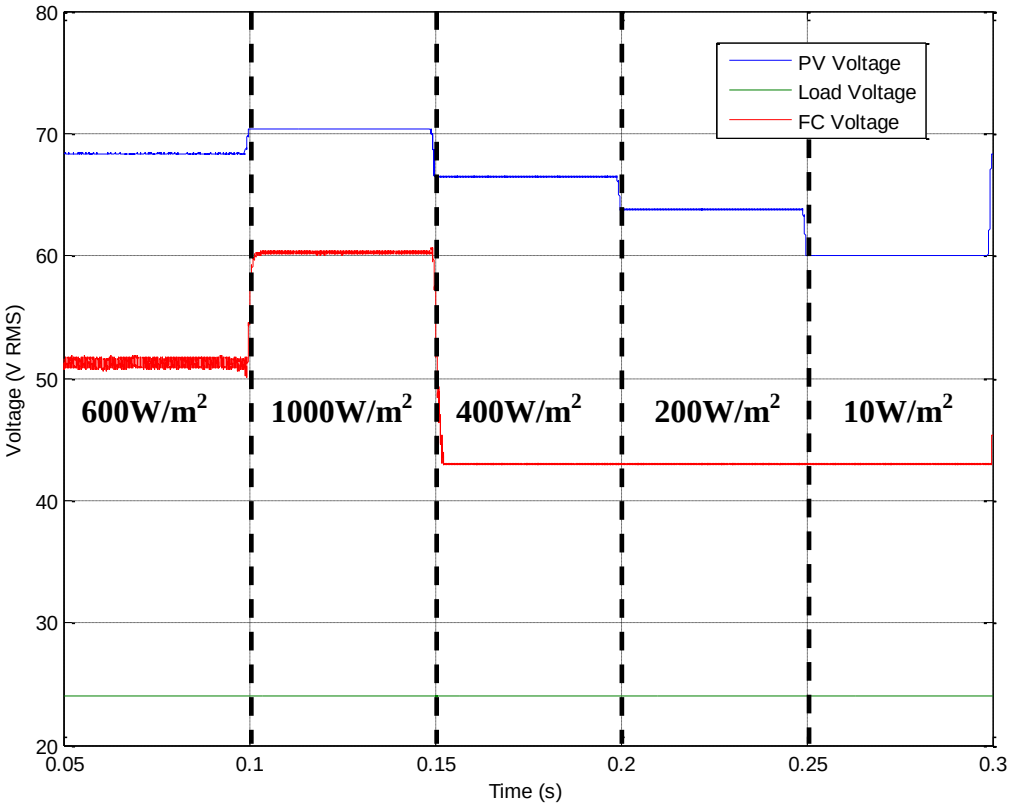

Fig 7.40: Load Voltages (RMS) Dynamics for Three Systems

Figure 7.41 shows the behavior of the PV, FC, Batteries and load powers. As can be seen from the figure, the PV power was varying with any variation in the irradiance increasing or decreasing its power output. It is noted that the FC supplied the additional power required to produce the 1.5kW. Also it can be appreciated that, when the PV and the FC were not able to produce enough power to maintain the 1.5kW at 120VAC, the battery supplied the additional power required. This simulation validates once again the ability of our control strategy to control the power generation of the system and to comply with the specifications. The system could supply the required 1.5kW at all moment.

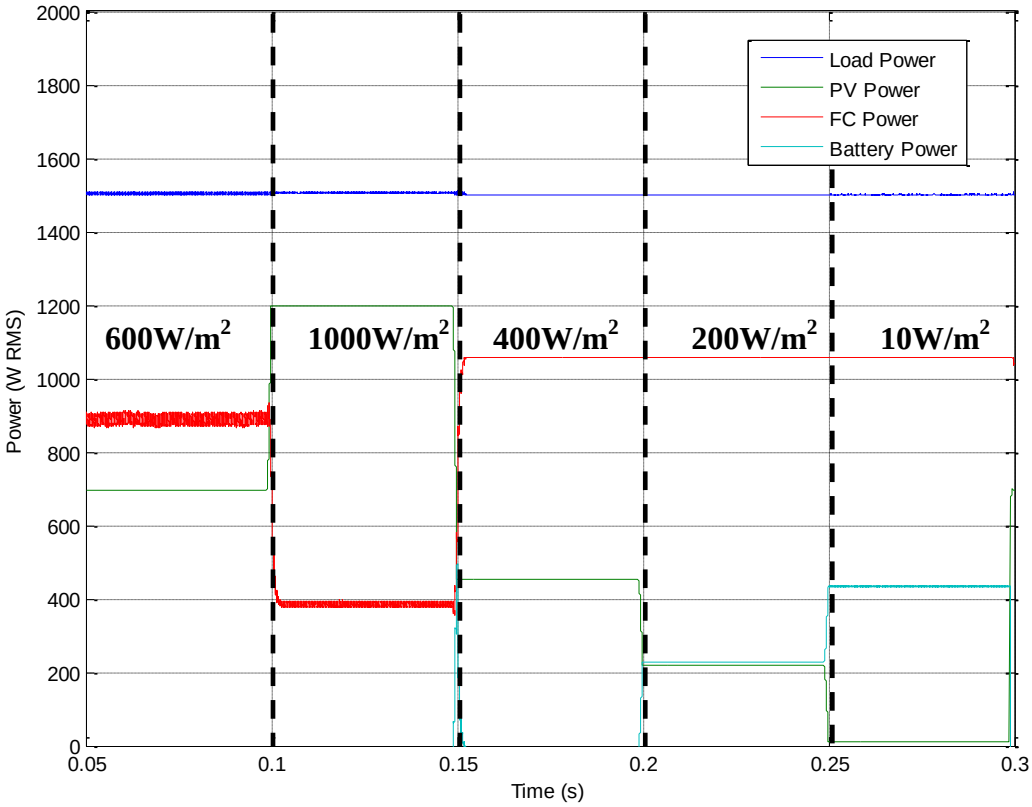

Fig 7.41: Power (RMS) Dynamics for Three Systems

8 Conclusions and Future Works

8.1 Conclusions

Simulation models of photovoltaic cells, fuel cells, batteries and dc/dc converters were used to analyze their behaviors when interconnected as a hybrid alternative power system and to facilitate the developing of control strategies to manage the power generation of these power sources while regulating the load voltage. Each energy source is connected to the load through dc/dc converters which, by controlling their duty cycle, control the power generated.

The solar irradiance reaching the photovoltaic cell and the temperature of the cell can be modified so it can recreate different environmental conditions such as daily values of solar irradiation and temperature levels. The load was a variable resistive load arranged in such a way that it would force our system to operate at each proposed operation mode. These operation modes were achieved applying the designed control strategy based on sliding mode control.

The control strategy of the hybrid alternative energy system use control laws specific to each power source in such a way that they would work together, in a hierarchical way, to achieve voltage regulation and to satisfy the power demand. The control laws used for each power source are based in sliding mode control. The primary system is in charge of

regulating the voltage while the other systems supplies extra power to help the primary system achieves its objective. The operation modes are being controlled by measuring voltages in the system and the controller determine the correct operation mode for the system.

Simulations shown validated the ability of our proposed system to operate well under statics and dynamics environmental and load conditions. The environmental conditions were varied within typical values to simulate realistic conditions. Load conditions were varied to simulate changes in the load's power demand. The control law implemented for the photovoltaic adjusted itself to follow the optimal voltage curve and force the PV voltage to follow the curve when maximum power mode was required. The control laws implemented for the auxiliaries systems adjusted themselves to the changes in the primary system.

Advantages in the power generation and voltage regulation were seen when a photovoltaic cell was connected directly to the load and when it was connected through our controller to the load. The power generated by the proposed system was higher and stable when operating in the maximum power mode and the load was varying while the power of the uncontrolled system was lower and varying as the load varies. When operating in voltage regulation mode, the load's voltage for the controlled system was regulated to a fixed level while the load's voltage of the uncontrolled system was dropping at each variation of the load.

8.2 Future Work

The following can be done for future works:

- The implementation of a dynamical fuel cell model that takes into consideration factors that affects the power output of the system such as the internal pressures of the reactants and the cell's temperature.
    - The model used for this work was a model that assumes constant pressures and constant temperatures. Using a model that takes into consideration those factors would give a more realistic behavior of the system.

- Simulations using different type of loads.
    - In this work, the load used for simulation was highly resistive. Loads such as inductive and capacitive load should be tested to analyze the system's behavior.

- Physical implementation of the system.
    - Only simulations were taken in consideration for this work. Some experimental results should be obtained to experimentally validate the control strategy.

References

[1]Global Wind Energy Council, Global Wind 2005 Report, www.gwec.net, 2006.

[2]R. Swisher, C.R. DeAzua, and J.Clendenin, "Strong winds on the horizon: Wind Power comes of age" Proc. IEEE, vol. 89, no. 12, Page(s).1754-1764, Dec. 2001

[3]Gross,G.;"Contributions of renewable energy resources to resource diversity" Power Engineering Society General Meeting, 2006. IEEE18-22 June 2006 Page(s):1. Digital Object Identifier 10.1109/PES.2006.1709497

[4]Ortiz,E."Modeling and Analysis of solar distributed generation"submitted PHD dissertation, Michigan State University, 2006.

[5]Chang, Liuchen; Ng, Cecilia, "A Solar Battery Charger with Improved Energy Utilization". 1994. Conference Proceedings. 1994 Canadian Conference on Electrical and Computer Engineering, 25-28 Sep 1994 Page(s):105 - 108 vol.1. Digital Object Identifier 10.1109/CCECE.1994.405650

[6]Triggianese, M.; Marino, P.; Morren, J.; de Haan, S.W.H.; "Reduction of Harmonics from MW-class Wind Turbines by Interlaced Active Front-Ends" IEEE International Symposium on Industrial Electronics", 2007. ISIE 2007.4-7 June 2007 Page(s):2607 - 2612 Digital Object Identifier 10.1109/ISIE.2007.4375019

[7]Swiegers, W.; Enslin, J.H.R.; "An Integrated Maximum Power Point Tracker for Photovoltaic Panels" IEEE International Symposium on Industrial Electronics, 1998. Proceedings. ISIE '98. Volume 1, 7-10 July 1998 Page(s):40 - 44 vol.1 Digital Object Identifier 10.1109/ISIE.1998.707746

[8]Singh, P. Rajagopalan, J. LaFollette, R. Fennie, C., Jr. Reisner, D.E. " Fuzzy logic-based solar charge controller for microbatteries" Conference Record of the Twenty-Eight IEEE Photovoltaic Specialists Conference, 2000. Page(s): 1726-1729

[9]Senjyu, T. Uezato, K. "Maximum power point tracker using fuzzy control for photovoltaicarrays" Proceedings of the IEEE International Conference on Industrial Technology, 1994. Page(s): 143-147. Digital Object Identifier: 10.1109/ICIT.1994.467196

[10]Jimenez, E. Ortiz-Rivera, E.I. Gil-Arias, O. "A dynamic maximum power point tracker using sliding mode control" COMPEL 2008. 11th Workshop on Control and Modeling for Power Electronics, 2008. page(s): 1-5. Digital Object Identifier: 10.1109/COMPEL.2008.4634685

[11]De Battista, H.; Mantz, R.J. "Variable structure control of a photovoltaic energy converter" IEE Proceedings in Control Theory and Applications. Volume 149, Issue 4, July 2002 Page(s):303 - 310 .Digital Object Identifier 10.1049/ip-cta:20020556

[12]Petchjatuporn, P.; Ngamkham, W.; Khaehintung, N.; Sirisuk, P.; Kiranon, W.; "A Solar-powered Battery Charger with Neural Network Maximum Power Point Tracking Implemented on a Low-Cost PIC-microcontroller" . International Conference on Power Electronics and Drives Systems, 2005. Volume 1, Page(s):507 - 510 Digital Object Identifier 10.1109/PEDS.2005.1619739

[13]Samangkool, K.; Premrudeepreechacharn, S.; "Maximum power point tracking using neural networks for grid-connected photovoltaic system". International Conference on Future Power Systems, 2005. 18-18 Nov. 2005 Page(s):4-5. Digital Object Identifier 10.1109/FPS.2005.204215

[14]Premrudeepreechacharn, S.; Patanapirom, N.; “Solar-array modeling and maximum power point tracking using neural networks”. Power Tech Conference Proceedings, 2003 IEEE Bologna.Volume 2, 23-26 June 2003 Page(s):5. Vol.2.Digital Object Identifier 10.1109/PTC.2003.1304587

[15]Springer Berlin/ Heidelberg. “Emerging Intelligent Computing Technology and Applications with Aspects of Artificial Intelligence”. Lecture Notes in Computer Science Volume 5755/2009. Page(s) 912-919. DOI 10.1007/978-3-642-04020-7_98

[16]Torres-Hernández, María E. 2007. “Hierarchical Control of Hybrid Power Systems”. UPRM Thesis Disertion. Webpage:”http://grad.uprm.edu/oeg/TesisDisertacionesDigitales /IngenieriaElectricaComputadoras

[17]Del Real, A.J, Arce, A.,Bordons, C. “Hybrid model predictive control of a two-generator power plant integrating photovoltaic panels and a fuel cell”. 46th IEEE Conference on Decision and Control, 2007. Page(s): 5447-5452. Digital Object Identifier: 10.1109/CDC.2007.4434550

[18]Michael, S., Utsler, J. “The use of genetic algorithm for the design and optimization of advanced multi-junction solar cells”. 48th Midwest Symposium on Circuits and Systems, 2005. Vol. 1. Page(s): 163 - 166. ISBN: 0-7803-9197-7

[19]Il-Song Kim, , Myung-Bok Kim, Myung-Joong Youn, “New Maximum Power Point Tracker Using Sliding-Mode Observer for Estimation of Solar ArrayCurrent in the Grid-Connected Photovoltaic System” IEEE Transactions on Industrial Electronics, Vol 53, No.4, August 2006, Page(s): 1027

[20]Galiana, B.; Algora, C.; Rey-Stolle, I.; Vara, I.G, “A 3-D model for concentrator solar cells based on distributed circuit units”, IEEE Transactions on Electron Devices, Volume 52, Issue 12, Dec. 2005 Page(s): 2552 – 2558. Digital Object Identifier 10.1109/TED.2005.859620

[21]AbdulHadi, M. Al-Ibrahim, A.M. Virk, G.S. “ Neuro-fuzzy-based solar cell model”, IEEE Transaction on Energy Conversion, Sept. 2004Volume: 19, Issue: 3 Page(s): 619- 624 ISSN: 1558-0059

[22]Fasooniehchi, A.R. Taherbaneh, M. , “A New Solar Cell Model for Evaluating Degradation of various il icon Cells at LEO and eO r its lran Telecommun. Res. Center, Tehran”; International Conference on Recent Advances in Space Technologies 3rd, 2007, 14-16 June2007 Page(s) 768-773 ISBN: 1-4244-1057-6

[23]Markvart, T. Landsberg, P.T. , “Solar cell model for electron transport in photosynthesis” , Conference Record of the Twenty-Ninth IEEE Photovoltaic Specialists Conference, 2002. 19-24 May 2002, P(s): 1348- 1351 ISSN: 1060-8371

[24]Ortiz-Rivera, Eduardo I; Peng, F.Z., "Analytical Model for a Photovoltaic Module using the Electrical Characteristics provided by the Manufacturer Data Sheet”, PESC’05. IEE 36th, vol. Page(s):2087-2091, 11-14 Sept.2005

[25]Correa, J.M.; Farret, F.A.; Canha, L.N.; Simoes, M.G.; “An electrochemical-based fuel-cell model suitable for electrical engineering automation approach”, 2004. IEEE Transactions on Industrial Electronics, Volume 51, Issue 5, Page(s):1103 - 1112 Digital Object Identifier 10.1109/TIE.2004.834972

[26]Dachuan Yu, S. Yuvarajan, “Electronic circuit model for proton exchange membrane fuel cells”,Science Direct Journal of Power Sources 142 (2005) Page(s): 238–242

[27]Mathworks," Simulink's Fuel Cell Model", SymPower System Toolbox. Matlab 2008b

[28]Ortiz-Rivera, E.I. Pan, Z. Jin Wang. "A mathematical model to describe the electrical characteristics for a fuel cell" IEEE Power Electronics Specialists Conference, 2008. Page(s): 559-561. ISBN: 978-1-4244-1667-7

[29]Femia, N.; Petrone, G.; Spagnuolo, G.; Vitelli, M. "Perturb and Observe MPPT technique robustness improved",2004 IEEE International Symposium on Industrial Electronics, Volume 2, 4-7 May 2004 Page(s):845 - 850 vol. 2

[30]Femia, N.; Petrone, G.; Spagnuolo, G.; Vitelli, M. "Optimization of perturb and observe maximum power point tracking method",IEEE Transactions on Power Electronics,Volume 20, Issue 4, July 2005 Page(s):963 – 973

[31]Weidong Xiao; Dunford, W.G. "A modified adaptive hill climbing MPPT method for photovoltaic power systems" Power Electronics Specialists Conference, 2004. IEEE 35th Annual Volume 3, 20-25 June 2004 Page(s):1957 – 1963.

[32]Atrash, H.; Batarseh, I.; Rustom, K. "Statistical modeling of DSP-based Hill-climbing MPPT algorithms in noisy environments" , Applied Power Electronics Conference and Exposition, 2005. Twentieth Annual IEEE. Volume 3, 6-10 March 2005 Page(s):1773 - 1777

[33]Yushaizad Yusof, Siti Hamizah Sayuti, Muhammad Latif, Zamri Che Wanik, "Modeling and Simulation of Maximum Power Point Tracker for Photovoltaic System" , National Power & Energy Conference (PECon) 2004 Proceedings, Kuala Lumpur, Malysa. Page(s): 88-93.

[34]Jae Ho Lee; HyunSu Bae; Bo Hyung Cho, " Advanced Incremental Conductance MPPT Algorithm with a Variable Step Size" Power Electronics and Motion Control Conference, 2006. 12th International Aug. 2006 Page(s):603 – 607

[35]Wu Libo; Zhao Zhengming; Liu Jianzheng, " A Single-Stage Three-Phase Grid-Connected Photovoltaic System With Modified MPPT Method and Reactive Power Compensation", IEEE Transaction on Energy Conversion, Volume 22, Issue 4, Dec. 2007 Page(s):881 - 886

[36]Hanifi Guldemir, " Sliding Mode Control of DC/DC Boost Converter", Journal of Applied Sciences 5(3), ISSN 1812-5654

[37]Il-Song Kim, "Robust Maximum power point tracker using sliding mode controller for the three-phase grid-connected photovoltaic system". Solar Energy 81(2007) Page(s): 415-414

[38]Il-Song Kim, Myung-Bok Kim, Myung-Joong Youn, "New Maximum Power Point Tracker Using Sliding-Mode Observer for Estimation of Solar Array Current in the Grid-Connected Photovoltaic System", IEEE Transactions on Industrial Eletronics, Vol. 53, No.4, August 2006, Page(s):1027-1036

[39]Alexis de Medeiros Torres, Fernando Antunes, Fernando Soares, "An artificial Neural Network-Based Real Time Maximum Power Tracking Controller for connecting a PV System to the grid", 1998 IEEE, 0-7803-4503-7/98 Page(s). 554-559

[40]Eduardo Ortiz, Fang Peng, "A Novel Method to Estimate the Maximum Power for a Photovoltaic Inverter System",2000 35th Annual IEEE Power Electronics Specialists Conference.

[41]A.M. Sharaf, Liang Yang, "An efficient Photovoltaic DC Village Electricity Scheme Using a Sliding Mode Controller", IEEE Conference on Control Applications, 2005, Page(s) 1325-1330.

[42]D.Georgakis,S.Papathanassiou, “Modeling of grid-connected fuel cell palnts”,National Technical University of Athen, Greece.

[43]Dachuan Yu, S. Yuvarajan, “Electronic circuit model for proton exchange membrane fuel cells”,Science Direct Journal of Power Sources 142 (2005) 238–242

[44]Hassan Moghbelli [1], Robert Vartanian, “A Green Hybrid Solar Cell and Fuel Cell Power Plant Generating Electricity and Water”, ASME 3rd International Conference on Energy Sustainability.July 2009

[45]R. Williams (1960). "Becquerel Photovoltaic Effect in Binary Compounds". The Journal of Chemical Physics 32 (5). Page(s). 1505–1514. doi:10.1063/1.1730950.

[46]A. E. Becquerel (1839). "Mémoire sur les effets électriques produits sous l'influence des rayons solaires". Comptes Rendus **9**. Page(s). 561–567.

[47]Perlin, John “From Space to Earth The Story of Solar Electricity”. Harvard University Press 1999. Page(s).147, ISBN 0-674-01013-2.

[48]D. M. Chapin, C. S. Fuller, and G. L. Pearson; J. “Applied Physics” , 1954,.Number 25, Page(s): 676.

[49]M. Patel, “Wind and Solar Power Systems”, Second Edition, Taylor & Francis Group, 2006.

[50]Geoffrey.landis “Graph of world shipments of photovoltaic arrays, in peak MW, as a function of year from 1980 to 2007

[51]Smil, Vaclav “Energy at the Crossroads” Global Science Forum Conference on Scientific Challenges for Energy Research,Paris, May 17-18, 2006. page 12. ISBN 0262194929

[52]Archer, Cristina. Jacobson, Mark. "Evaluation of Global Wind Power” Journal of Geophysical June 2005, Vol. 110, DOI:10.1029/2004JD005462

[53]Miyamoto, Kazuhisa "Energy conversion by photosynthetic Organisms” Renewable biological systems for alternative sustainable energy production (FAOAgricultural Services Bulletin - 128) Chapter 2. ISBN 92-5-104059-1

[54]Energy Information Administration."World Consumption of Primary Energy by Energy Type and Selected Country Groups, 1980-2004".International Energy Annual 2006

[55]Energy Information Administration. "World Total Net Electricity Consumption, 1980-2005”.International Energy Annual 2006

[56]Matthias Loster, “ Total Primary Energy Supply:Required Land Area” TPES 2006.

[57]Wielstich, W. “Handbook of fuel cells: advances in electrocatalysis, materials, diagnostics and durability”.Vol 6. 2009

[58]"Batteries, Supercapacitors, and Fuel Cells: Scope". Science Reference Services. 20 Aug 2007

[59]US Department of Energy, Office of Fossil Energy “Fuel Cell Handbook”. Fifth Ed. Oct 2000.ISBN 1410219607

[60]George Wand. "Fuel Cells History, part 1". Fuel Cell Today.June 2006. Article 1104. Page(s): 14.

[61]Grove, William Robert "On Voltaic Series and the Combination of Gases by Platinum", Philosophical Magazine and Journal of Science (1839), ,Vol. XIV Page(s) 127-130.

[62]Princeton University chemistry lab website “History of Fuel Cells http://www.princeton.edu/~chm333/2002/spring/FuelCells/fuel_cel ls-history.html

[63]Smithsonian National museum of American History “Fuel Cell History Project website” http://americanhistory.si.edu/fuelcells/index.htm

[64]Spaceaholic.com. "Apollo Space Program Hydrogen Fuel Cells" Link: http://www.spaceaholic.com/apollo_artifacts.htm

[65]Smithsonian National museum of American History “Fuel Cell History Project website” http://americanhistory.si.edu/fuelcells/index.htm

[66]U.S. Department of Energy, Energy Efficiency and Renewable Energy. http:// www1.eere. energy. gov/ hydrogen and fuel cells

[67]Vonhelmolt, R "Fuel Cell Vehicles:Status 2007". Journal of Power Sources Vol. 165: Page(s): 833, DOI:10.1016/j.jpowsour.2006.12.073

[68]Palmer, D. "Hydrogen in the Universe". NASA. http://imagine.gsfc.nasa.gov/docs/ask_astro/answers/971113i.html

[69]Dresselhaus, Mildred. "Basic Research Needs for the Hydrogen Economy". Argonne National Laboratory, U.S. Department of Energy, Office of Science Laboratory. http://www.sc.doe.gov/bes/hydrogen.pdf

[70]Miessler, Gary L.; Tarr, Donald A. “Inorganic Chemistry” (3rd ed.). Prentice Hall . (2003)..ISBN 0130354716

[71]Emsley, John (2001). "Oxygen: Nature's Building Blocks: An A-Z Guide to the Elements". Oxford, England, UK: Oxford University Press. Page(s). 297–304. ISBN 0198503407

[72]Cook, Gerhard A.; Lauer, Carol M."Oxygen". The Encyclopedia of the Chemical Elements (1968) . Page(s). 499–512. LCCN 68-29938.

[73]Chris Rayment ,Scott Sherwin, "Introduction to Fuel Cell Technology",Department of Aerospace and Mechanical Engineering, University of Notre Dame, Notre Dame, IN 46556, U.S.A. May 2, 2003

[74]Garcia B.J,;Sethruraman, V.A;Weidner, J.W;White, R.E;Dougal, R. "Mathematical Model of a Direct Methanol Fuel Cell". Journal of Fuel Cell Science and Technology ASME, Nov 2004. p43-48

[75]M.Dargahi; J.Rouhi; M.Rezanejad; M.Shakeri. "Maximum Power Point Tracking for Fuel Cell in Fuel Cell/Battery Hybrid Power Systems"European Journal of Scientific Research,ISSN 1450-216X Vol.25 No.4 (2009), Page(s).538-548

[76]M.Y. El-Sharkh, A. Rahman, M.S. Alam, P.C. Byrne, A.A. Sakla, T.Thomas, 2004. "A dynamic model for a stand-alone PEM fuel cell power plant for residential applications", J. Power Sources, Vol. 138, No. 1–2, Page(s). 199–204.

[77]Ticianelli,F;Derouin,C;Redondo,A;Srinivasan,S "Methods to Advance Technology of Proton Exchange Membrane Fuel Cells" Electrochemistry Society, 135.9, 1988 Page(s)2209-2214

[78]Hanifi Guldemir, " Sliding Mode Control of DC/DC Boost Converter", Journal of Applied Sciences 5(3), ISSN 1812-5654

[79]Il-Song Kim, “Robust Maximum power point tracker using sliding mode controller for the three-phase grid-connected photovoltaic system”. Solar Energy 81(2007) pag. 415-414.

[80]A.M. Sharaf, Liang Yang, “An efficient Photovoltaic DC Village Electricity Scheme Using a Sliding Mode Controller”, IEEE Conference on Control Applications, 2005, Page(s) 1325-1330.

[81]Global Wind Energy Council, Global Wind 2005 Report, www.gwec.net, 2006.

[82]Gross, G.; “Contributions of renewable energy resources to resource diversity” Power Engineering Society General Meeting, 2006. IEEE18-22 June 2006 Page(s):1 Page(s). Digital Object Identifier 10.1109/PES.2006.1709497

[83]Ahmed, M.M.; Sulaiman, M., "Design and proper sizing of solar energy schemes for electricity production in Malaysia," Power Engineering Conference, 2003, Page(s). 268-271, 15-16 Dec. 2003

[84]Hassan Khalil, “Non Linear Control”, 3rd Edition. Prentice Hall, December 2001. ISBN-10: 0130673897

APPENDIX A Photovoltaic Module Datasheets

A1 Siemens SP75

Solar module SP75		
Electrical parameters		12 V/6 V
Maximum power rating P_{max}	[Wp] 1)	75
Rated current I_{MPP}	[A]	4.4/8.8
Rated voltage V_{MPP}	[V]	17.0/8.5
Short circuit current I_{SC}	[A]	4.8/9.6
Open circuit voltage V_{OC}	[V]	21.7/10.9
Thermal parameters		
NOCT 2)	[°C]	45 ±2
Temp. coefficient: short-circuit current		2.06 mA / °C
Temp. coefficient: open-circuit voltage		-.077 V / °C

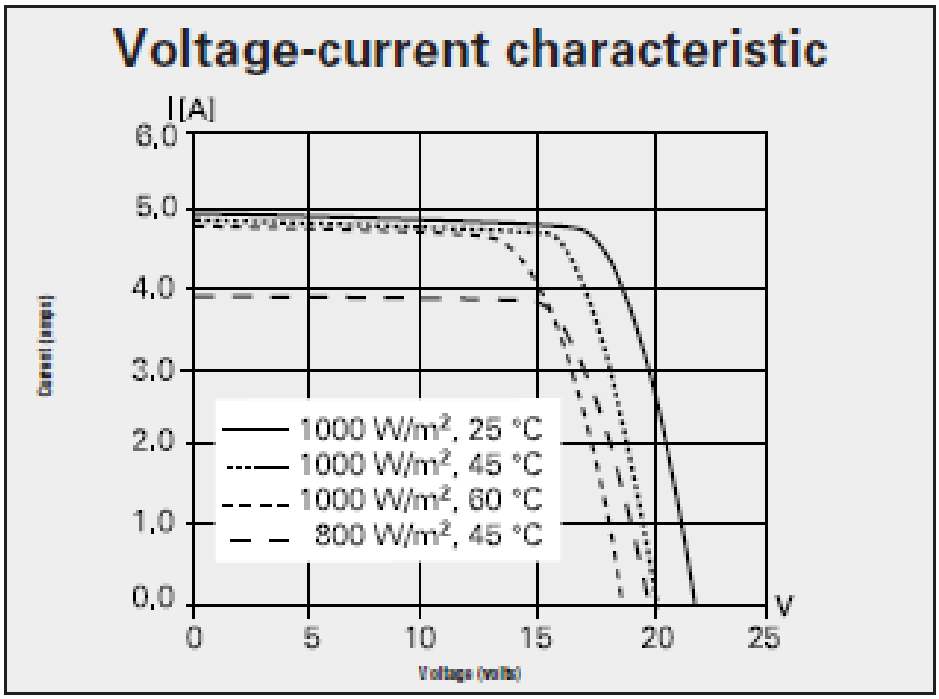

A2 Shell SPQ80

	Shell PowerMax™	Ultra 80-P
Rated power	P_r	80W
Peak power	P_{mpp}*	80W
Module efficiency	η	12.7%
Maximum system voltage	V_{sys}	600V (UL); 715V (TUV);
Peak power voltage	V_{mpp}	16.9V
Peak power current	I_{mpp}	4.76A
Open circuit voltage	V_{oc}	21.8V
Short circuit current	I_{sc}	5.35A
Series fuse rating	I_{fuse}	20A
Minimum peak power	$P_{mpp\ min}$	76W
Tolerance on peak power	%	+/- 5

Temperature coefficients

αP_{mpp}	%/°C	-0.43
αV_{mpp}	mV/°C	-72.5
αI_{sc}	mA/°C	0.8
αV_{oc}	mV/°C	-72.5

A3 SLK60m6 Datasheet

Electrical Data

Power max. (±5%)	P_{mpp}	210 Wp
Voltage mpp	V_{mpp}	30.6 V
Current mpp	I_{mpp}	6.86 A
Open Circuit Voltage	V_{oc}	37.2 V
Short Circuit Current	I_{sc}	7.52 A

Data related to standard test conditions (STC): 1000W/m² radiation, spectrum AM 1.5 and cell temperature 25ºC.

Dimensions

Dimensions (tolerance ±2mm)	955x1580 mm²
Thickness with frame, including junction box	40 mm
Approximate weight	17 kg

Module temperature coefficients

Nominal Operation Cell Temperature	NOCT	43±2 ºC
Power coefficient	$T_k(P_n)$	-0.43%/ºC
Open circuit voltage	$T_k(V_{oc})$	-127mV/ºC
Short circuit current	$T_k(I_{sc})$	+2.2mA/ºC

NOCT Nominal operation cell temperature: Radiation 800W/m², ambient temperature 20ºC, wind speed 1 m/s.

Operation Limits

Maximum system voltage	750 V_{dc}
Operation temperature	-40ºC a +85ºC
Wind resistance	200 km/h
Hailstone max. diameter	25 mm
Hailstone speed impact	23 m/s

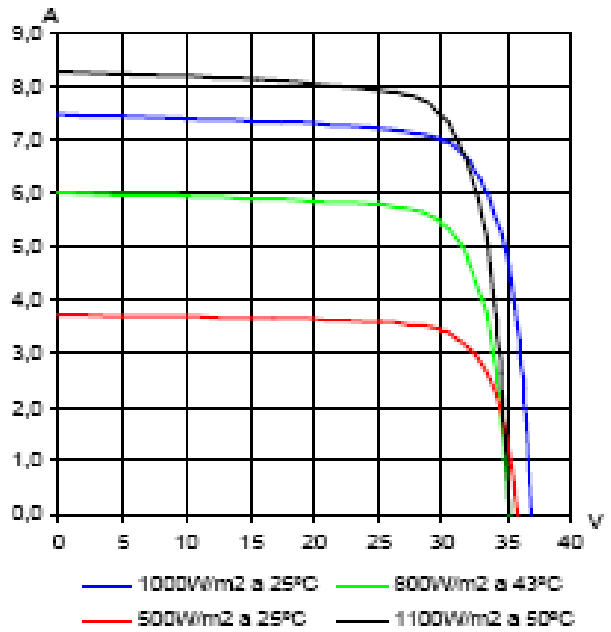

A4 Solarex SX-5 Data Sheet

Typical Electrical Characteristics	
Maximum power (Pmax)	4.5W
Voltage at Pmax (Vmp)	16.5V
Current at Pmax (Imp)	0.27A
Guaranteed Minimum Pmax	4W
Short-circuit current (Isc)	0.3A
Open-circuit voltage (Voc)	20.5V
Temperature coefficient of Isc	(0.065±0.015)%/°C
Temperature coefficient of Voc	–(80±10)mV/°C
Temperature coefficient of power	–(0.5±0.05)%/°C
NOCT	47±2°C

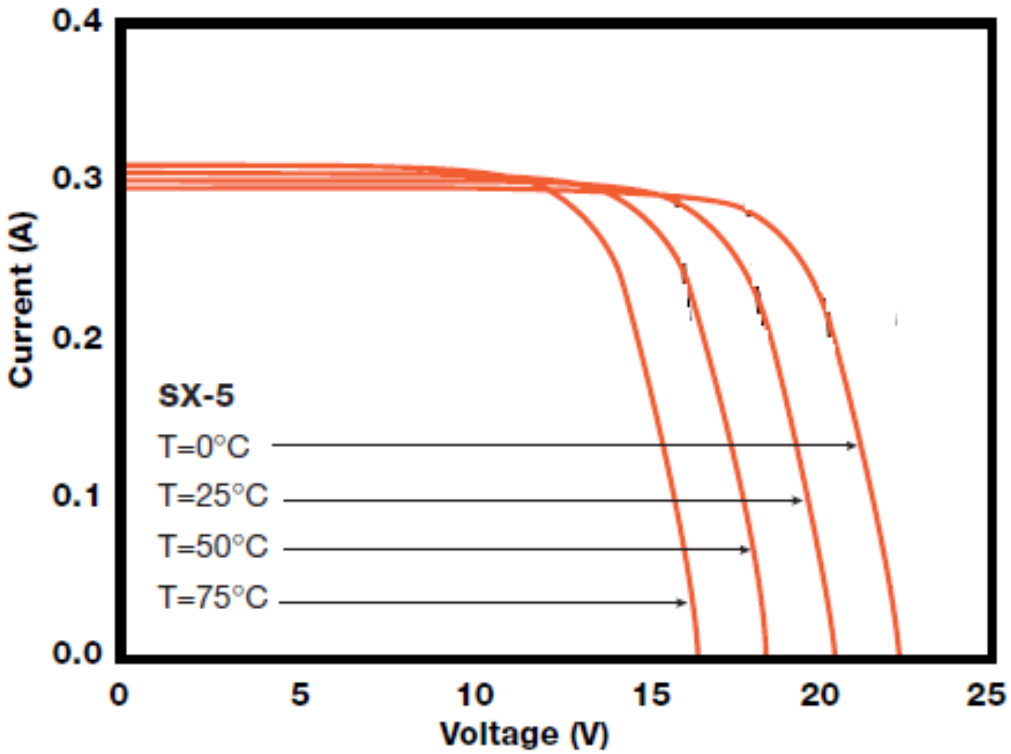

A5 Solarex SX-10 Data Sheet

Typical Electrical Characteristics	
Maximum power (Pmax)	10W
Voltage at Pmax (Vmp)	16.8V
Current at Pmax (Imp)	0.59A
Guaranteed Minimum Pmax	9W
Short-circuit current (Isc)	0.65A
Open-circuit voltage (Voc)	21.0V
Temperature coefficient of Isc	(0.065±0.015)%/°C
Temperature coefficient of Voc	–(80±10)mV/°C
Temperature coefficient of power	–(0.5±0.05)%/°C
NOCT	47±2°C

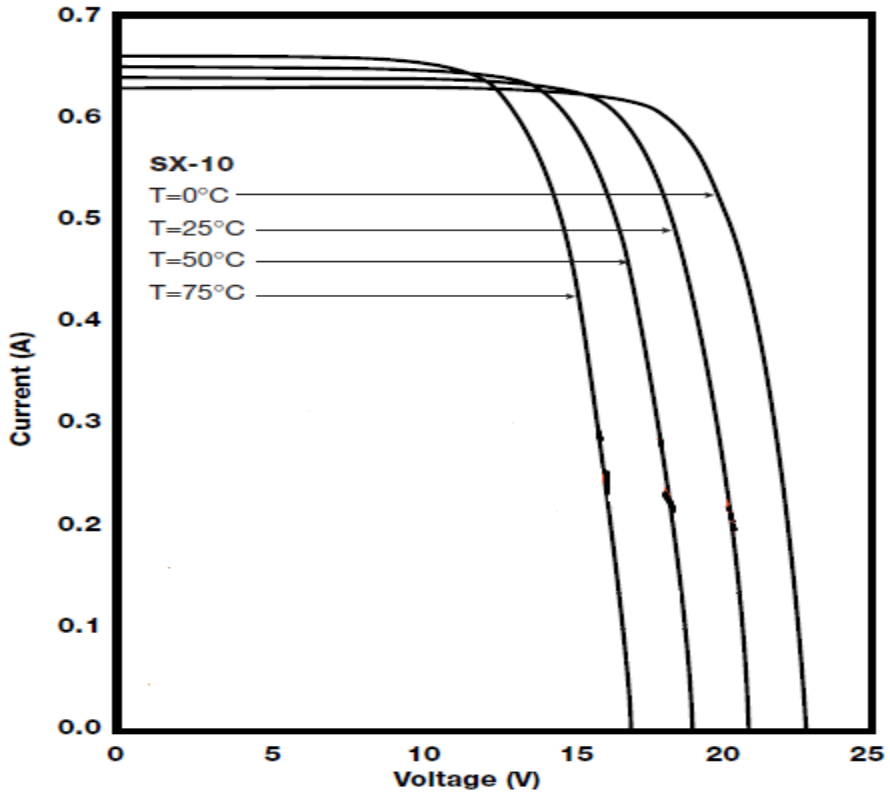

APPENDIX B Fuel Cells Datasheets

B1 Horizon H-100

Type of fuel cell	PEM
Number of cells	24
Rated power	100W
Rated performance	14V@7.2A
Output voltage range	13V-23 V
Weight (with fan & casing)	0.95kg(2.1lbs)
Size	143x109x94mm(5.6x4.3x3.7in)
Reactants	Hydrogen and Air
Rated H_2 consumption	1.4l/min(83in³/min)
Hydrogen pressure	0.4-0.45Bar(5.8-6.5PSI)
Controller weight	0.4kg(0.88lbs)
Hydrogen supply valve voltage	12V
Purging valve voltage	12V
Blower voltage	12V
Ambient temperature	5-35°C(41-95°F)
Max stack temperature	65°C(149°F)
Hydrogen purity	99.999% dry H2
Humidification	Self-humidified
Cooling	Air (integrated cooling fan)
Start up time	Immediate
Efficiency of system	40%@14V

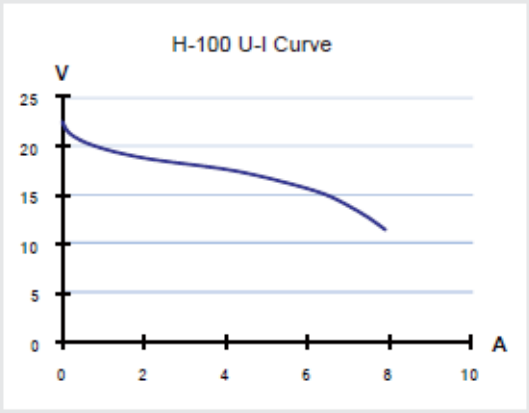

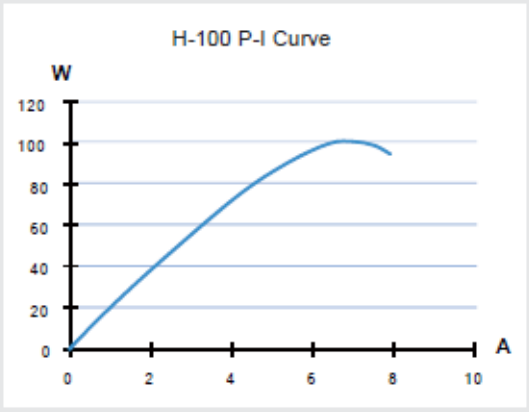

B2 Horizon H1000

Type of fuel cell	PEM
Number of cells	72
Rated power	1000W
Rated performance	43V@23.5A
Output voltage range	39V-69V
Weight (with fan & casing)	4.2kg(9.3lbs)
Size	324x220x122mm(12.8x8.7x4.8in)
Reactants	Hydrogen and Air
Rated H_2 consumption	14l/min(847in³/min)
Hydrogen pressure	0.5-0.6Bar(7.2-9.4PSI)
Controller weight	0.45kg(0.99lbs)
Hydrogen supply valve voltage	12V
Purging valve voltage	12V
Blower voltage	12V
Ambient temperature	5-30°C(41-86°F)
Max stack temperature	65°C(149°F)
Hydrogen purity	99.999% dry H2
Humidification	Self-humidified
Cooling	Air (integrated cooling fan)
Start up time	Immediate
Efficiency of system	40%@43V

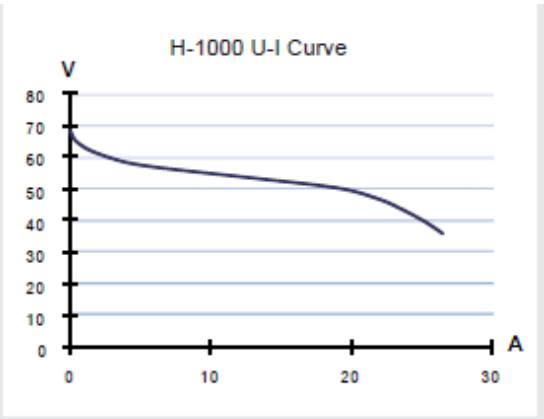

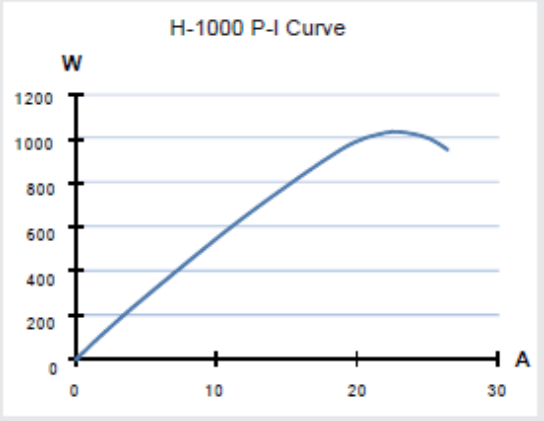

APPENDIX C Battery Model

C1 Simulink's Battery Model

Battery Figure

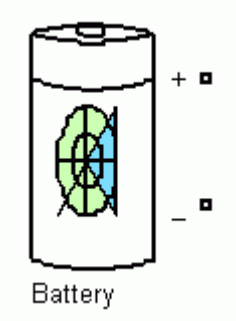

The Battery block implements a generic model parameterized to represent most popular types of rechargeable batteries.

The equivalent circuit of the battery is shown below:

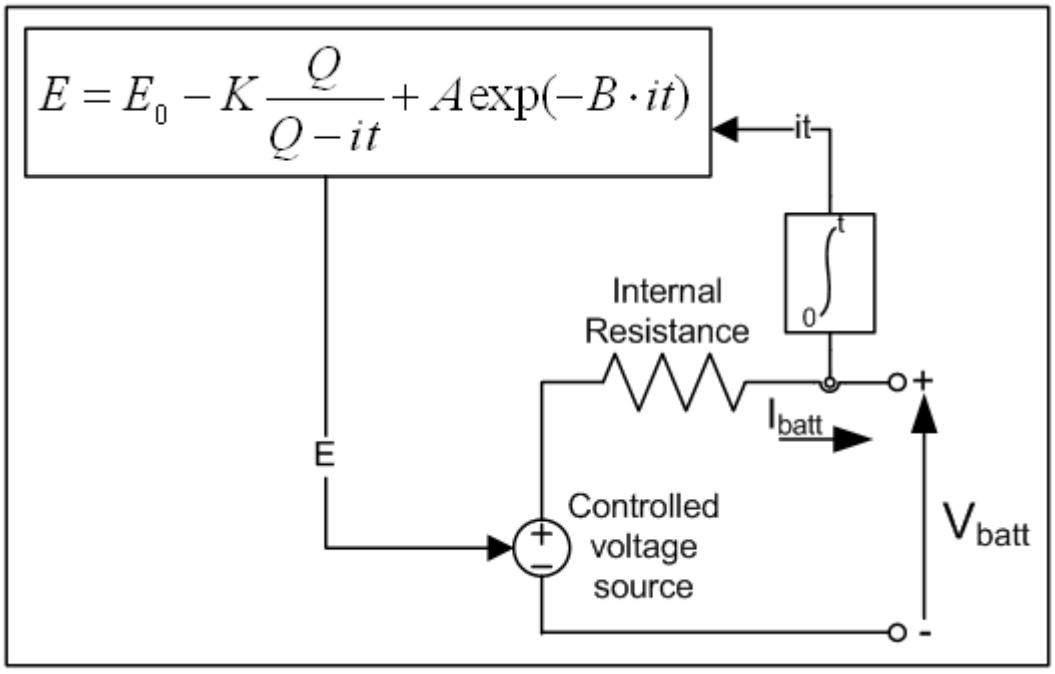

where,

E = No load voltage (V)

E0 = Constant voltage (V)

K = Polarization voltage (V)

Q = Battery capacity (Ah)

A = Exponential voltage (V)

B = Exponential capacity (Ah)-1

All the parameters of the equivalent circuit can be modified to represent a particular battery type, based on its discharge characteristics. A typical discharge curve is composed of three sections:

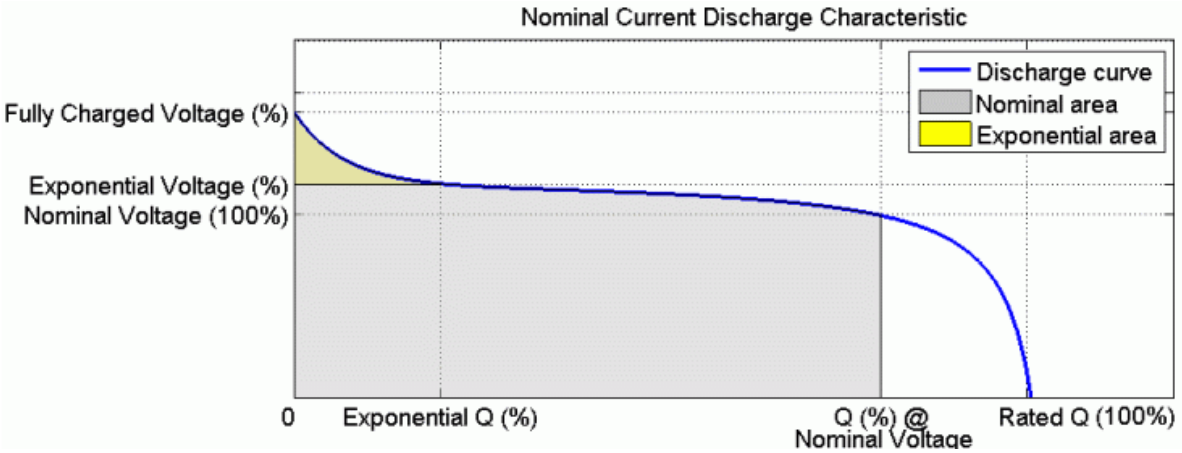

The first section represents the exponential voltage drop when the battery is fully charged. The width of this region depends on the battery type. The second section represents the charge that can be extracted from the battery until the voltage drops below the battery nominal voltage. Finally, the third section represents the total discharge of the battery, when the voltage drops rapidly.

When the battery current is negative, the battery will recharge following a charge characteristic as shown below: